AFRL-HE-WP-TR-2004-0149

United States Air Force Research Laboratory

University of South Carolina CB Support, Basic Research in Materials and Techniques for Optical Computing Standoff Sensors

Michael L. Myrick
University of South Carolina
Office of Sponsored Programs
901 Sumter Street, Room 51
Columbia SC 29208

October 2004
Final Report: 13 June 2001 – 12 June 2004

Human Effectiveness Directorate
Biosciences and Protection Division
Counterproliferation Branch
E5183 Blackhawk Road
Aberdeen Proving Ground MD 21010-5424

When US Government drawings, specifications or other data are used for any purpose other than definitely related Government procurement operation, the Government thereby incurs no responsibility nor any obligation whatsoever, and the fact that the Government may have formulated, furnished, or in any way supplied the said drawings, specifications or other data, is not to be regarded by implication or otherwise, as in any manner licensing the holder or any other person or corporation, or conveying any rights or permission to manufacture, use, or sell any patented invention that may in any way be related thereto.

Please do not request copies of this report from the Air Force Research Laboratory. Additional copies may be purchased from:

National Technical Information Service
5285 Port Royal Road
Springfield, Virginia 22161

Federal Government agencies registered with the Defense Technical Information Center should direct requests for copies of this report to:

Defense Technical Information Center
8725 John J. Kingman Rd., Ste 0944
Ft. Belvoir, Virginia 22060-6218

TECHNICAL REVIEW AND APPROVAL

AFRL-HE-WP-TR-2004-0149

This report has been reviewed by the Office of Public Affairs (PA) and is releasable to the National Technical Information Service (NTIS). At NTIS, it will be available to the general public, including foreign nations.

This technical report has been reviewed and is approved for publication.

FOR THE DIRECTOR

//signed//
STEPHEN R. CHANNEL, DR-IV
Director, AF CBD Tech Base Programs
Air Force Research Laboratory

REPORT DOCUMENTATION PAGE

Form Approved
OMB No. 0704-0188

PLEASE DO NOT RETURN YOUR FORM TO THE ABOVE ADDRESS.

1. REPORT DATE *(DD-MM-YYYY)*	2. REPORT TYPE	3. DATES COVERED *(From - To)*
01-10-2004	Final Report	13 Jun 2001 - 12 June 2004

4. TITLE AND SUBTITLE

University of South Carolina CB Support, Basic Research in Materials and Techniques for Optical Computing Standoff Sensors

5a. CONTRACT NUMBER
F33615-00-2-6059

5b. GRANT NUMBER

5c. PROGRAM ELEMENT NUMBER
61384B

6. AUTHOR(S)

Michael L. Myrick

5d. PROJECT NUMBER
0600

5e. TASK NUMBER
060001

5f. WORK UNIT NUMBER
06000101

7. PERFORMING ORGANIZATION NAME(S) AND ADDRESS(ES)

University of South Carolina
Office of Sponsored Programs
901 Sumter Street, Room 51
Columbia SC 29208

8. PERFORMING ORGANIZATION REPORT NUMBER

9. SPONSORING/MONITORING AGENCY NAME(S) AND ADDRESS(ES)

Air Force Research Laboratory, Human Effectiveness Directorate,
Biosciences and Protection Division, Counter Proliferation Branch
E1583 Blackhawk Road
Aberdeen Proving Ground MD 21010-5424

10. SPONSOR/MONITOR'S ACRONYM(S)

11. SPONSOR/MONITOR'S REPORT NUMBER(S)
AFRL-HE-WP-TR-2004-0149

12. DISTRIBUTION/AVAILABILITY STATEMENT

Approved for public release, distribution is unlimited.

13. SUPPLEMENTARY NOTES

14. ABSTRACT

Research demonstrated that multivariate optical elements (MOEs) and imaging MOEs (IMOEs) could be designed, fabricated and characterized. These devices are the computing elements of multivariate optical computing. Results of the first MOE tests revealed that near-theoretical performance could be obtained in the simple situation tested. Mid-infrared, near-infrared and Raman spectra were acquired for nearly 50 organophosphorus compounds. Measurements were made on B. globigi, and comparisons to paper was made. A prototype camera system based on an IMOE was constructed and demonstrated to work in the UV-Vis region. Improved sampling methods for bacterial spores were developed. Spectroscopy of autoclaved spores and spores devoid of DPA was reported. An instrument was designed and built to measure scattering matrix elements of single particles. It is the belief of this laboratory and our AF technical representative that rugged instruments based on these concepts can be made much more inexpensively to become an important part of the chemical and biological detection and identification program of the DOD as well as homeland defense.

15. SUBJECT TERMS

16. SECURITY CLASSIFICATION OF:			17. LIMITATION OF ABSTRACT	18. NUMBER OF PAGES	19a. NAME OF RESPONSIBLE PERSON
a. REPORT	b. ABSTRACT	c. THIS PAGE			Dr. Burt V. Bronk
Unclas	Unclas	Unclas	SAR	82	19b. TELEPHONE NUMBER *(Include area code)* 410-436-1813

THIS PAGE INTENTIONALLY LEFT BLANK

TABLE OF CONTENTS

FIGURES

FIGURE PAGE

1.0 INTRODUCTION

Multivariate optical computing was introduced by Myrick theoretically in 1998 and first shown to be realizable in 2001 under this contract. This measurement tool is based on specialized interference filters called multivariate optical elements (MOEs) that encode spectral pattern vectors for simplified pattern recognition in complex spectroscopy, replacing conventional spectrometers in many dedicated applications. It is the belief of this laboratory and our Air Force technical representative that rugged instruments based on these concepts can be made much more inexpensively to become an important part of the chemical and biological detection and identification program of the DOD as well as homeland defense.

This report summarizes work performed under AFRL grant number F33615-00-2-6059 between June 13, 2001 and June 12, 2004, titled "University of South Carolina CB Support: Basic Research in Materials and Techniques for Optical Computing Standoff Sensors". The organization of the report is as follows:

1. Introduction
2. Aims
3. Findings of the Investigator
4. Chronological list of written publications
5. List of professional personnel associated with the project.
6. Related Activities: Meetings/Conferences
7. Discoveries and Inventions
8. Other grants related to F33615-00-2-6059
9. Appendixes

2.0 AIMS

Broadly, the purpose of this project has been to explore the idea of using simple optical elements to do the job of more complex and costly spectroscopic hardware in measuring chemical concentrations and determining chemical composition via optical spectroscopy. Work of this type is called multivariate optical computing, a name given it in a 1998 publication in the journal Analytical Chemistry.

The underlying theme of this work is that the spectroscopic patterns that provide meaningful chemical information in complex systems can be encoded into the spectrum of a simple optical interference filter. To ascertain whether this is feasible, and if feasible then under what conditions and with what certainty, this project explores the basic theory of multivariate optical computing as well as the materials, algorithms and systems used for bringing the concept to life.

In pursuit of this aim, the USC research team undertook a wide variety of investigations. We had a number of outside collaborations including one under a subcontract with Dr. Jozsef Czege of Uniformed Services University of the Health Sciences in Bethesda, MD. Among the activities under this contract were development of design algorithms, measurements of optical spectra of samples in transmittance, diffuse reflectance and grazing angle specular reflectance, process

control algorithms, theoretical analysis of the limitations of our ability to fabricate optics, spectral radiometry of detectors and light sources, construction of prototype systems, construction of imaging systems, measurements of the optical constants of materials used in fabrication, literature searches and reviews, plus measurements of organic materials, thin films and other processes for making defined interference layers. In addition, we conducted a study of the spectroscopy of mixtures of organophosphorus compounds and other organic liquids, developed tools to fabricate optical elements more precisely, evaluated a new algorithm for design of imaging elements, developed a system to permit measurement of organic compounds in the near-infrared, investigated the spectroscopy of bacterial spores and of envelope paper and other postal materials, developed a prototype system for measuring the presence of bacterial spores on paper, and investigated the spectroscopy of bacterial spores for the purpose of distinguishing spore types from one another. We also measured the optical spectroscopy of bacterial spores before and after autoclaving and studied the effects of the process on their optical spectra. With assistance from Peter and Barbara Setlow of University of Connecticut, we spectroscopically studied spores devoid of DPA to understand the effects of DPA on the optical spectra of spores. We also developed a full theory of precision in multivariate optical computing that permits MOC to be quantitatively compared to other types of measurements, and reveals the factors that influence precision. A new method for improved spectroscopic measurement of bacterial spores was developed with much higher precision that methods previously in existence. Also, a system for the rapid measurement of Mueller scattering matrix elements from single particles was designed. The angular distribution of these elements has been shown to give information about the particles size, shape and optical properties. An early prototype of this system was constructed and partially evaluated. If further development of such a system takes place, we envision an instrument which serially delivers from a particle absorption information from MOE's and combines this with information from the Mueller matrix scattering to automatically improve very rapid classification of an unknown aerosol particle.

The following report describes some of the salient features of our work.

3.0 FINDINGS OF THE INVESTIGATOR

3.1 SYNTHESIS OF MULTIVARIATE OPTICAL ELEMENTS FOR POINT MEASUREMENTS

A major focus was to develop and improve tools for the design of multivariate optical elements (MOEs). All initial work (prior to the beginning of this program) was aimed at spectral matching algorithms (SMAs). SMAs are used to design MOEs by attempting to design a thin-film structure whose interference-governed spectrum matches a desired target spectrum. The "match quality" of the filter spectrum to the target spectrum was characterized by a figure of merit (FOM) that generally expresses the percent transmission difference between the two across a range of wavelengths. Target spectra were derived from chemometric interpretation of sample spectroscopy. SMAs are conceptually and practically identical to design methods for any type of tailored-spectrum optical interference filter, including the very sophisticated commercially-available packages used by thin-film designers at custom coating houses. While such algorithms have been well known, they are by no means easy to implement for general MOE design. There

are serious problems, both conceptual and practical, relating to how well data noise should be included in the target spectrum, for example. In addition, relating the film thickness sensitivities for layers of a MOE to the chemical prediction quality desired for an MOE is by no means straightforward or simple. Thus it was recognized at the beginning of this project that SMAs are not ideal for MOE design.

The USC team undertook software development for the synthesis of interference coatings based on a "standard error of prediction" figure of merit. This new design algorithm bypasses many of the problems associated with the old SMA approach by finding an optimal design for the MOE at each given level of MOE complexity.

This work began with a written code that calculates the transmittance of a multilayer film as a function of angle, wavelength and optical constants, including absorbance. The second stage of the work was the incorporation of this algorithm into an optimization code. This optimization code at the moment uses a pseudo-Newton gradient descent algorithm to optimize the thicknesses of materials in a multilayer that is given it as a starting point. A number of permutations on this basic theme were tried. The USC team has thus far found that random starting positions for optimization are preferable to a SMA-derived starting point. The ultimate reason behind this remains essentially unknown; one possible explanation is that an SMA-derived starting point limits the available space that can be sampled easily during optimization. Random starting points have generally produced results that outperform SMA-initiated optimizations.

The new algorithms have been the subject of both a manuscript (currently submitted) and a preliminary patent application.

3.2 Manufacturing Tolerances

The question of how closely a fabricated filter has to match its objective, theoretical spectrum before its performance as an MOE degrades was addressed by the USC team. This question is of great importance in determining whether it is feasible to manufacture an MOE suitable for general application. Theory was developed on this topic by taking a conservative approach to tolerance. The USC team used a "bandpass selection" filter set to select the spectral region in which a MOE should work. The new theory provides an exact definition for the actual bandpass region of importance, and how the spectral tolerances where the band begins and ends. It also tells us how the tolerance changes with wavelength.

The key equations of note were found to be:

$$1. \qquad \Delta t(\lambda) = \frac{V_{co}}{V(\lambda)},$$

$$2. \qquad V_{ex} + V_{co}(\lambda_R - \lambda_L) - \frac{SEP^2}{2k} = 0$$

In Equation 1, V stands for variance, Δt is the tolerance in transmittance, co means "at the cutoff wavelength", and λ is wavelength. In equation 2, SEP is the standard error of prediction in the calibration, R and L mean "at the right and left cutoffs", respectively. ex means "excluded", and k is the gain factor relating the regression vector to the predicted value. These two equations are of principal importance in determining the permissible error tolerance in filter design and manufacturing, and for determining the bandpass of the coating. Their derivation and use are described in the attached manuscript, "Fixed Tolerance Determination for Multivariate Optical Elements" which was published in Fresenius J. Anal. Chem. 369(2001), 351-5.

The consequence of this investigation was the finding that ideal performance in an MOE would be extremely difficult to achieve in practice. In the specific example chosen for the manuscript, the designed MOE required some spectral regions to have 0.2% errors in transmittance or better for ideal performance. This level of error was found to be unachievable in practice for a fixed design. That is, the accumulated error expected in the fabrication of a fixed-design MOE would quickly mount to levels greater than the theoretical tolerance at the most critical wavelengths. This lead the USC team to the "variable-design" MOE concept that is a subject of current, ongoing research.

3.3 Demonstration of Multivariate Optical Computing

The USC team completed the SEP coating synthesis programming and applied it to two simple chemical problems to determine how this solution to film design works. One of these examples is shown below as Figure 1.

Figure 1 gives a set of optical spectra for mixtures of two dyes. The two dyes have optical spectra that overlap one another throughout the wavelength region covered. The samples were made by random generation so that the concentrations of the two dyes are independent of one another. Consequently, each dye other simulates a random interfering species for measurement of the other.

Simple bandpass filtering was found to work poorly for the measurement of the target chemical species in the mixture represented in Figure 1. The SEP approach, on the other hand, gave the spectral design illustrated in Figure 2 below.

Figure 3 shows the result of actual manufacture of this coating (at normal incidence, not the 45 degrees incidence at which it would be used).

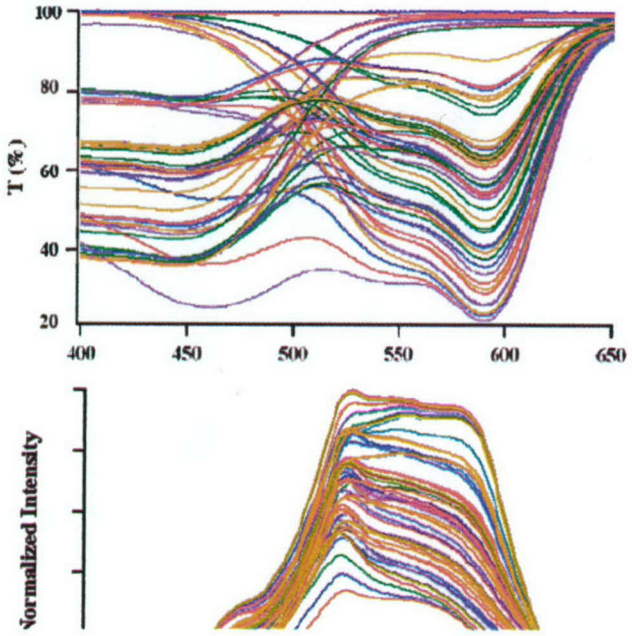

Figure 1. Binary dye spectra. Top: transmission spectra of binary dye mixtures. Bottom: spectra corrected for source radiance, detector response, and filter bandpass.

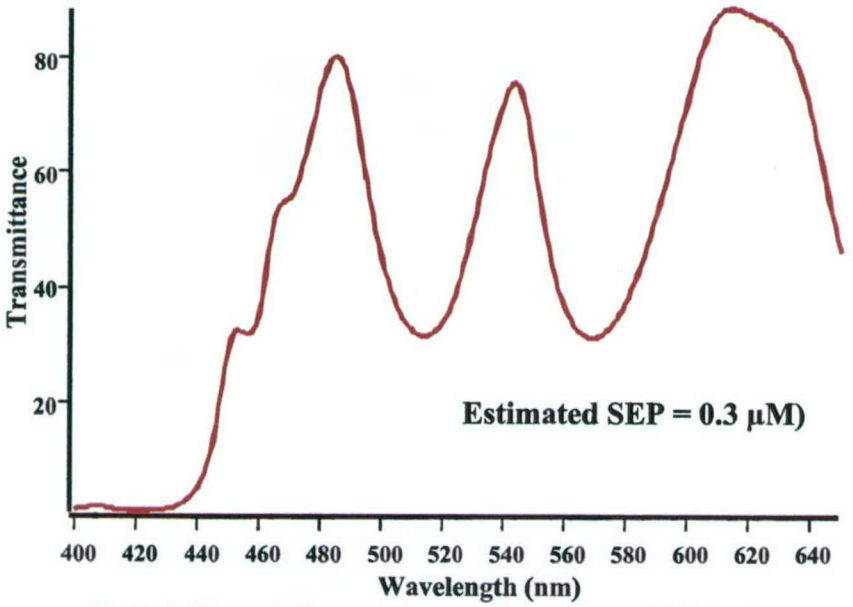

Figure 2. Theoretical transmittance spectrum of an MOE designed for the data in Figure 1 at 45 degrees angle of incidence.

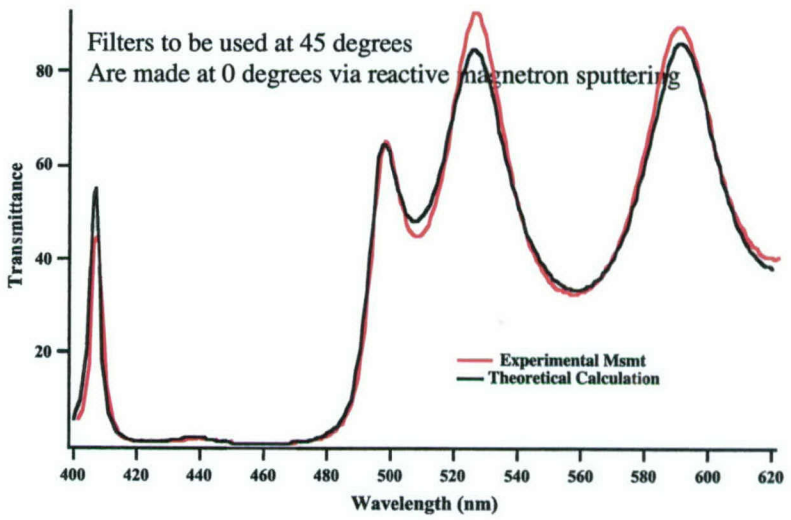

Figure 3. Real (as fabricated) and theoretical spectrum of the MOE in Figure 2 at 0 degrees angle of incidence.

Figure 4 below shows a schematic of the point-detection system into which the Figure 3 MOE was placed for demonstration purposes. Figure 5 shows a photograph of the actual prototype instrument.

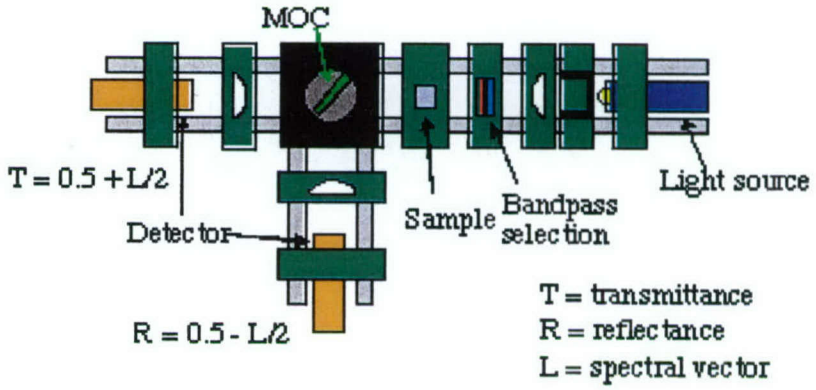

Figure 4. Schematic of Multivariate optical computing prototype system for single-point transmission measurements.

The actual prototype is shown in the following photograph:

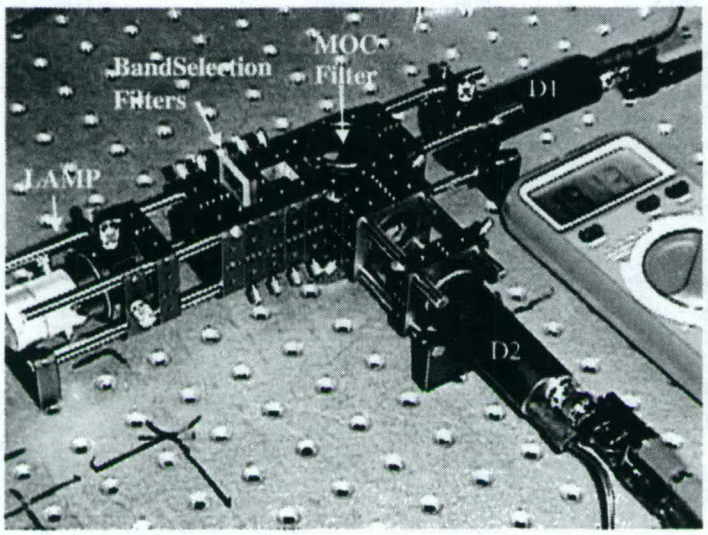

Figure 5. Photograph of prototype system illustrated in Figure 4.

Figure 6 shows that the system obtained 0.68 μM SEP rather than 0.3 μM, which was the theoretical optimum. The reduction in precision was found to be due to (a) imprecision in the manufacture of the MOE and (b) the algorithm for design that was limited to a single angle of incidence (no angular dispersion). This was the first successful demonstration of the multivariate optical computing principle.

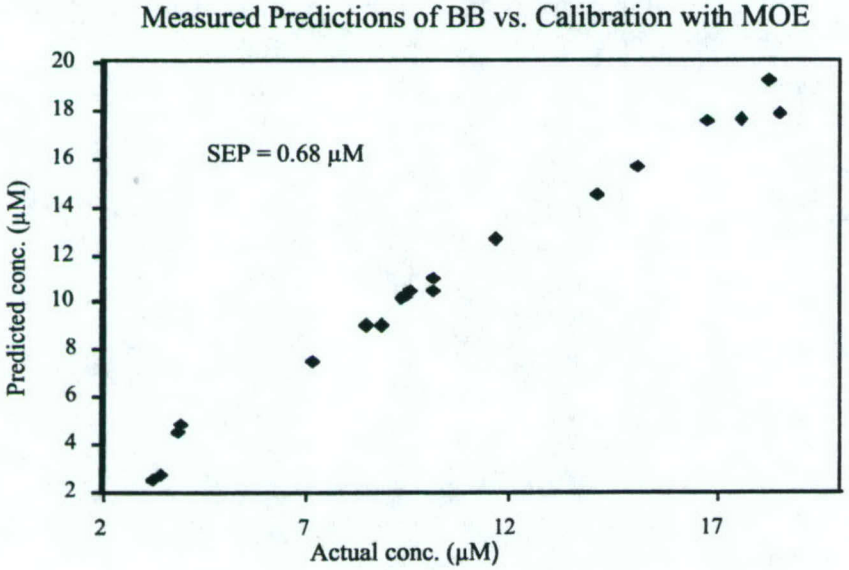

Figure 6. Results from the MOE built for demonstration purposes.

3.4 ANGLE-INVARIANT MOEs FOR IMAGING SPECTROSCOPY

As mentioned above, early forms of MOEs were designed to work with collimated light (see Figure 7 below).

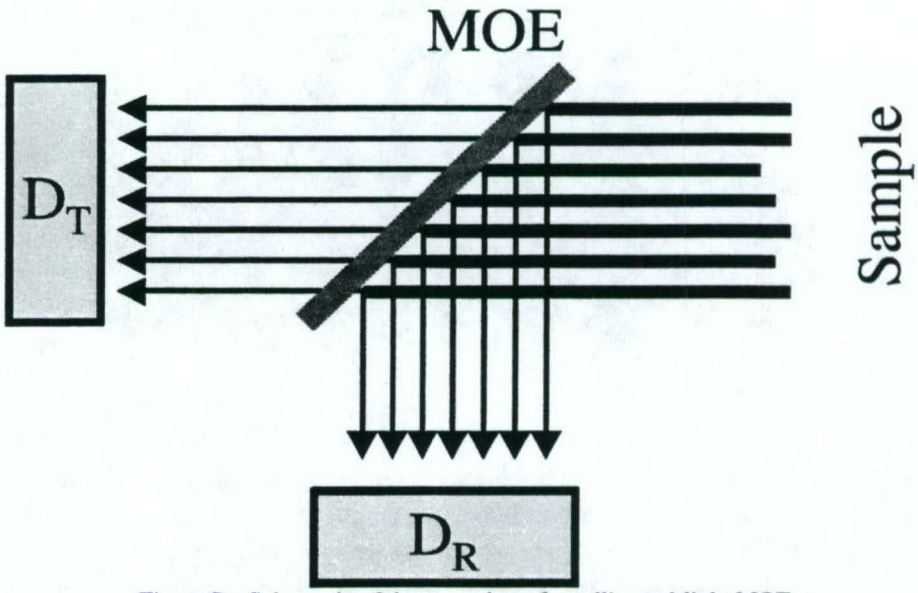

Figure 7 – Schematic of the operation of a collimated-light MOE

Imaging applications require the analysis of light from various angular positions in a field of view. This is illustrated in Figure 8 below.

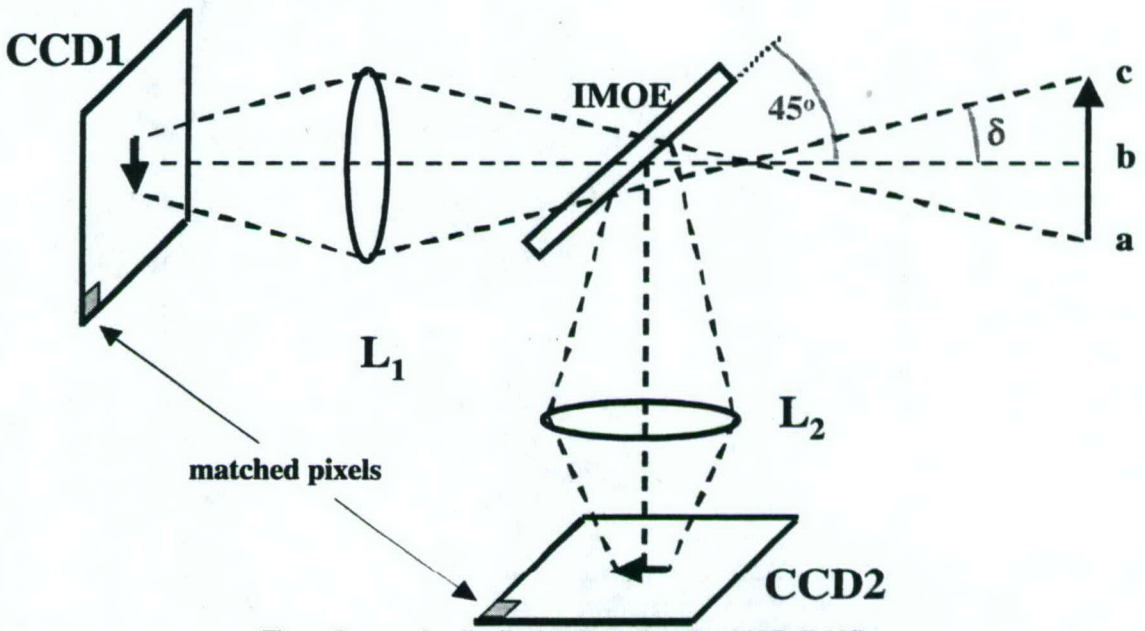

Figure 8 – angular distribution for an imaging MOE (IMOE)

The preceding figure helps illustrate the point that light analyzed during imaging operations comes into the instrument off collimation. This light needs to be tolerated well over a designed range of angles for imaging multivariate optical computing to function. In order to accomplish this, a new algorithm was developed ("Design of Angle-Tolerant Multivariate Optical Elements for Chemical Imaging" Appl. Optics. 41 (2002), 1936-1941) that simulated the effects on the MOE spectrum of light impinging from different angles, and that optimizes the average prediction error over the entire angular range. The performance of this algorithm is illustrated in Figure 9, which shows the prediction error for the MOE from the last section as the angle deviates from its designed angle of 45 degrees, and compares it to an IMOE designed for the same measurement. We found that small ranges of angles could be tolerated by design, although the greater the range of angles to be tolerated, the poorer the performance was likely to become.

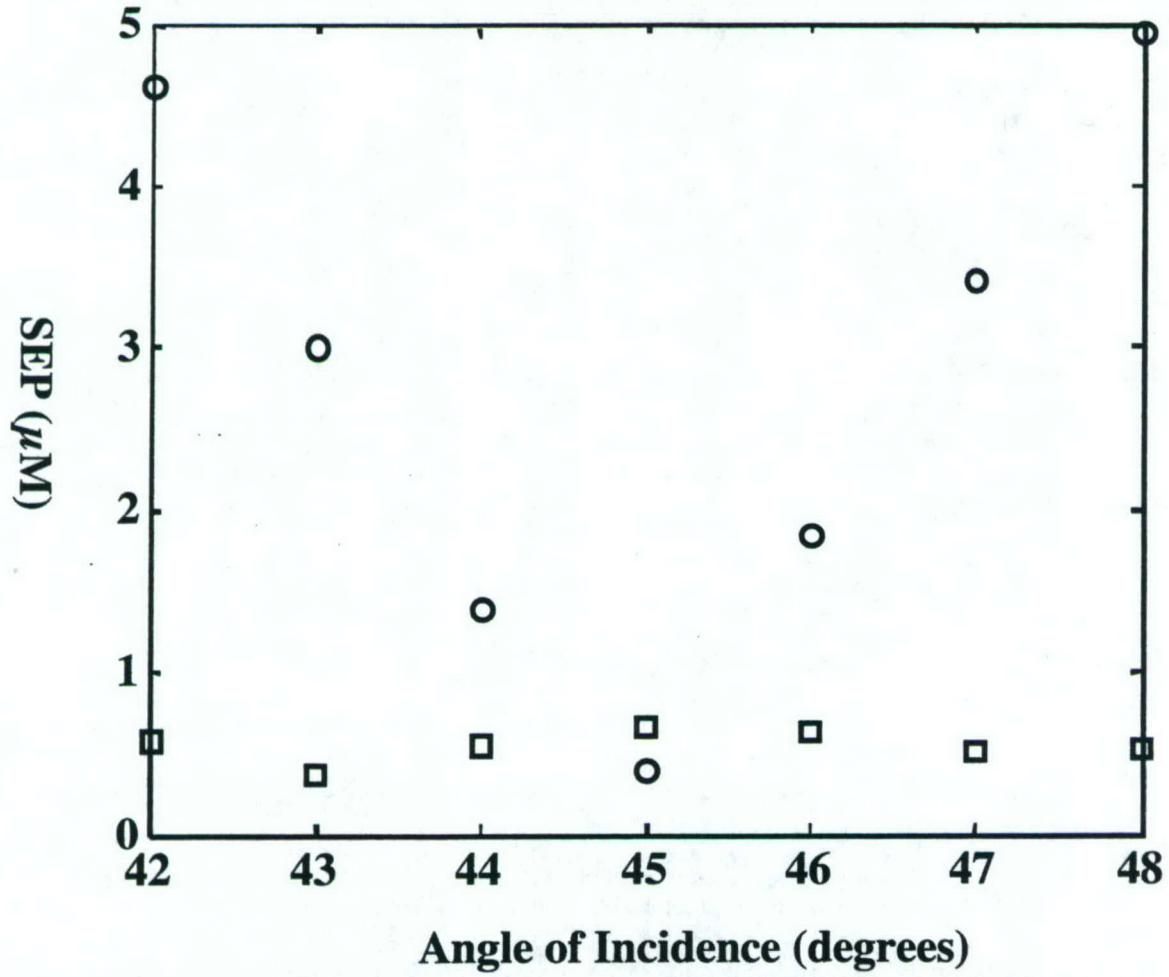

Figure 9. SEP as a function of angle for MOEs designed for 45-degree operation. (circles) SEP for the point MOE designed in the last section. (squares) SEP for an IMOE designed with the new angle-invariant algorithm.

The explanation for how a MOE can be designed for optimal performance over a range of incident angles is provided in detail in the manuscript ("Design. . .") describing the algorithm.

3.5 Near-infrared and mid-infrared spectroscopy of organophosphorous compounds

A goal for the first year of this project was to record the near-infrared and mid-infrared spectroscopies of a number of organophosphorous compounds. 47 compounds were selected; their structures and spectra were provided in a previous report.

Of particular interest is the near-infrared spectral region, which contains overtone and combination band absorbances. Only two of the compounds studied this year differed in the nature of the atom doubly-bonded to phosphorous. Tetraethylpyrophosphate and tetraethyldithiopyrophosphate differ only in that the former contains oxygen, while the latter contains sulfur, doubly-bonded to phosphorous. The near-infrared spectroscopy of these com-

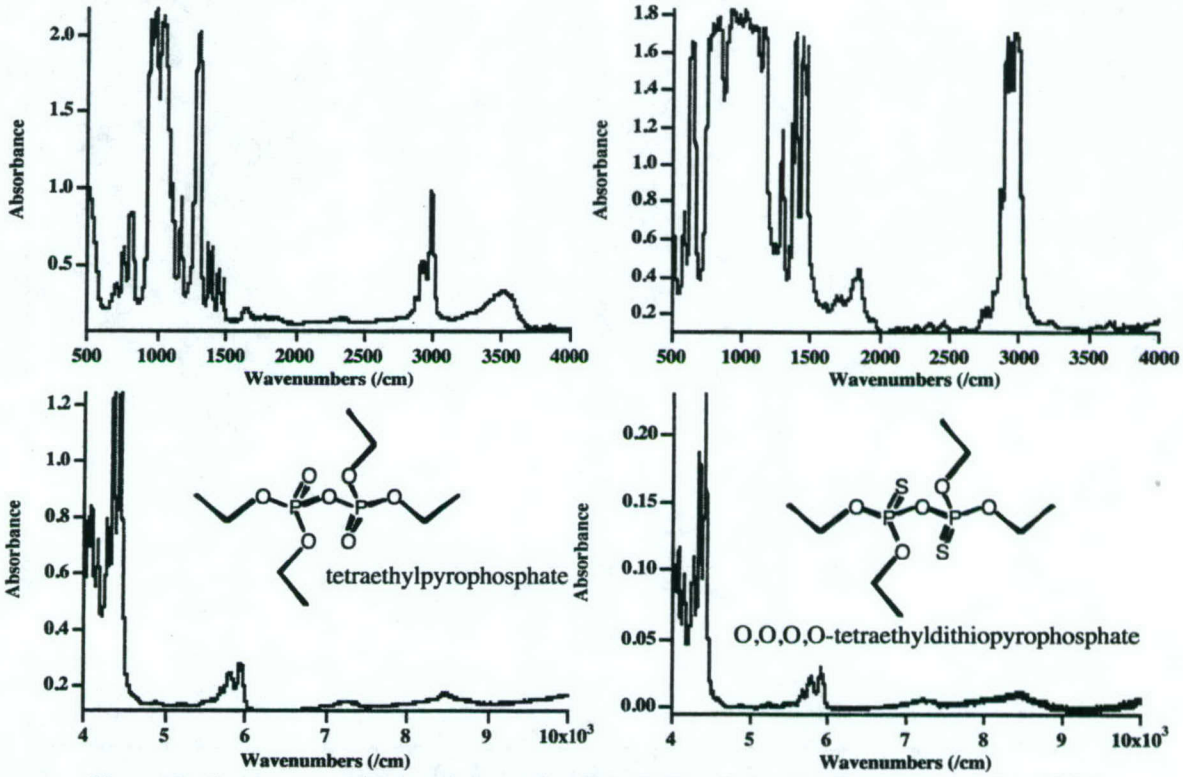

Figure 10. Spectroscopy of tetgraethylpyrophosphate (left) and tetraethyldithiopyrophosphate(right). Top: mid-infrared absorbance. Bottom: near-infrared absorbance.

pounds exhibits a combination band that is distinctly different in the two species, and is strongly correlated with the behavior of two bands appearing in the mid-infrared spectral region. Specifically, two mid-infrared modes for the oxygen species at 1371.1 and 1445.9 cm^{-1} couple with a C-H stretching vibration at 2987.2 cm^{-1} to produce combination bands at 4345.8 and 4431.6 cm^{-1}. For the sulfur species. modes at 1367.8 and 1443.5 cm^{-1} couple with a C-H vibration at 2976.1 cm^{-1} to form combination bands at 4340.5 cm^{-1} and 4425.9 cm^{-1}. The importance of these modes is that they reproduce in the near-infrared the observed differences in

the mid-infrared. The mid-IR modes (between 6.9 and 7.1 micrometer wavelength) are diagnostic for the P=S and P=O assignment in these molecules. However, they occur at a wavelength that is very difficult to measure due to blackbody emission and other for other reasons. The combination bands show the same intensity differences that the fundamentals show, but appear between 2.2 and 2.3 micrometers in wavelength. This wavelength region is transparent to high-quality silica optics and can be measured with higher-quality detectors. While the intrinsic strength of these absorbances is an order of magnitude less than those in the mid-infrared region, much of that loss can be compensated by improved detector quality and the loss of the blackbody continuum background that is so troublesome in both active and passive measurement of the mid-infrared region.

Optical spectra, including Raman spectra, of all samples have been obtained, but the research is still in progress to the extent that a detailed analysis of the optical spectra is still being performed. Preliminary data is available to DOD chemical researchers on request. An appendix below gives the names of the compounds studied, plus the types of spectra available for them.

3.6 NIR SPECTROSCOPY OF MIXTURES OF ORGANOPHOSPHORUS COMPOUNDS AND OTHER ORGANIC LIQUIDS

We demonstrated that multivariate optical elements can be designed for determinations based on the near-infrared C-H overtones of organic compounds.

Samples of dimethylmethylphosphonate (DMMP) and ethyl acetate in carbon tetrachloride solvent were prepared according to random number generation. Optical transmission spectra were measured on a Mattson Infinity AR-60 FTIR/FTNIR spectrometer in 1-cm pathlength quartz cells with air reference. Candidate detectors for the NIR spectral window were selected. These were Germanium photodiodes manufactured by Sciencetech, Inc. A light source consisting of a 6W/6V lamp (Linos Photonics) was measured as a candidate illumination system for point measurements. Measurements of spectral radiance of candidate light sources and spectral efficiency for candidate detectors were made with an Optronic Laboratories calibration system.

Figure 11 shows the experimental setup for implementing the single-filter design in a simple transmission measurement. In this system, a spatial filter and collimating lens is used to restrict the angular dispersion of light reaching a single filter. A single optical element is used in a beamsplitter arrangement, with part of the light passing through the sample being reflected and part being transmitted. The spectrum of the 45-degree optical element is designed to be precisely $T(\lambda)=0.5 +/- L(\lambda)$, where T is the filter transmittance and L is proportional to the loading of a spectral vector obtained via principal components regression of a chemical system. The reflectance is adequately represented by $R(\lambda)=0.5 -/+ L(\lambda)$. The difference between these values is proportional to the spectral regression vector, while the sum of the two is independent of the spectral vector.

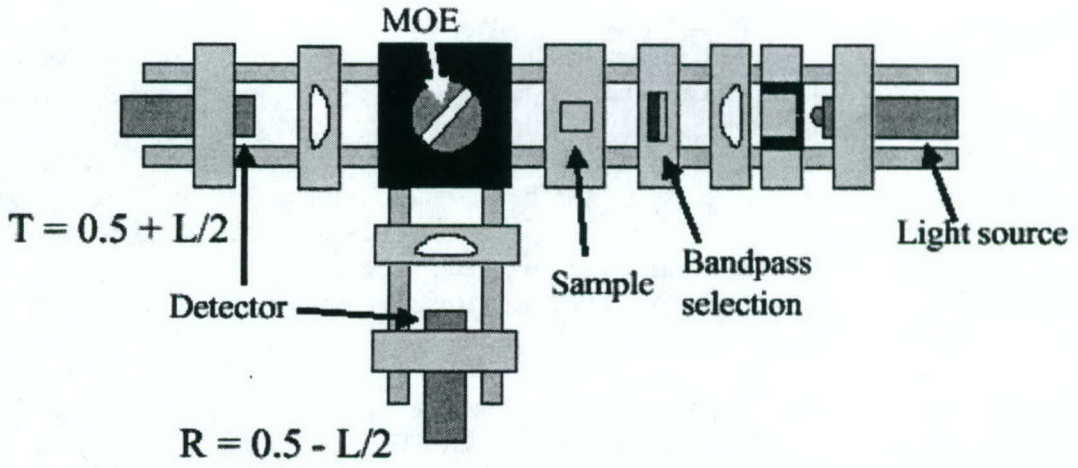

Figure 11. Schematic diagram of a simple single-element system for the prediction of chemical properties based on the transmission spectroscopy of samples in cuvettes. In this design, MOE is the multivariate optical element, the bandpass selection filters are simple colored glass filters that roughly limit the spectral window, the detectors are matched, T and R stand for transmittance and reflectance on the scale of zero to one, and L is the scaled regression vector of the MOE.

The optical computation of chemometric predictions is inherently radiometric in nature. Absorbance is non-linearly related to the intensity of light passing through a sample and is difficult to represent exactly. Sample transmittance is directly related to radiometric quantities in our measurement scheme. Unfortunately, while Beer's law relates absorbance linearly to concentration, sample transmittance is not as simply related. Therefore, the number of principal components required to describe a radiometric data set is greater than the number of independent species.

Figure 12 shows the NIR absorption spectra for two organic chemicals, dimethylmethylphosphonate (DMMP) and ethyl acetate (EA), and carbon tetrachloride solution in the region between 1,000 and 2,500 nm. Figure 13 shows transmission spectra for a series of 40 mixtures of these compounds, mixtures in which the concentrations of the two compounds are varied independently of one another based upon a random number generation. DMMP was arbitrarily selected as the analyte, while EA was treated as a random interferent. These 40 mixtures provide a starting point for development of a suitable regression vector for DMMP that could be incorporated into a single-element multivariate optical element (MOE).

Model Compounds/DMMP, Ethyl Acetate in CCl_4

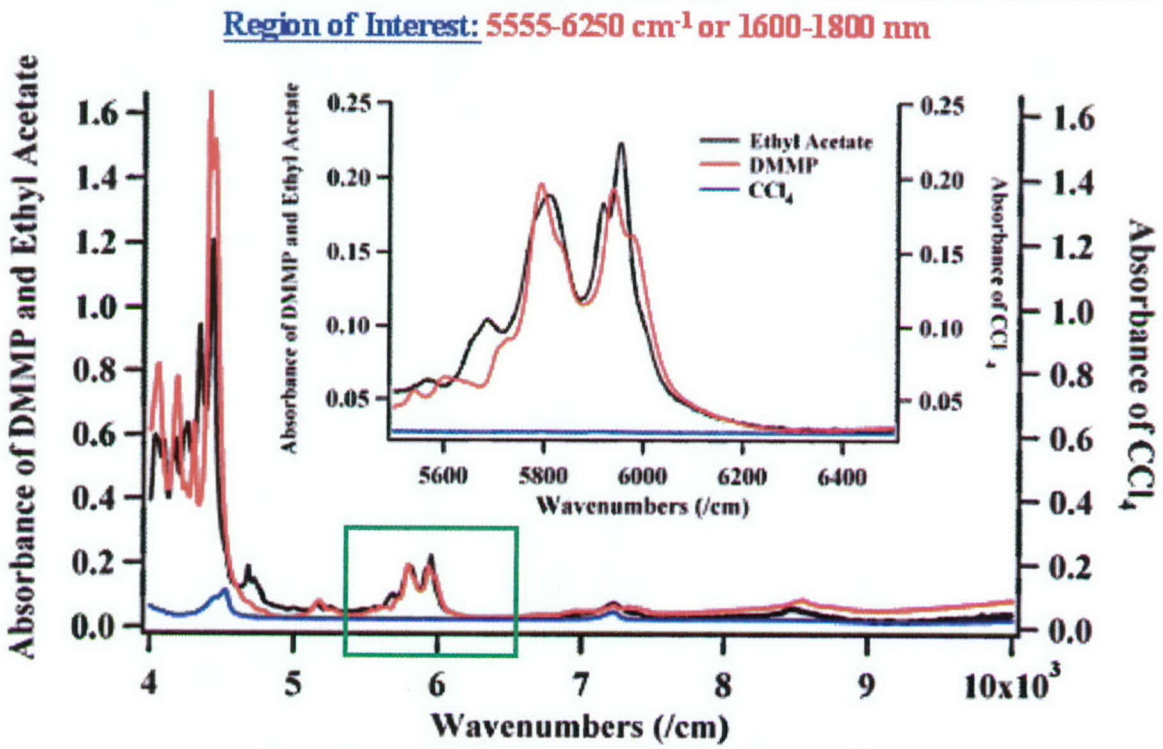

Figure 12. Absorption spectra for solutions of two chemicals, DMMP and EA,used in this report. Carbon Tetrachloride is superimposed on both spectra to show no interference in the C-H region (~5,250-6,250 cm^{-1}).

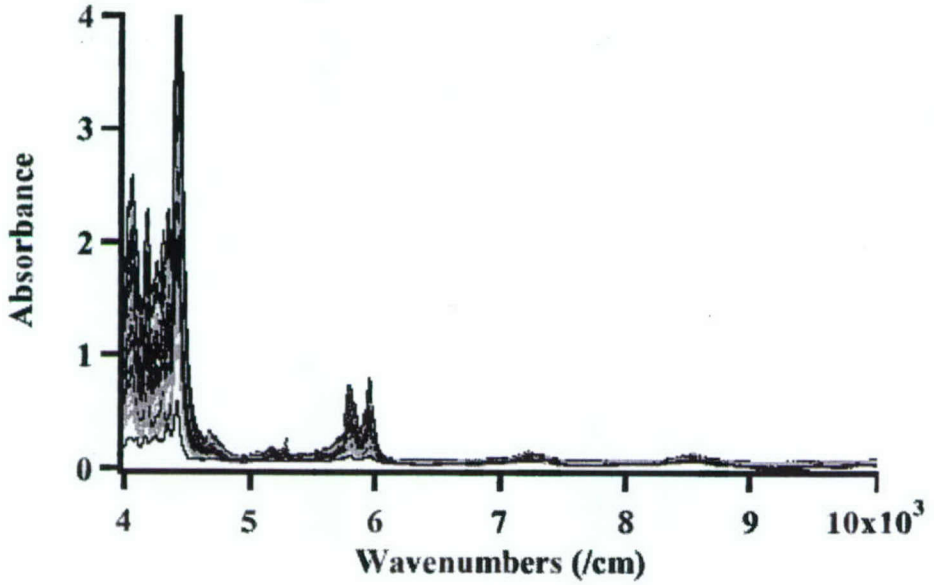

Figure 13. Transmission spectra for 40 mixtures of DMMP and EA using random concentrations of both compounds. The maximum concentration of each was limited so that absorbances of the two compounds individually would not be more than 0.4 in the C-H region (~5,250-6,250 cm^{-1}).

Before calculation of a regression vector, the transmission spectra were converted into system units by measuring the spectral radiance of the light source to be used for illumination of the sample, the transmittance of an idealized spectral bandpass filter set, and the spectral sensitivity of the detector selected for the measurement. The product of these factors with the sample transmittance spectra gives the system-corrected spectra shown in Figure 14.

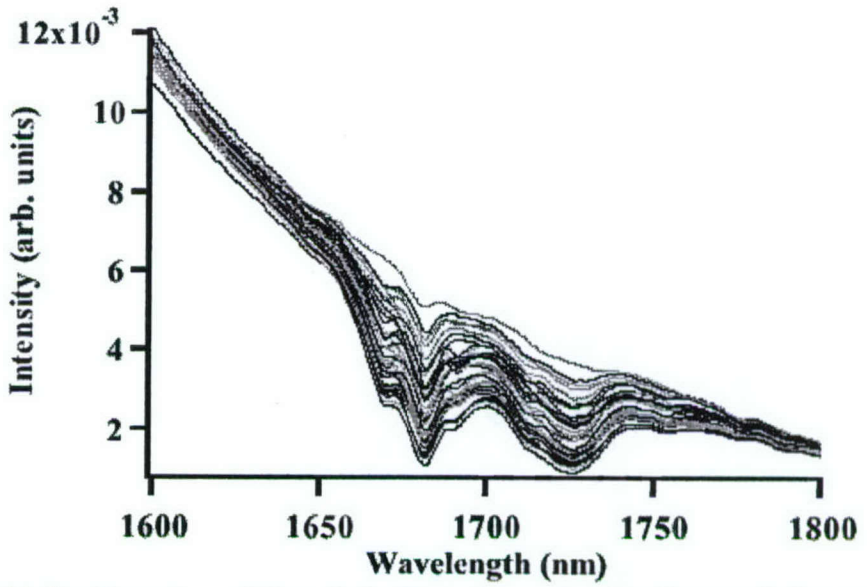

Figure 14. Sample spectra used for analysis. These data are based on the transmission spectra in Figure 13, plus the spectral radiance of the tungsten light source, the spectral sensitivity of the germanium detectors, and the transmission spectra described in the experimental section.

The results of a 4-factor principal components regression of the data in Figure 14 are shown in Figure 15. In this figure, triangles represent validation samples, while black dots represent calibration samples. The standard error of prediction (SEP) for this calibration is 0.0310 μM. The regression vector that produces this calibration is shown in Figure 16, normalized to unit length. This vector could be used to design a MOE by appropriate scaling. The scaling of the vector into the MOE is somewhat arbitrary, limited only by a need to end with realistic transmittance values.

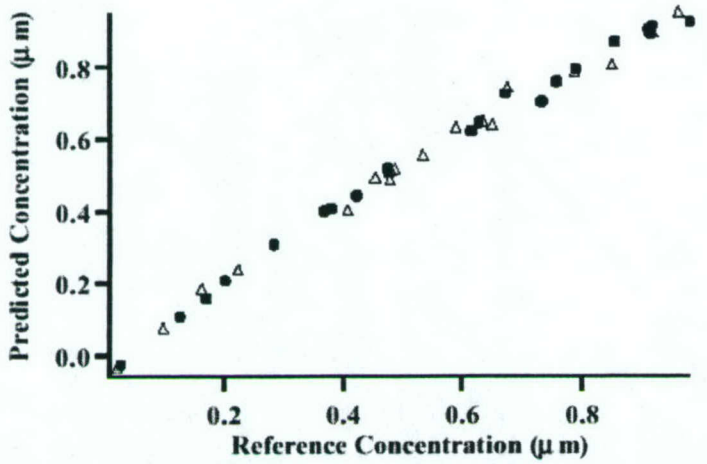

Figure 15. Calibration based on Figure 14 data. Filled Circles: Calibration set. Open Triangles: Validation set. SEP = 0.0310 μM for the validation set.

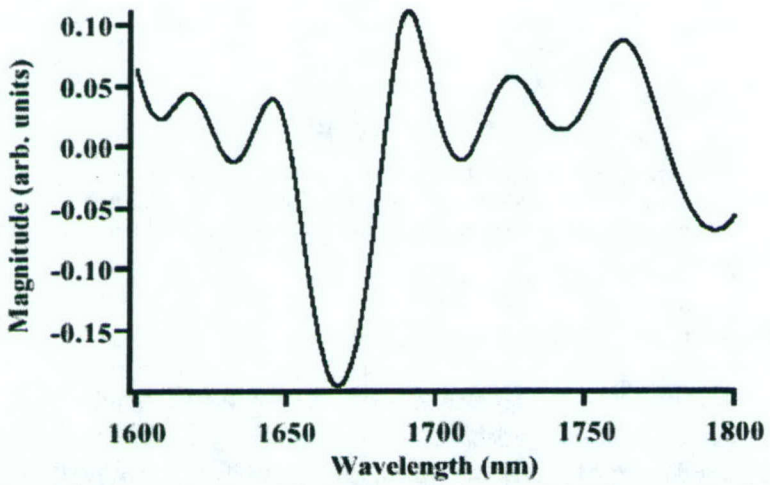

Figure 16. Regression vector for the calibration shown in Figure 15. The vector has been scaled to unit length.

In a second and more promising approach, random number generation produces a random multilayer structure that is then used as a starting point for an in-house algorithm that iterates this structure to find a result that can be characterized as "the best solution at this level of complexity". The in-house algorithm uses the original data (Figure 14) to optimize the structure of the MOE coating in a way that minimizes the SEP. Figure 17 shows the "vector relaxed" result, although the "relaxed" result is very different from the target based on the regression analysis that is given in Figure 15, the SEP produced by this vector is similar, 0.0643 μM. This relaxed design has the benefit of creating a thinner filter in comparison to the direct design, having a total thickness near 2.5 micrometers vs. 26 micrometers for the direct design, and requiring significantly less computation time.

At the time of this final report, the MOE for measuring DMMP in thepresence of EA has not yet been fabricated. This represents work still in progress.

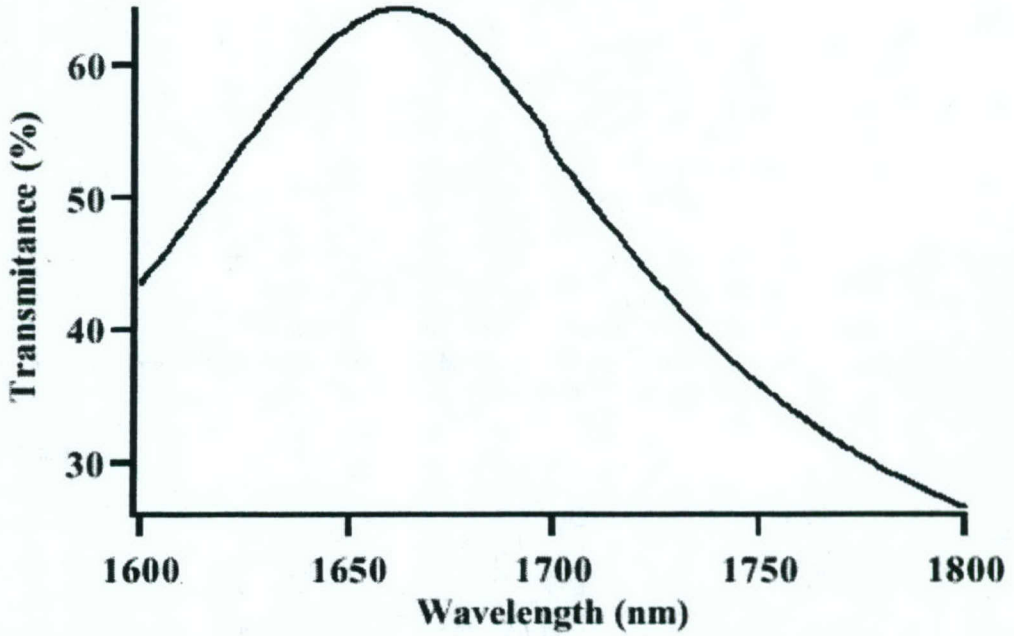

Figure 17. MOE transmission spectrum at 45 degrees angle-of-incidence based on vector relaxation from a partial direct solution as described in the text. This solution can be construed as the best solution at this level of complexity in the MOE. This design should give an SEP of 0.0643 μM.

3.7 DEVELOPMENT OF TOOLS TO FABRICATE OPTICAL ELEMENTS MORE PRECISELY

Deposition-correction algorithms. All new algorithms for design require two formats. The first is a pure MATLAB code written for design. The second is a LabVIEW-linked MATLAB code that performs online redesign of the MOE during production. Each time that we describe a new development in our algorithms, it must be mirrored in the LabVIEW-linked codes that are used to fabricate coatings. At the moment, our system works to "correct" the thicknesses are all remaining layers for errors in the fabrication of preceding layers. If a modified MATLAB code were not mirrored in LabVIEW, these redesigns would be to a different set of criteria than desired – an imaging MOE could be redesigned as a single-angle MOE, for instance, during fabrication.

Inclusion of substrate absorbance in algorithms. As our work moves first into the NIR and then into the MIR, our original assumption of non-absorbing substrates becomes invalid. The effect of this is to change the way that the Fresnel reflectivity calculation is done (now it must be a complex calculation instead of a real calculation) at both interfaces, and multiple reflections must be accounted for by a modified infinite series. No longer do reflectance and absorbance sum to unity, which was an assumption of our earlier work.

Explicit calculation of reflectance in algorithms. Thin films and substrates both exhibit absorbance in the NIR and MIR regions. Since reflectance and transmittance no longer sum to unity, they must each be explicitly calculated. The computation is complex both in the numerical sense and in the coding sense, since absorbance and non-normal incidence each cause calculations to be more difficult and time-consuming. Fortunately, a major text by MacLeod of Arizona State University provides details on the theory behind these calculations.

3.8 EVALUATION OF A NEW ALGORITHM FOR DESIGN OF IMAGING ELEMENTS

Figure 18 below shows an experimental design for a mixture of two organic dyes that absorb in the visible region. We selected these dyes because we were familiar with them from our earlier point-measurement demonstration.

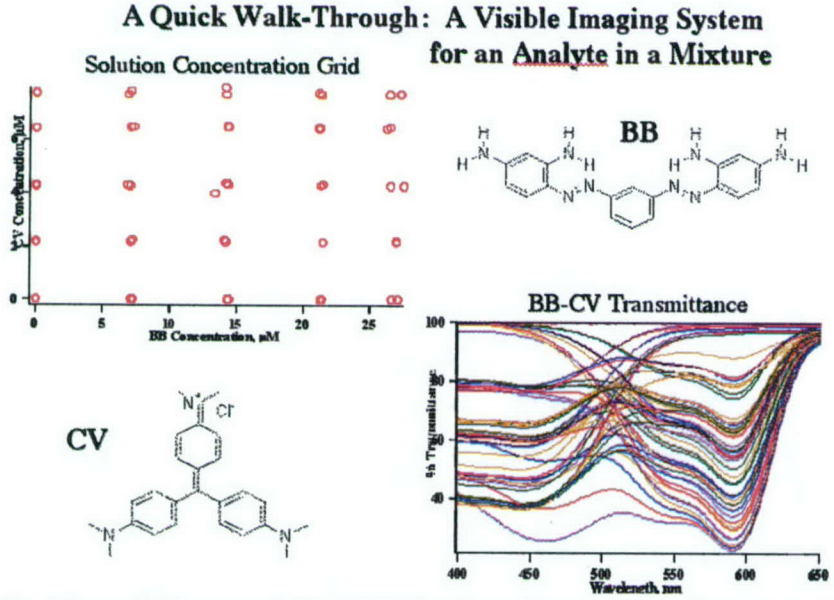

Figure 18. Bismarck Brown and Crystal Violet dyes, the experimental concentration grid measured, and the experimental transmission spectra of a set of samples on which an imaging MOE was based.

Figure 19 shows the result of convolving the spectra of the dyes with the system response measured for a specific experimental apparatus (shown below). These spectra were input to the IMOE design algorithm, and a response shown in the Figure 19 was obtained for a theoretical 14-layer filter, averaged over all angles within the cone of acceptance of the optical system.

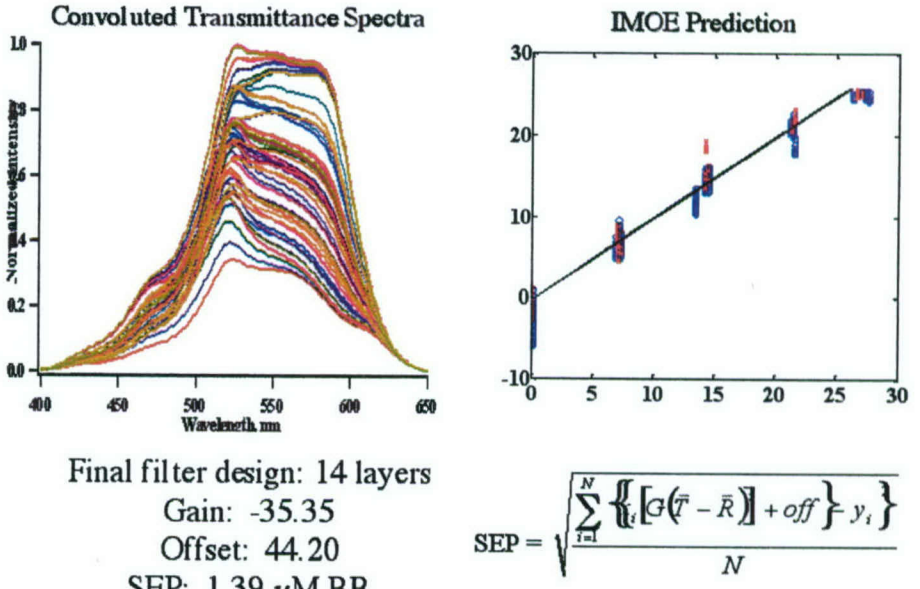

Figure 19. Convolved BB/CV spectra with theoretical predictability for an imaging IMOE system.

Figure 20 shows the spectral profile and regression vector expected for the IMOE theoretically to give the results shown in Figure 19. The standard error in prediction is shown in the Figure 20 as a function of the designed angle. The asymmetric nature of the result is not unexpected because of the way the spectral vector varies as the angle of incidence changes.

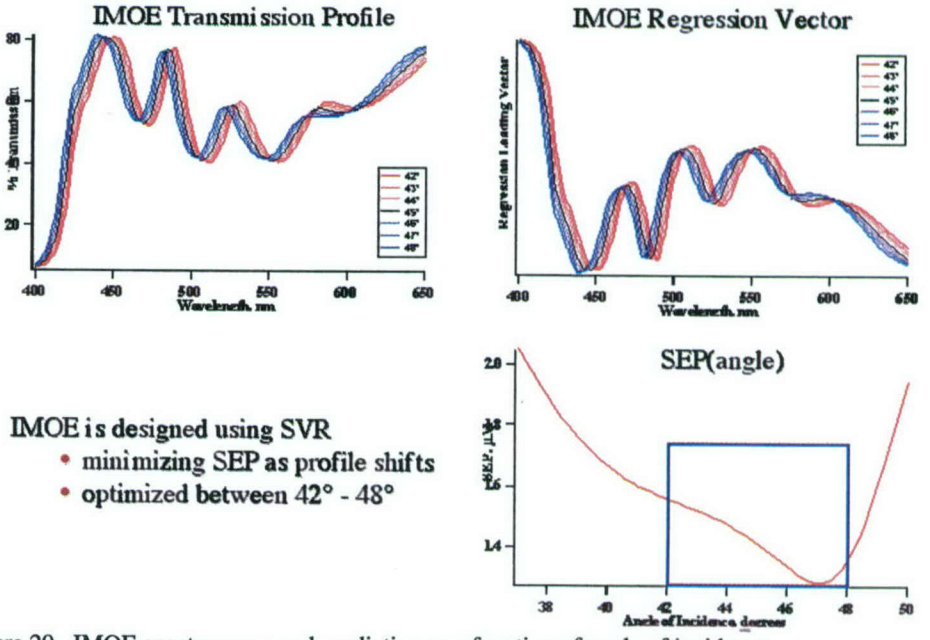

Figure 20. IMOE spectroscopy and prediction as a function of angle of incidence.

Figure 21 shows the experimental result for the IMOE spectrum. This IMOE was constructed with monitoring at normal incidence. This experiment taught us that a theoretical result requires measurement at the same angle of incidence that will be used in the experimental application of the IMOE.

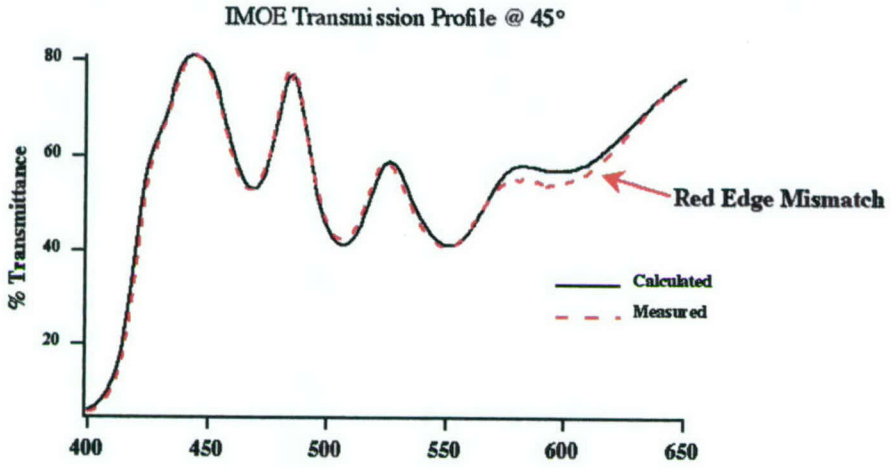

Figure 21. Experimental vs. theoretical IMOE spectra.

The optical system used for the tests is shown in Figure 22. A single camera was used with a fixed mounting, and a swiveling sample arm was tested. Two sequential images were acquired and evaluated off-line.

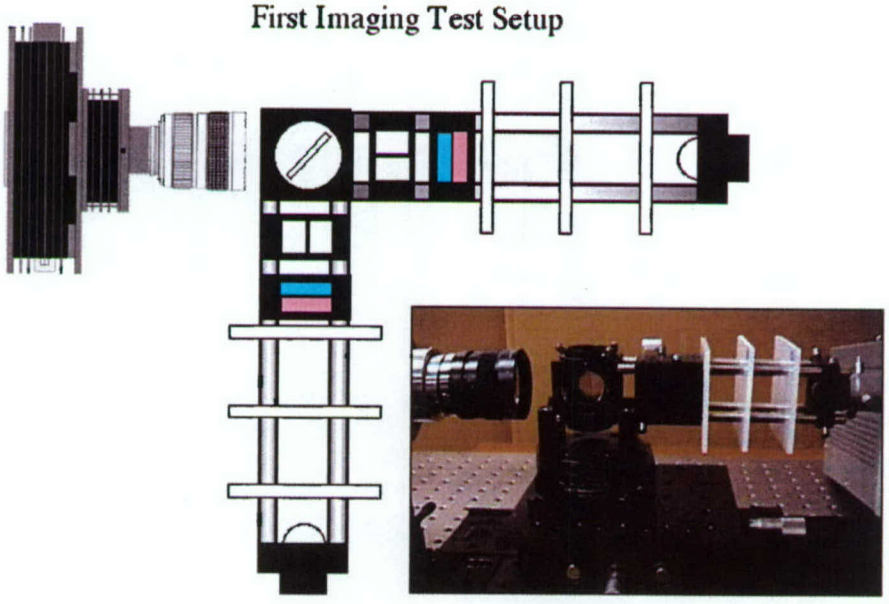

Figure 22. Outline and photograph of a swiveling optical mount for testing the IMOE performance.

The performance was measured with a standard and sample sandwiched together in the sample compartment. Two images were acquired, one in transmitted light, one in reflected light. Figure

23 shows an example set of images, with the differences in the image shown as T-R in the same figure. The T-R figure is color coded to indicate positive or negative differences.

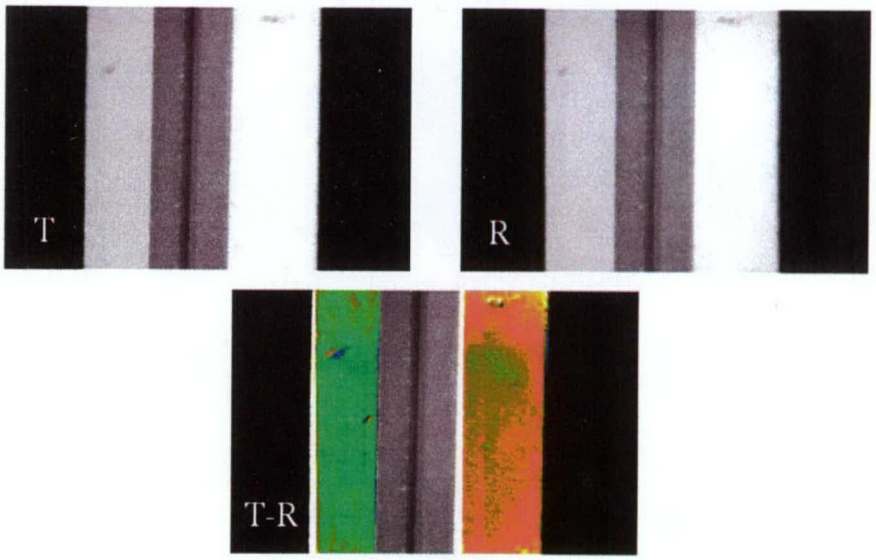

Figure 23. T, R and T-R images from the Figure 12 setup.

Figure 24 shows a series of images with increasing analyte concentration and random interferent concentration. We found in these studies that IMOEs do function, but that a simple T-R design does not adequately take uneven illumination of the scene into consideration. In other words, a different approach to quantitatively interpreting IMOE results was needed. This has now lead us toward a concept we call the "panoptical" sensor, because this permits us to evaluate many different types of samples simultaneously using a single IMOE.

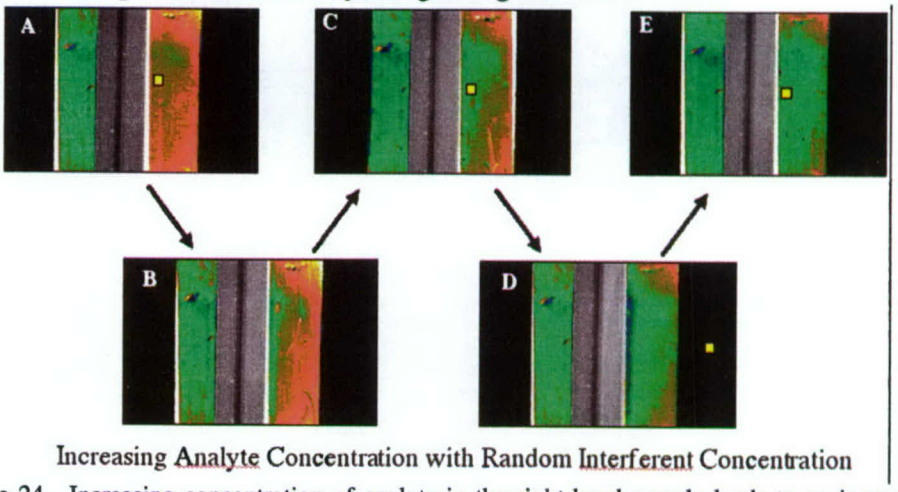

Figure 24. Increasing concentration of analyte in the right-hand sample leads to an increasing result from the IMOE, even when an overlapping interferent is present in a random concentration.

3.9 DEVELOPMENT OF A SYSTEM TO PERMIT MEASUREMENT OF ORGANIC COMPOUNDS IN THE NEAR-INFRARED

Calculations have been made which show the practicality of fabricating a MOE filter which will demonstrate for the first time that the optical computing technique will be useful for analyzing mixtures at near infrared (NIR) wavelengths. This technique was first demonstrated by this laboratory for two dyes absorbing in visible wavelengths and was published as the cover article in Analytical Chemistry in March, 2001. A host of factors influence the achievability of useful NIR MOEs. Among these are knowledge of the optical constants of materials, ability to monitor deposition processes in the NIR, and – perhaps most critically – the availability of good spectral limiting filters. The NIR absorbance of organic compounds is by no means spread evenly through the NIR region, but is concentrated in specific portions of the electromagnetic spectrum. The C-H overtone region near 5500 cm-1 energy is one region of particular significance – it is at a low enough energy to be relatively intense, yet at a high enough energy to be detected with relatively high-quality germanium detectors. The main difficulty we have faced in using this region for NIR measurements is that spectral limiting is necessary. Germanium detectors (and all other detectors for this region) are not limited to detecting the narrow region containing the C-H overtone. Instead, they detect wide swaths of the electromagnetic spectrum outside the region of interest. As was done in the visible tests, a set of bandpass filters was necessary to restrict the measurement. Interference filters are not suitable for this task, since there is too much variability in them. Colored glass filters, unfortunately, are not available with much selectivity in the NIR region. The best colored glass combination we could identify only restricted the wavelengths detected to the 1000-1800 nm region – still a very large spectral window when we only need about 50-100 nm of that region.

We believe we have solved this very serious problem with a new type of optical longpass filter based on the solid-state absorbance of the element germanium. The detectors we use are limited to about 1800 nm because that's where the absorbance of germanium becomes too low to be useful for a detector. However, the absorbance of germanium is actually quite low at 1800 nm, so that a thin film of the material should have nearly total transmission there. The attenuation becomes very great near 1600 nm, so that a germanium film should allow us to restrict the design of MOEs for the NIR to only a 100-200 nm wide region. Since pure germanium is a very controllable material, we should be capable of making very reproducible films of the material ourselves. This is a major development that will allow us to isolate a smaller spectral window with important chemical group absorbances in it. The consequence of using a smaller total band is that the design of MOEs can be dramatically simplified.

Example: Band selection for NIR measurement of organophosphorus compounds

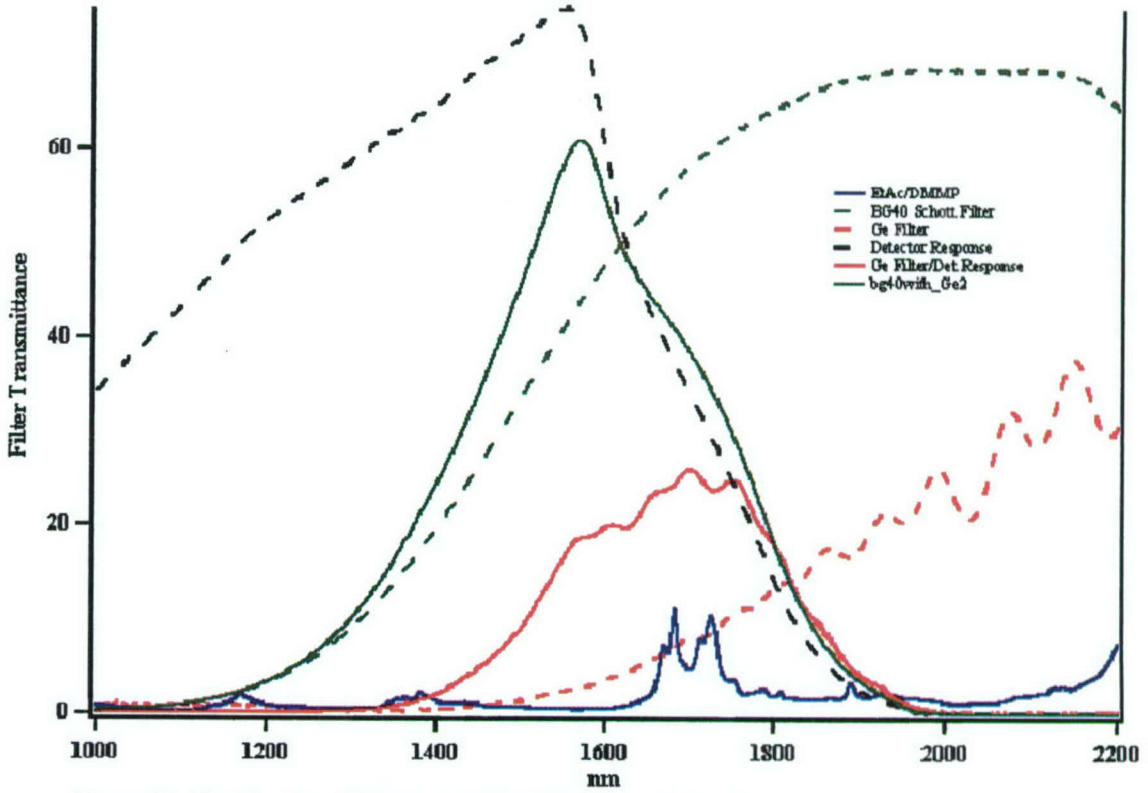

Figure 25. Combination of detector cutoff and film transmission characteristics of a germanium thin film provides a spectral window centered on the C-H region of organic compounds.

Our initial work with germanium filters has shown that, with little effort, we can produce filters that perform better than those that are commercially available. We are still in the process of perfecting our methods. We believe we have solved this very serious problem with a new type of optical longpass filter based on the solid-state absorbance of the element germanium, as well as with filtering media based on chemicals such as D_2O and H_2O that can be used to isolate specific regions of the electromagnetic spectrum. These tools are being applied in a variety of design processes for NIR multivariate optical computing elements today.

3.10 INVESTIGATION OF THE SPECTROSCOPY OF BACTERIAL SPORES AND OF ENVELOPE PAPER AND OTHER POSTAL MATERIALS

Prior to entering into the presently concluding contract we had not contemplated applying the methods of this laboratory (MOE etc.) to problems of identification of biological particles. With the collaboration and guidance of this contract work by Dr. Bronk of AFRL at U.S. Army ECBC, we realize the importance of this research to defense against biological attack. The lab required some updating for collaboration in determining IR properties of microorganisms. We approached this by procuring an inverted biological microscope, and an IR (reflecting optics)

microscope. Students were trained in the use of these new instruments. Arrangements were made to obtain prepared microorganisms of various important species. IR spectra were obtained of various spore types, and measurements of the spores dispersed onto paper were performed.

Figure 26 below shows an example of the reflectance spectra of *B. Globigii* vs. standard envelope paper.

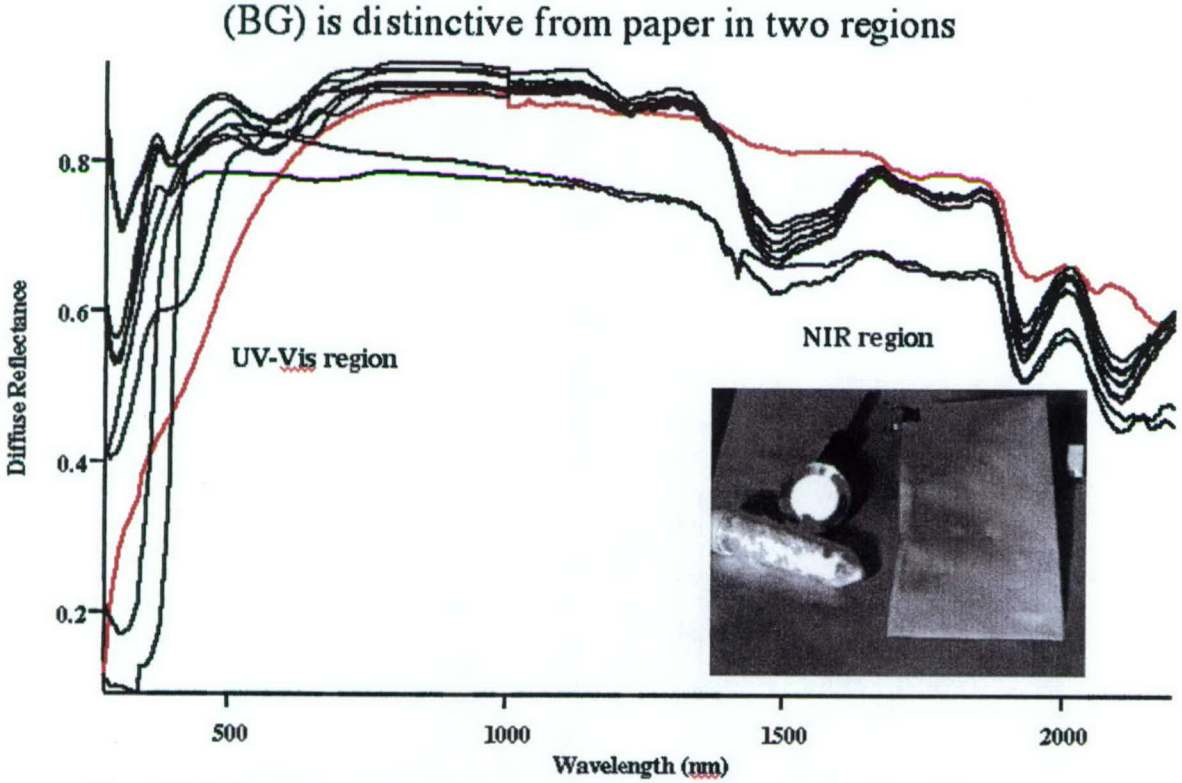

Figure 26. Reflectance spectra of bacterial spores of B. Globigii and a series of standard papers. The inset photograph shows a NIR reflectance image of BG samples and a standard white paper envelope in the 1500 nm region. As expected from the spectroscopy in this figure, smudges of BG are observed on the paper as increased reflectance in this region compared to the paper.

Based on the results of our studies, it was apparent that standard paper had greater reflectance than spores in the UV-blue region, but a lower reflectance in the 1500 nm region. The differences in the MIR region were also quite pronounced.

3.11 DEVELOPMENT OF A PROTOTYPE SYSTEM FOR BACTERIAL SPORES ON PAPER

Based on our results above, an IMOE was designed for spores based on the UV-blue region because we had in our possession several small blue-sensitive CCD cameras. Figure 27 shows the layout of the system, using a twin periscope design to produce two images together on the same camera simultaneously, rather than two separate images that had to be collected sequentially as done earlier with the first prototype for imaging analysis.

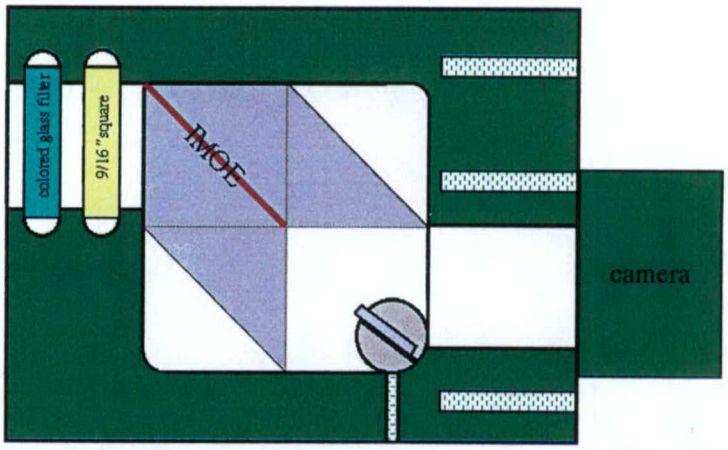

Figure 27. A twin periscope optical system with a small mirror was used to project two images onto the same camera elements simultaneously.

The final appearance of the "spore camera" is shown in Figure 28 below.

Figure 28. The "spore camera" based on the design of Figure 17 is shown with LEDs for light sources and a handheld computer attached for data display.

An example of the images acquired from the camera are shown in Figure 29.

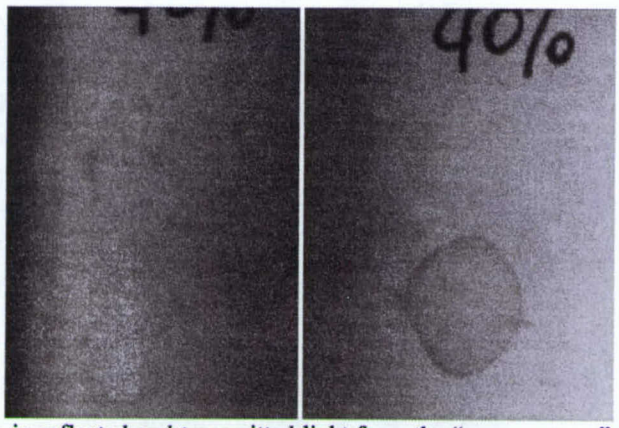

Figure 29. Images in reflected and transmitted light from the "spore camera" in Figure 28. The subject here is a standard envelope with a stain of BG spores. Both images are of the identically same area and were recorded simultaneously. These are from an individual frame of the camera. The difference in the two images is a marker of where spores are present.

3.12 INITIAL INVESTIGATION OF THE SPECTROSCOPY OF BACTERIAL SPORES FOR THE PURPOSE OF DISTINGUISHING SPORE TYPES FROM ONE ANOTHER

The laboratory began developing some expertise at recording infrared spectral of bacterial spores of different types with the intention of pursuing a project to determine whether spores are differentiable based on their infrared spectroscopy. By the end of Y2, a student had begun work on this project and was recording initial data. An example of an infrared microspectroscopic measurement of *B. Subtilis* spores is shown below as Figure 30, with a comparison to standard envelope paper.

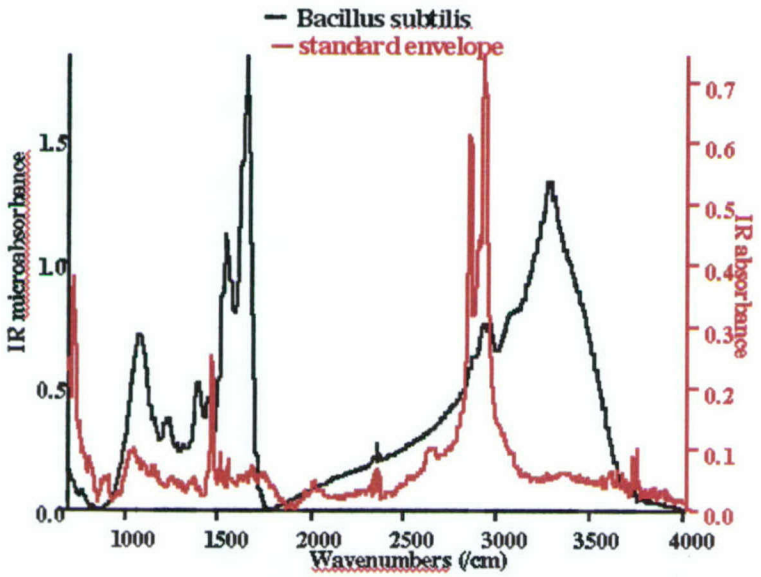

Figure 30. IR microspectrograph of *B. Subtilis* spores compared to standard paper.

3.13 PARTICLE LIGHT SCATTERING MEASUREMENTS

It is expected that any deliberate exposure of our armed forces to a biological pathogen would most likely come in the form of an airborne microorganism. The size, shape and optical characteristics of such an aerosol obtained by light scattering measurements would give some classification information which could automatically be correlated with spectral information obtained with MOE's. It was therefore decided to investigate methods for obtaining angular distributions of Mueller matrix elements rapidly and at multiple wavelengths from a stream of single aerosol sized particles. This section explains some new methods successfully explored in the pursuit of these aims.

As it is well known from the literature measuring a Muller matrix element requires, in general, measurements with two differently conditioned input light beams. However, our final goal was to measure single particle scattering in which case the particle flies through the measuring device in a relatively short time. This means that either we had to find a new single step method or we had to be able to change the input light polarization very fast. The latter case had several disadvantages: (a) it required expensive/nonavailable fast cameras, fast data processing; (b) it does not scale well for faster particles; (c) however fast our detection is, the particle can change its orientation uncontrollably between two measurements so the two measurements won't refer to the same particle orientation; etc.

We had several ideas for the single step method. One was to divide the spectrum of the input white light into a series of bands with specially designed filters, condition them comb-like to two different, appropriately polarized states, and use this specially spectrally polarized light as input beam. The detector has an inline imaging spectrograph so the resulting data set will contain enough data to calculate the S34/S11 matrix element. It turned out, however, that the necessary filters are rather hard to make and the whole optical path, being too long, would waste a lot from the light intensity.

The other method is based on the fact that practically all the Muller matrix measurements require a retarder in the input light path. Retarders are usually considered better if they are broadband, so their retardance changes slowly with the wavelength. In our case the situation is just the opposite. We used a retarder which had several full retardance cycles over the spectral range we detected. Orienting its fast axis at 45 degree to a polarizer we obtain a nearly periodically changing polarization with as many periods as we like (depending on the thickness of the retarder).

If we let a vertically polarized beam go through a retarder with fast axis at $\pi/4$ angle to the vertical then, at 0, $\pi/4$, $\pi/2$, $3\pi/4$, ...,$k\pi/4$, ... retardances, we get vertically, left circularly, horizontally, right circularly, etc. polarized light with elliptically polarized one in between. If we append a horizontal polarizer (analyzer) after the retarder then we can visualize these changes as it can be seen in Figure 31.

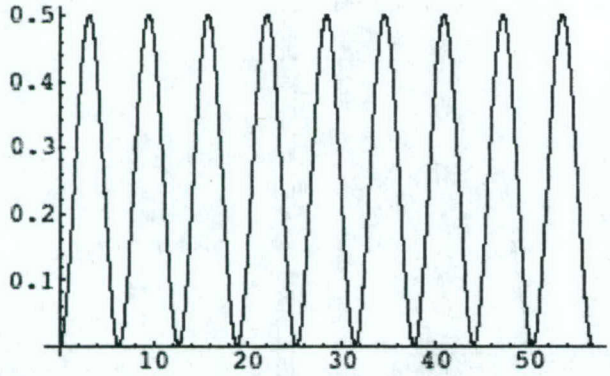

Figure 31. The dependence of the light intensity on the retardance if a beam goes through a vertical polarizer, a retarder with fast axis at 45 degree and a horizontal analyzer.

This means that putting the retarder between crossed polarizers and measuring the spectrum of white light before and after the analyzer we can determine the change of the retardance with the wavelength. How can we use this retardance "spectrum" to measure scattering Muller matrix elements in a single step? This is almost straightforward now. For example, if we use a vertical polarizer and a multiple order retarder with 45 degree fast axis and use a 45 degree polarizer before the detector channels then the detector will see the following scattered light intensity at retardance x:

$$S11 + S31 - (S12 + S32)*\cos(x) - (S14 + S34)*\sin(x)$$

or, if we have spherical particles or random suspension of homogeneous particles and so having S31, S32 and S14 equal to zero (7), then:

$$S11 - S12*\cos(x) - S34*\sin(x)$$

We use the result shown in Figure 31 to determine the dependence of the retardance of our retarder on the wavelength. If the difference between the ordinary and extraordinary index does not depend on the wavelength then the retardance can be simply calculated from the d thickness, the Δn index difference and the λ wavelength :

In real life, however, we have to allow a slight wavelength dependence for the index difference. Also, if we normalize the data in Figure 32a with the lamp spectrum in Figure 32b we still don't get the constant amplitude black line in Figure 32c; we have to normalize it empirically due to the imperfections of the analyzer. But performing all these normalizations we can get a very good fit of the experimental data and a sufficiently exact empirical $x(\lambda)$ function as it can be seen in Figure 32c..

We acquired a higher resolution SCION 1/2" ccd camera which made possible to use a broader spectral range and better signal to noise ratios. The multiple order retarder is a ThorLabs WPMQ05M-1310 model which can be used in the infrared measurements, too. We decided to build a separate infrared instrument. In the infrared, the polarizer sheets used in the visible don't work; we had to put separate high contrast IR polarizers in every detector channel (model NT47327 from Edmund Industrial Optics). The smallest available polarizers have 12mm

diameter so the collector lenses had to be replaced with similar sizes and the whole collector had to be redesigned from scratch.

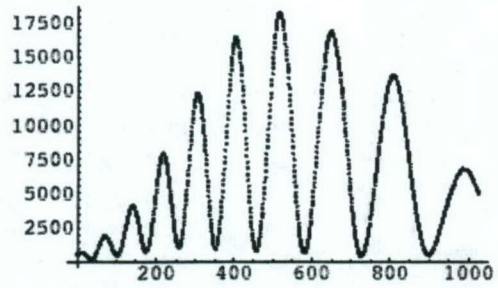

Figure 32a.
The spectrum of the input light with putting the retarder between crossed polarizers.

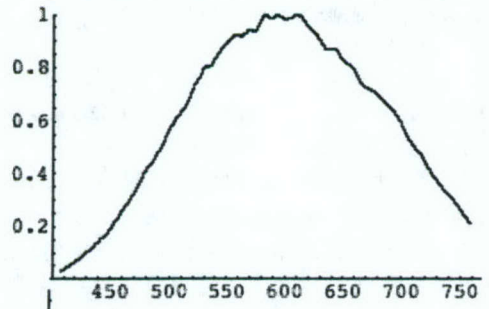

Figure 32b.
The spectrum of the input light after the polarizer and the retarder used to partially normalize the curve in Figure 2a.

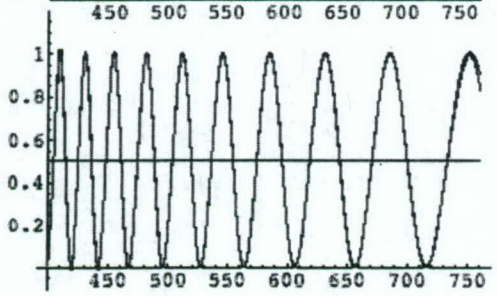

Figure 32c.
Fitting the normalized experimental data (black line) with the theoretical curve (red line).

$$x(\lambda)=2*d*\Delta n/\lambda$$

The infrared measurements required a sensitive infrared camera. We chose the SU640-1.7RT-D Indium Gallium Arsenide camera from Sensors Unlimited, Inc. which has 640x480 pixels and fairly sensitive up to 1.7 micron wavelength. The camera does not have an interface compatible with our system so I had to design and build an appropriate interface module for it. For the particle stream measurements we used an Inkjet Aerosol Generator from Edgewood Aerosol Science. It can generate up to 5000 particles per second and it has a heated column to evaporate the liquid from the generated particles. With using the present visible light source we needed long exposure times, therefore a low noise camera. We purchased a low noise cooled ccd camera from QImaging, model Retiga EXi.

We were looking for an intense infrared light source, in the Sensors Unlimited camera's wavelength range, which has smooth continuous spectrum and collimates well. A relatively new development looked very promising: the supercontinuum generating photonic crystal fiber. We purchased the SC-5.0-1040 model from Blaze Photonics and an appropriate mode locked MicroChip nano laser (model NP-10620-100) from JDS Uniphase.

Using the calibrated multiple order retarder we can measure scattering Muller matrix elements with a single shot of a camera now. In Figure 33 we show a typical frame to measure S34 for 300 nm polystyrene bead suspension. The first band is the retarder calibration which is described in details above. The next contains the lamp spectrum, the third has lines from a neon lamp which serves wavelength calibration purposes. The remaining 19 bands come from 19 fibers collecting scattered light in the scattering plane from 20 to 140 degrees. The input light is conditioned with a vertical polarizer and a multiple order retarder with 45 degree angle to the horizontal. A sheet polarizer with 45 degree polarization angle is placed before the light collecting fibers. (A photograph of the setup is shown in Figure 36 in the first year progress report.) In this case, along a band, the camera will detect the following intensities:

$$S11(\lambda) - S12*\cos(x(\lambda)) - S34*\sin(x(\lambda))$$

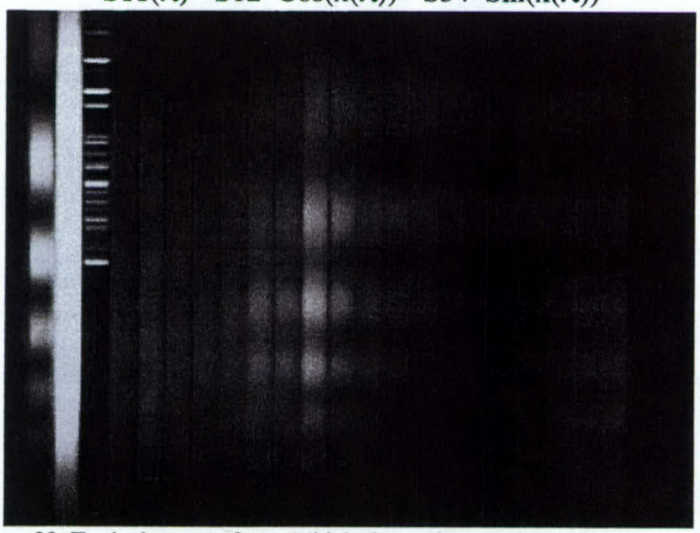

Figure 33. Typical camera frame which shows the retardance, lamp spectrum, and wavelength calibration bands together with the 19 angular channel spectra.

If we approximate the wavelength dependence of the Muller matrix elements with a "polynomial" (with degrees from -1 to +2) then we can easily determine the S34/ S11 or the S12/S11 normalized matrix elements. (S11 in this case is not the real S11 matrix element because we attenuated the low angle bands with neutral density filters to avoid the saturation of the camera.) To make our S11 smoother, so in the above approximation we don't need higher order polynomials or even different kind of probe functions, we normalized the bands with the measured lamp spectrum.

A typical fit is shown in Figure 34a and 34b. Figure 34a visualizes the quality of the fit while Figure 34b shows the "S11" component of the fit. These curves come from a 503 nm bead scattering measurement in the 53.33 degree channel.

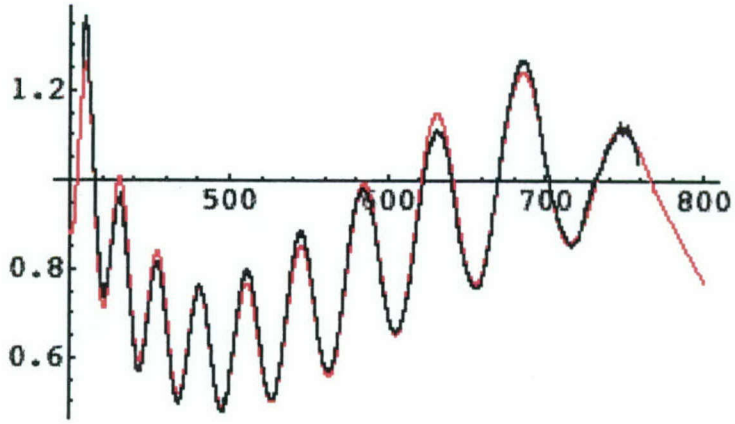

Figure 34a.
Typical fit (red) of the experimental data (black). The horizontal axis represents the wavelength in nm.

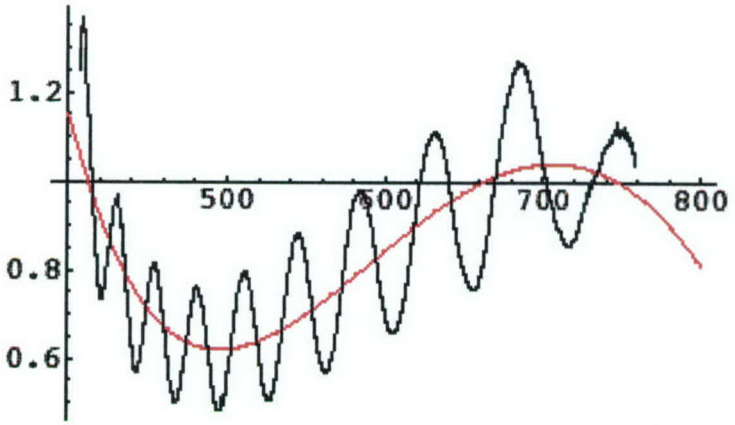

Figure 34b.
The "S11" component (red curve) of the fit shown in Figure 34a.

If we assemble the S34/S11 ratios from these fits into a two dimensional surface then we get what is shown in Figure 35a and 35b. Figure 35a shows the S34/S11 for 300 nm beads while Figure 35b is the same surface for 503nm beads. Figures 36a and 36b show samples of individual S34/S11 curves at 500nm wavelength for 300nm and 503nm beads, respectively. If we remove the 45 degree polarizer from before the collector fibers then the camera will detect the following matrix element combinations:

$$S11(\lambda) - S12*\mathrm{Cos}(x(\lambda)) - S14*\mathrm{Sin}(x(\lambda))$$

In this case we did not omit the theoretically zero matrix elements. The representative, very near to zero curve for S14/S11 in Figure 37 proves the consistency of the theory and practice of our new fast method of determining scattering Muller matrix elements.

With the new single step method we were ready to proceed toward our final goal: measure single particle polarized light scattering. As single particles scatter million times less light than a suspension of them, logically the next step was to measure scattering from an airborne particle stream. We put 1g/l NaCl solution into the cartridge of the Edgewood particle generator and carefully heated the column to evaporate the solvent from the generated droplets. The process required to balance several parameters: the carrier air flow had to be sufficiently low to increase

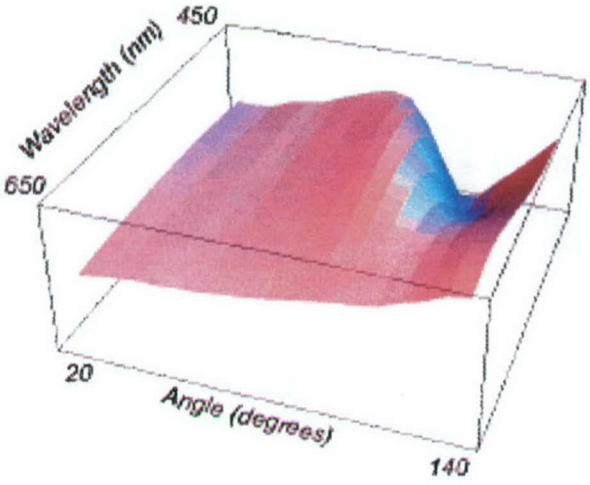

Figure 35a.
The S34/S11 matrix element surface for 300 nm polystyrene beads.

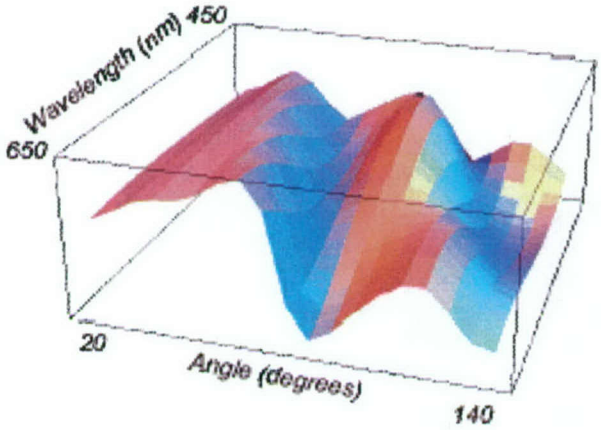

Figure 35b.
The S34/S11 matrix element surface for 503 nm polystyrene beads.

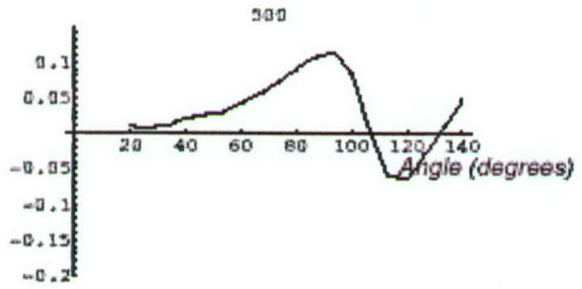

Figure 36a.
Scattering angle dependence of the S34/S11 matrix element for 300 nm beads at 500 nm wavelength.

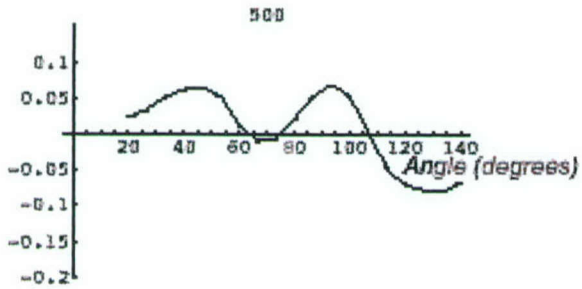

Figure 36b.
Scattering angle dependence of the S34/S11 matrix element for 503 nm beads at 500 nm wavelength.

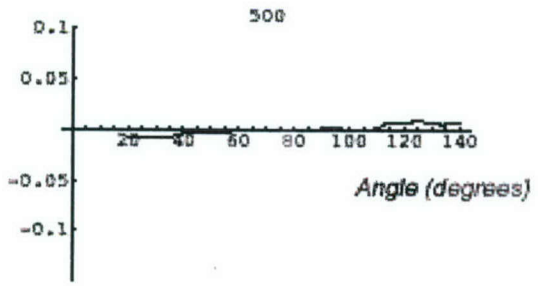

Figure 37. Consistency test. Theoretically zero S14/ S11 matrix element measurement. The result for 300 nm beads at 500 nm wavelength is shown.

the dwelling of the particles in the light beam but fast enough to have them flowing through the beam and not going upward with the warm carrier flow. In Figure 38 we show the camera frame of the scattering: the exposure time was 20 second, the nominal particle flow was ~5000/s. The evaluation for S12/ S11 (for simplicity we did not use the 45 deg output filter), however, did not show any expected S12/S11 pattern so we measured the size distribution of the particles collecting them on a microscope slide. In Figure 39 we show a typical picture of the particles.

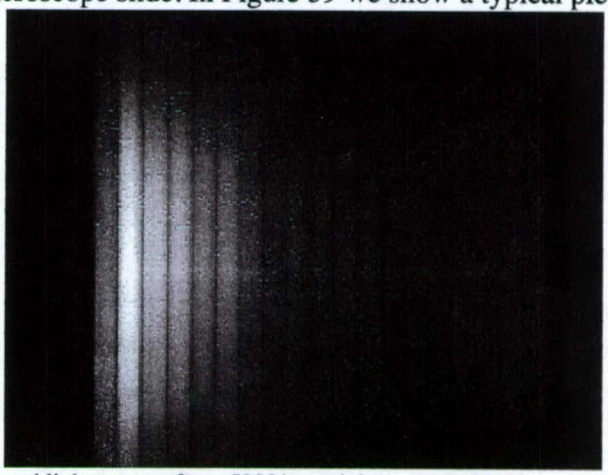

Figure 38. Scattered light spectra from 5000/s particle stream with 20 seconds exposure time.

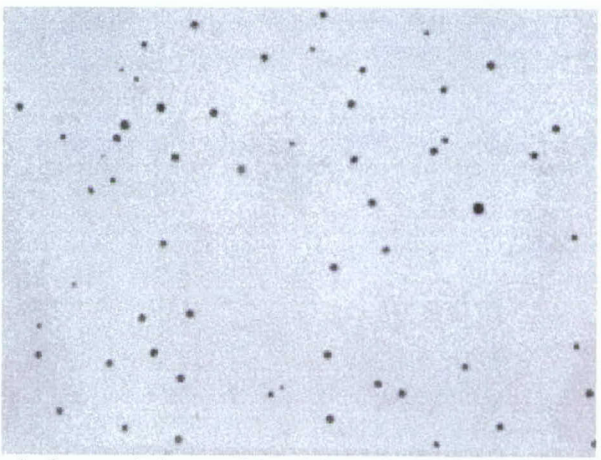

Figure 39. Typical microscopic image of the NaCl particles collected on a microscope slide.

Measuring the area of a few thousand spots and calibrating the magnification with a stage micrometer we could determine the size distribution of the particles. As it can be seen from Figure 40a, b and c there were two populations in the distribution with ~8 and 4 micrometer diameters. With visible light, in the scattering of this big particles we expect fast oscillations of S12 with the scattering angle which can not be resolved with the 6.33 degree detector spacing even for the 4 micron particles. Further size reduction did not seem practical taking that the 20 second exposure (with maximal gain) was close to the limit of the SCION camera, the particle generator could not generate more particles, and the intensity of the illuminator also was set to the maximum. As we already mentioned, we attacked the problem in several ways: switched to infrared up to 1.7 micron wavelength and applied an intensity scalable supercontinuum generating illuminator. Also, we acquired a low noise cooled camera to attempt long exposure, visible measurements on smaller particles. With these changes the successful measurement of polarized scattering from ~3 micrometer particles seems easily attainable. Because of serious administrative delays in the ordering of the necessary parts, however, the new measuring setup is only at near completion as of writing the present report.

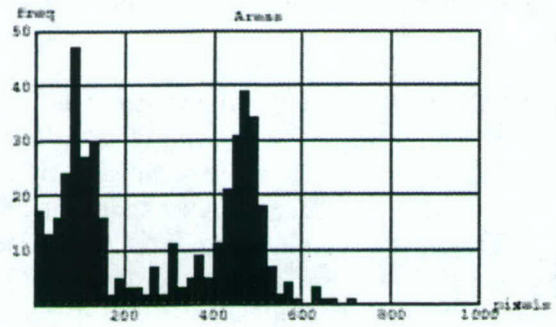

Figure 40a.
Particle area distribution in pixel units.

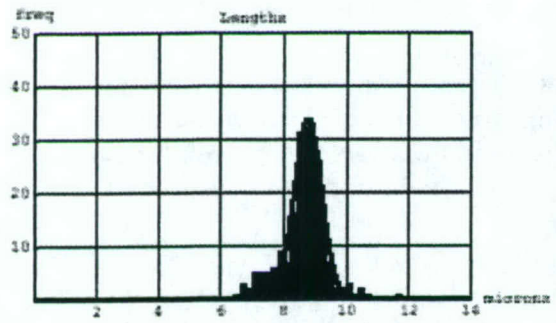

Figure 40b.
The distribution of the diameter of the bigger particle population with lognormal distribution fit. The average is 8.79 μ m.

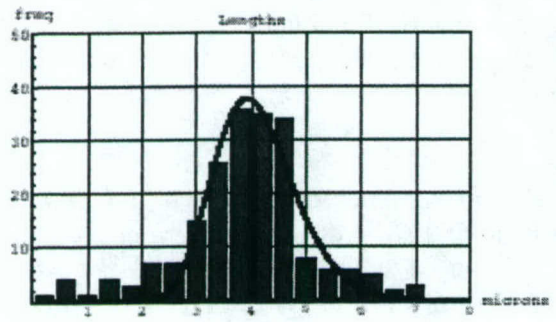

Figure 40c.
The distribution of the diameter of the smaller particle population with lognormal distribution fit. The average is 4.11 μ m.

3.14 Infrared Studies of Genetically-Modified Endospores

We performed a detailed study of the contribution of the mid-infrared absorbance of CaDPA salt to the IR spectrum of *B. subtilis* by FTIR reflectance microscopy. This analysis was made possible by the creation of genetically engineered organisms incapable of producing DPA or its salt.

The *B. subtilis* strains used in this work were PS832 (wild-type) and FB122 (*sleB spoVF*). These strains are isogenic except for the two mutations in strain FB122, and are prototrophic derivatives of strain 168. The *sleB* geneand *spoVF* operon in strain FB122 have been deleted and replaced with spectinomycin and tetracycline resistance genes, respectively. The *spoVF* operon encodes DPA synthetase and as a consequence *spoVF* strains cannot synthesize DPA during sporulation, and the DPA-less spores that are produced are very unstable and spontaneously germinate and lyse. The *sleB* gene encodes one of the two redundant enzymes that degrade the spore's peptidoglycan cortex upon spore germination. Since the other cortex lytic enzyme, CwlJ, requires CaDPA for its action, spores of strain FB122 lacking both DPA and SleB are stable and can be isolated in dormant form.

Spores of *B. subtilis* strains PS832 (wild-type) and FB122 (*sleB spoVF*) were prepared at 37°C on 2xSG medium agar plates without antibiotics. The spore preparations were cleaned with numerous suspensions in water followed by centrifugation, as well as several sonication treatments until the preparations were free (> 98%) of sporulating cells, germinated spores or cell debris as determined by phase contrast microscopy. These spore samples were lyophilized and stored dry. Analyses of DPA in these spore preparations showed that the spores of strain PS832 contained 83μg DPA/mg dry spores, similar to values obtained previously for wild-type *B. subtilis* spores, while the FB122 spores had ≤ 2_g (0.2%) DPA/mg dry weight.

Just before FTIR reflectance microspectroscopic analyses, the previously cleaned spores were again suspended in water, rinsed, sonicated, and centrifuged, after which the supernatant fluid was removed and discarded. This procedure was repeated twice to further clean the samples of any extraneous materials. The spores were finally suspended in water and oven-dried to a film on a gold-coated microscope slide.

CaDPA was prepared from $Ca(NO_3)_2$ and sodium dipicolinate. The resulting solution was cooled slowly to allow crystallization. The CaDPA crystals were collected by vacuum filtration and recrystallyzed with hot distilled water. Dilute solutions of dipicolinic acid (obtained from Acros organics) in methanol and aqueous CaDPA were prepared. One drop of each solution was placed on a gold microscope slide for reflectance microspectroscopy and oven-dried at 50°C (less than 30 min in all cases).

The averaged normalized and baseline corrected absorbance spectra of spores of *B. subtilis* strains PS832 (wild-type) and FB122 (*sleB spoVF*) from 650-4000 cm^{-1} are shown in Fig. 41A. The spectra of *B. subtilis* spores of strain PS832 represent typical mid-infrared endospore spectra. The most prominent vibrations in mid infrared spore spectra are due to the amide A at 3300 cm^{-1} (N-H stretching), amide I at 1650 cm^{-1} (carbonyl stretching), and the amide II at 1540 cm^{-1} (a combination of C-N stretching and N-H bending vibrations) protein bands. Other

assignments in these typical endospore spectra are lipid C-H stretching from 2850-2960 cm^{-1}, and the vibrations at 1443 cm^{-1} and 1388 cm^{-1}, assigned as pyridine ring vibrations and symmetric carboxylate stretching respectively.

The mid-infrared absorbance spectra for the *B. subtilis* FB122 (DPA-less) spores (Fig. 41, A and B) were observed to be similar to those obtained for autoclaved spores, in which DPA had been lost through the pressurized moist heat of the autoclaving process. Specifically, the absorbance spectra of strain FB122 noticeably lack absorption bands, shown in Fig. 41B for the expanded spectral region of 650–1800 cm^{-1}, at 1580 cm^{-1} , 1280 cm^{-1} , 768 cm^{-1}, 729 cm^{-1}, and 706 cm^{-1}, previously associated with DPA and its calcium chelate salt.

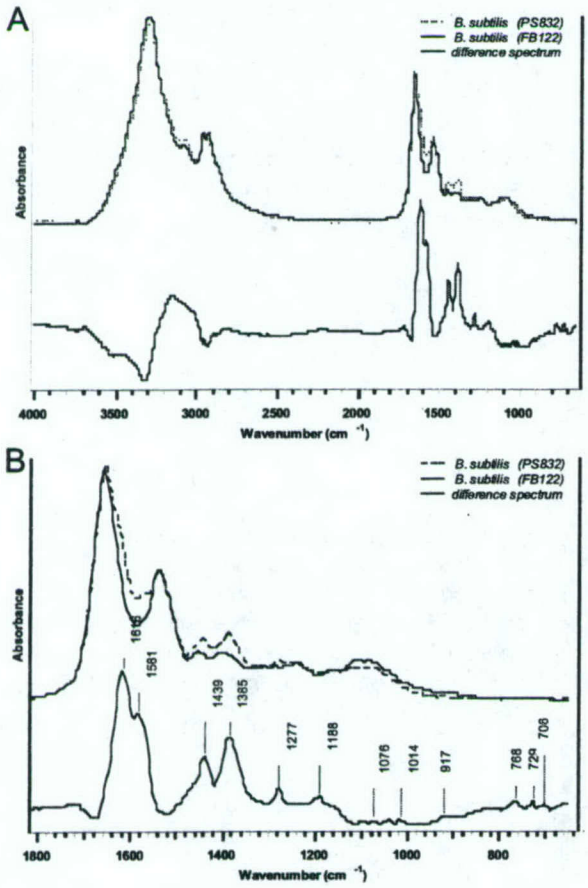

Figure 41.

(A) Absorbance spectra from 650-4000 cm^{-1} of spores of *B. subtilis* strains PS832 (wild-type) and *B. subtilis* FB122 (*sleB spoVF*). Spectra were averaged, baseline corrected and vector normalized. Offset below, the corresponding difference spectrum obtained by one-to-one subtraction of spectra of strain FB122 (*sleB spoVF*) from strain PS832 (wild-type). The difference spectrum is shown increased by a factor of 4.5.

(B) The same spectra are shown in the expanded region 650-1800 cm^{-1} with vibration bands labeled.

A difference spectrum (Fig. 41A) was calculated by the one-to-one subtraction of the normalized spectra of *B. subtilis* FB122 (DPA-less) spores from that of spores of strain PS832. It was noted that the positive peak values for the difference spectrum given in Fig. 1B closely match those reported for the difference between vegetative and sporulated bacteria and associated with DPA and it calcium chelate salt. In addition to the peaks missing in the FB122 absorbance spectra mentioned above, difference spectroscopy revealed missing asymmetric and symmetric carboxylate stretching absorptions at 1620 cm^{-1} and 1385 cm^{-1} respectively, a pyridine ring

stretch at 1439 cm^{-1}, as well as missing absorptions at 1188 cm^{-1}, 1072 cm^{-1}, 1014 cm^{-1}, 918 cm^{-1}, 829 cm^{-1} and 660 cm^{-1}.

Difference spectroscopy (Fig. 41A) revealed negative absorptions at 3310 cm^{-1} (N-H amide A stretching) and 2870-2960 cm^{-1} (C-H stretching). This information suggests FB122 (*sleB spoVF*) spores contain relatively more proteins and/or lipids than strain PS832 (wild type). Furthermore, negative absorptions at 3500 cm^{-1} (O-H stretching) and 1670 cm^{-1} (O-H bending) suggest DPA-less spores of strain FB122 have relatively more water content that those of PS832.

Spectra of CaDPA and DPA were obtained for comparison (Fig. 42, A and B).

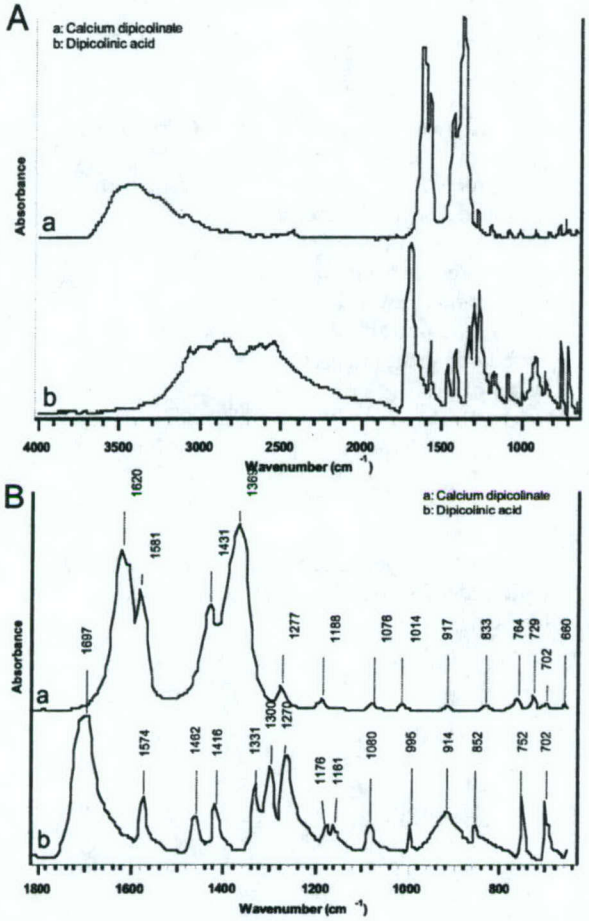

Figure 42.

(A) Mid-infrared absorbance spectra from 650-4000 cm^{-1} of calcium dipicolinate (a) and dipicolinic acid (b).

(B) The corresponding spectra of calcium dipicolinate (a) and dipicolinic acid (b) expanded from 650-1800 cm^{-1}, with vibrational bands labeled, illustrating that the difference spectrum shown in Fig. 1 closely resembles the spectrum of the CaDPA. The spectra were averaged and offset for clarity.

Shoulders in the dipicolinate spectra (Fig. 42B) at approximately 1605 cm^{-1} and 1388 cm^{-1} ($\Delta\nu$ = 217cm^{-1}) suggest unconverted sodium dipicolinate (Na_2DPA). The remaining spectral features show that the difference spectrum given in Fig. 41 is dominated by dipicolinate only. When DPA is deprotonated to form the carboxylate, the O-H stretching band, from 3400-2700 cm^{-1} (Fig. 42A) is replaced with an absorption band from 3100-3600 cm^{-1}, confirming CaDPA exists as a hydrate. Upon the formation of CaDPA, the characteristic carboxylic acid group vibration at 1695 cm^{-1} is replaced by the asymmetric and symmetric -COO^- vibrations, observed at 1620 cm^{-1} and 1369 cm^{-1} respectively in the CaDPA spectrum (Fig. 42B). These vibrations of crystalline

CaDPA differ only slightly from the difference spectrum in Fig. 41B due to environmental factors.

To determine the minimum amount of DPA that could be observed in a difference spectrum like the one in Fig. 41, and thus the minimum amount of DPA one would be able to detect in a sample of *B. subtilis* FB122 by FT-IR microspectroscopy, the following method was used. The DPA spectrum in Fig. 42B was normalized to the same absorbance intensity (0.0083) of CaDPA at 701 cm^{-1} (the out-of-plane C-H bend) as this vibration has the smallest frequency shift after the formation of the carboxylate and may thus exhibit the smallest change in oscillator strength on deprotonation. The root mean squared (RMS) noise in the difference spectrum in Fig. 41 was calculated to be 2.28×10^{-4}, equivalent to 1% of the normalized DPA carbonyl absorbance intensity at 1695 cm^{-1}. This absorbance is the strongest in DPA, therefore, in order to detect DPA with a signal to noise ratio (SNR) equal to 1, it must be present in excess of 1.0% w/w in FB122 spores.

3.15 Infrared Studies on Gold-Coated Filtering Substrates

Alumina membrane filters have a highly ordered structure compared to organic membranes, with a standardized porosity and chemical inertness. We built on previous work to develop a simple but superior method for preparing samples of bacterial endospores for study by FTIR microspectroscopy and scanning electron microscopy. Although the use of filters for bacteria studies has been previously reported, we introduce a unique method of bacterial microorganism detection and quantification by filtration of *Bacillus subtilis* (BS) spores on gold-coated porous alumina filters. This method concentrates the spores in a sample onto the filter surface while simultaneously providing a highly reflective substrate for FTIR microspectroscopy in a single step. Moreover, the technique provides even distribution of endospores on the surface, which improves the reproducibility of sampling. The porosity (200 nm) of the alumina filters ensures the total retention of all the bacterial spores (1-2 μm in length). In our work, we used a 100 nm thick coating of gold that that is thin enough to allow filtration and yet optically thick enough to act as an excellent gold mirror.

Endospores of *Bacillus subtilis* strain PS832, a prototrophic laboratory strain derived from strain 168, were prepared in 2xSG medium at 24 °C. Although strain PS832 is derived from strain 168 which is the most commonly used laboratory stain, DNA sequencing demonstrates negligible differences between the two strains. The PS832 endospore preparations were cleaned by repeated suspension in water followed by centrifugation until the preparations were free of sporulating cells, germinated spores or cell debris (>95%) as determined by phase contrast microscopy. These spores were then lyophilized and stored dry.

A stock spore suspension was prepared by mixing 21.2 mg of the spore preparation with 50 mL of deionized ultrafiltered water (DIUF) (Fisher Scientific, Fairlawn, NJ). The solution was prepared in an amber bottle and was stored at 5 °C. Before filtration the solution was sonicated for 15 min and then 0.15 mL solution was removed and mixed with 0.85 mL of DIUF water. This 1 mL solution was sonicated for 15 min, and then diluted to 50 mL with DIUF water and

then sonicated for 15 additional min in order to minimize spore aggregation. Following sonication, the spores were filtered through Au coated Anodiscs™ (Whatman, Fisher Scientific).

The Anodiscs™ used were 47 mm in diameter with a nominal 0.2 μm pore size. They were coated with a Au layer having a thickness of ~100 nm using a CrC-100 sputtering system (Plasma Sciences Inc., Lorton, VA). The filter membranes were transferred to a vacuum filtration system with a holder for 47 mm filters (Fisher Scientific). The filter membranes were fragile, and care was taken to ensure that the samples studied here were free of cracks after filtering. To the vacuum filtration system was added the bacterial spore suspension; the suspension was allowed to settle for approximately 30 seconds until the suspension ceased visibly moving. Vacuum filtration was then applied in order to achieve even distribution of individual spores throughout the surface of the Anodisc™. After filtration, the disks were transferred to an oven at 50 °C and dried for 15 minutes. Three filtration disks were prepared, using the same volume of the same stock suspension, following the above method in order to examine the disk-to-disk variability.

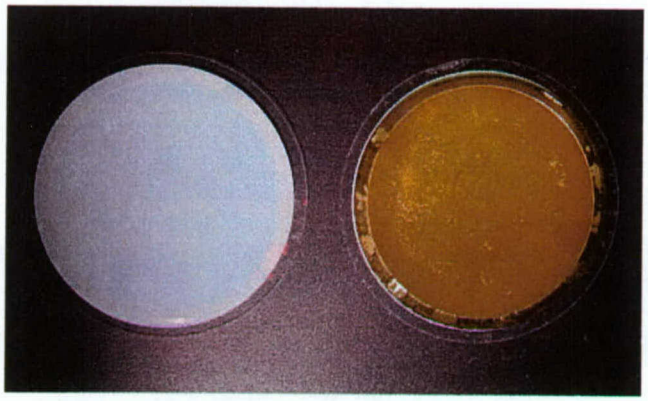

Figure 43. Photographs of Whatman Anodiscs™ before and after gold coating (~100 nm).

A common sampling procedure for bacterial microspectroscopy is to deposit a drop of a suspension of bacteria or spores onto a gold-coated glass slide and air-dry the sample before spectra collection. The distribution of spores achieved by this method is usually very uneven: Results from our laboratory[33] have shown an average relative standard deviation of 0.67 based on IR microspectroscopy using an aperture of 100 x 100 μm^2 on such samples. Spore aggregation and separation of components during drying result in large differences in spectral intensity and unreliable quantification of bacterial endospores.

When endospores are filtered through a fine gold-coated alumina filter such as the one shown in Figure 43, a more even distribution of endospores is observed via SEM, as seen in Figure 44.

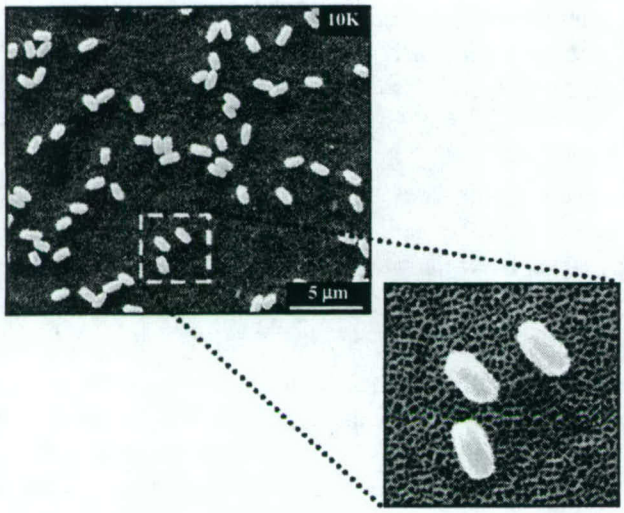

Figure 44. SEM images of Bacillus subtilis (BS) endospores dispersed on a Au-coated Anodisc™ membrane. Magnification was 10,000X

In this characteristic image, bacterial endospores are found primarily as individuals, unaggregated and settled on top of the relatively flat filter surface. The enlarged section of the SEM image shows the structure and size of pores on the gold-coated Anodisc™ . Additionally, the image confirms that the gold sputtered onto the Anodisc™ surface was not thick enough to block the pores of the membrane. As can be seen in Figure 44 the BS endospores were free of other particulates, such as debris from the growth medium, as a result of the extensive cleanup prior to arrival in our laboratory. A typical spectrum collected from a 100 x 100 μm^2 area with the FTIR microscope on the gold-coated Anodisc™ is shown in Figure 45, along with the same spectrum after baseline correction by the automated algorithm, and shows the characteristic bands observed in other infrared studies of bacterial endospores.

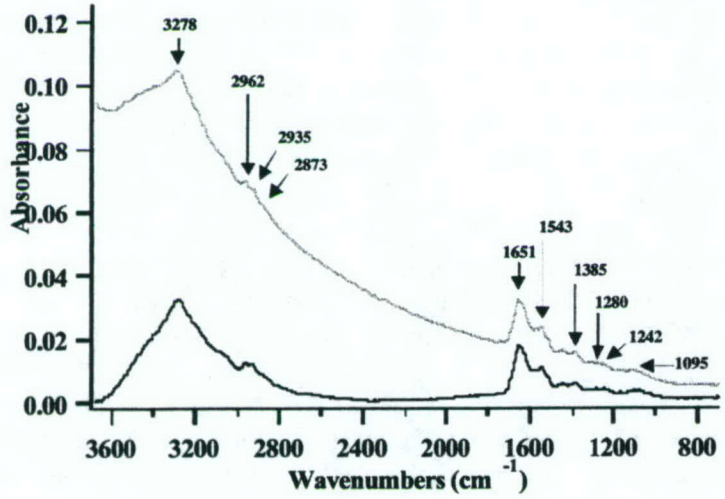

Figure 45. Spectrum collected in a 100 x 100 μm^2 area by the FTIR microscope from a Au-coated Anodisc™ co-adding 64 scans with 8 cm^{-1} resolution. Labels for peaks are described in the text. The spectrum is baseline corrected as described in the text.

Previously observed absorbances at 3278 cm^{-1}, 1651 cm^{-1}, 1543 cm^{-1} and 1280 cm^{-1} (reported to be the Amide A, I, II[3] and Ca dipicolinate bands[11]) are observed in agreement with the literature values. A few other absorbances are also prominently observed in Figure 45: 2962 cm^{-1}

(asymmetrical methyl C-H stretch) 2935 cm^{-1} (asymmetrical methylene C-H stretch), 2873 cm^{-1} (symmetrical methyl C-H stretch), 1385 cm^{-1} (symmetrical carboxylate C-O stretch), 1242 cm^{-1} (from the asymmetrical P=O stretch of $>PO_2$) and 1095 cm^{-1} (from the symmetrical P=O stretch of $>PO_2$).

The average number of endospores calculated from ten images per sample in a 100 x 100 μm^2 area was 1335 ±72, 1397 ±85, and 1337 ±49 spores for Disk 1, Disk 2, and Disk 3, respectively. The relative standard deviations (RSDs) of the three filter samples were 5.4%, 6.1% and 3.7%, respectively, all greater than the RSD (2.7%) expected from simple particle counting statistics given by $1/\sqrt{N}$, where N is the average number of spores. The greater variability found on each sample is an indication that the porous structure is not uniform across the surface of the 2-inch diameter disks, causing the rate of filtration to vary slightly across the surface of the sample.

If the samples each were presented with the same number of spores to filter, the average numbers of spores measured by SEM across the samples should be nearly the same. While the experimental values were qualitatively similar, the mean of the averages from the three disks was found to be 1356 ±35 endospores per 100 x 100 μm^2. This represents an experimental RSD of the mean of 2.6%. This disk-to-disk variability of the spore count is above the expected variability (0.8 % RSD) of the mean of ten measurements based on simple particle counting statistics. Assuming that the membrane prohibits the passage of spores (no spores were detected in the filtrate), then the fact that SEM shows a greater disk-to-disk variability than expected from particle counting statistics likely implies imprecision in the number of spores filtered through the membrane due to heterogeneity of the stock suspensions, and can be attributed to fluid sampling errors.

The average intensity of the vibrational absorbance of Amide A at 3278 cm^{-1} in the observed spectra was calculated to be 0.0270 ±0.0016, 0.0297 ±0.0016, and 0.0288 ±0.0021 for Disk1, Disk 2, and Disk 3, respectively. The LD50 estimate for human exposure to *Bacillus anthracis* spores (based on primate studies) is reported to be between 2,500 and 55,000 for acute inhalation exposure. Done appropriately, these data suggest that FTIR is in principle capable of detecting spores at a level below the LD50 estimate, especially considering that *B. subtilis* spores are significantly smaller than those of *B. anthracis*. This would require concentration of the spores into a relatively small area.

The mean of the average baseline-corrected intensities for the Amide A absorbance from the three membranes was calculated to be 0.0285 absorbance units with a RSD of the mean of 4.82%. Again, the particle-counting RSD of 0.8% is expected to represent the ultimate precision of the FTIR measurement.

FTIR measurements showed a greater RSD than the SEM particle counts, and this poorer precision can be attributed to the relatively low absorbance (A ≤0.03) being detected. The RSD observed for vibrational absorbances weaker than the Amide A band increased with decreasing average absorbance, consistent with this origin for the higher RSD compared to SEM particle counts. The added imprecision observed in FTIR of the Amide A band can thus be attributed primarily to instrument and measurement noise.

Even with the slight non-uniformity of the porous alumina membranes and including fluid-sampling errors, the relative standard deviation of the Au-coated Anodisc™ measurements show an approximate 10-fold improvement over the relative standard deviation obtained by drying drops of a suspension on a gold-coated glass slide in our laboratory, as reported above.

4.0 CHRONOLOGICAL LIST OF WRITTEN PUBLICATIONS (19)

Spectral Tolerance Determination for Multivariate Optical Element Design
M.L. Myrick, S. Soyemi, H. Li, L. Zhang and D. Eastwood
Fres. J. Anal. Chem. 369(2001), 351.

Spectroelectrochemical Study of the Oxidative Doping of Polydialkylphenyleneethynene using Iterative Target Transformation Factor Analysis
Una Evans, O. Soyemi, M. Doescher, U. Bunz, L. Kloppenberg, M.L. Myrick
Analyst 126 (2001), 508.

Field Applications of Stand-off Sensing using Visible/NIR multivariate optical computing.
D. Eastwood, O. Soyemi, J. Karunamuni, L. Zhang, H. Li, and M.L. Myrick
SPIE 4199 (2001), 105.

Design and Testing of a Multivariate Optical Element (MOE): The First Demonstration of Multivariate Optical Computing for Predictive Spectroscopy
O. Soyemi, D. Eastwood, L. Zhang, H. Li, J. Karunamuni, P. Gemperline, R.A. Synowicki, M.L. Myrick
Anal. Chem. 73 (2001), 1069.

Novel Filter Design Algorithm for Multivariate Optical Computing
O.O. Soyemi, P.J. Gemperline, L. Zhang, D. Eastwood, H. Li, and M.L. Myrick
SPIE 4205 (2001), 288.

Simple Optical Computing Device for Chemical Analysis
O.O. Soyemi, P. J. Gemperline, L. Zhang, D. Eastwood, H. Li,, and M.L. Myrick
SPIE 4284 (2001), 17.

Interference Filter Refinement for Array-Based Fluorescimetric Sensing
J. Karunamuni, K.E. Stitzer, D. Eastwood, K.J. Albert, D.R. Walt, S.B. Brown and M.L. Myrick
Optical Engineering 40 (2001), 888-95.

A Single-Element All-Optical Approach to Chemometric Prediction
M.L. Myrick, O. Soyemi, J. Karunamuni, D. Eastwood, H.Li, L. Zhang, A.E. Greer and P. Gemperline
Vibrational Spectroscopy 28 (2002), 73-81.

Multivariate Optical Elements Simplify Spectroscopy
M.L Myrick
Laser Focus World 38 (2002), 91-94.

Application of Multivariate Optical Computing to Simple Near-Infrared Point Measurements
M.L. Myrick, O.O. Soyemi, M.V. Schiza, J.R. Farr, F.G. Haibach, A.E. Greer, H. Li and R.J. Priore
SPIE 4574 (2002), 208-215.

Application of Multivariate Optical Computing to Near-Infrared Imaging
M.L. Myrick, O.O. Soyemi, F.G. Haibach, L. Zhang, A.E. Greer, H.Li, R.J. Priore, M.V. Schiza and J.R. Farr
SPIE 4577 (2002), 148-157.

A Nonlinear Optimization Algorithm for Multivariate Optical Element Design
O.O. Soyemi, F.G. Haibach, P.J. Gemperline and M.L. Myrick
Appl. Spectrosc. 56 (2002), 477-487.

Design of Angle-Tolerant Multivariate Optical Elements for Chemical Imaging
O.O. Soyemi, P.J. Gemperline, M.L. Myrick
Appl. Optics. 41 (2002), 1936-1941.

Online Reoptimization of Filter Designs for Multivariate Optical Elements
Frederick G. Haibach, Ashley E. Greer, Maria V. Schiza, Ryan J. Priore, Olusola O. Soyemi and Michael L. Myrick
Applied Optics 42 (2003), 1833-1838.

The Growth and Characterization of a Porous Aluminum Oxide Film formed on an Electrically Insulating Substrate
Paul G. Miney, Paula E. Colavita, Maria V. Schiza, Ryan J. Priore, Frederick G. Haibach, and Michael L. Myrick
Electrochem. Solid State Lett 6 (2003), B42-B45.

A New Optically Reflective Thin Layer Electrode (ORTLE) Window: Gold on a Thin Porous Alumina Film used to observe the Onset of Water Reduction
Paul G. Miney, Maria V. Schiza, M. L. Myrick
Electroanal. 16 (2004), 113-119.

Miniature Stereo Spectral Imaging System for Multivariate Optical Computing
Ryan J. Priore, Frederick, G. Haibach, Maria V. Schiza, Ashley E. Greer, David L. Perkins and M.L. Myrick
Appl. Spectrosc. 58 (2004) 870-873.

Effects of Autoclaving on Bacterial Endospores Studied by Fourier Transform Infrared Microspectroscopy

D.L. Perkins, C.R. Lovell, B.V. Bronk, B. Setlow, P. Setlow and M.L. Myrick
Appl. Spectrosc. 58(2004) 749-753.

Precision in Multivariate Optical Computing
Frederick G. Haibach and M. L. Myrick
Applied Optics 43 (2004), 2130-2140.

Improved Dispersion of Bacterial Endospores for Quantitative Infrared Sampling on Gold Coated Porous Alumina Membranes
Maria V. Schiza, David L. Perkins, Ryan J. Priore, B. Setlow, P. Setlow, Burt V. Bronk, M. L. Myrick
Appl. Spectrosc. (in press, 2004).

5.0 LIST OF PROFESSIONAL PERSONNEL ASSOCIATED WITH THE PROJECT

Michael L. Myrick, Professor and Principal Investigator
Joszef Czege, Subcontract PI for light scattering (USUHS)
Burt V. Bronk, Biophysicist, AFRL at U.S. Army ECBC
Peter Setlow, Professor, University of Connecticut Health Center
Barbara Setlow, University of Connecticut Health Center
J. Karunamuni, postdoctoral associate (ending 9/00)
L. Zhang, postdoctoral associate (ending 5/00)
Y. Yan, postdoctoral associate
U. Evans, postdoctoral associate (beginning 3/01)
M.V. Schiza, postdoctoral associate (beginning 5/01)
D. Eastwood, postdoctoral associate (ending 6/01)
O.O. Soyemi, postdoctoral associate (ending 7/01)
F.G. Haibach, postdoctoral associate (beginning 8/01)
A.E. Greer, graduate associate (beginning 5/01)
P.E. Colavita, graduate associate (beginning 5/01)
R.J. Priore, graduate student (beginning 5/02)
D.L. Perkins, graduate student (beginning 5/02)
H. Li, M.S. student (ending 9/01)
L. Profeta, student (beginning 5/04)

6.0 RELATED ACTIVITIES: MEETINGS AND CONFERENCES (56)

The Growth of Aluminum Oxide Thin Films and their Potential Application in Sensor Technology
P.G. Miney, M.V. Schiza, P.E. Colavita, R.J. Priore, F.G. Haibach, D.L. Perkins and M.L. Myrick.
Presented at 205th Electrochemical Society Meeting, San Antonio, TX, May 9-13, 2004.

Multivariate Optical Computing: Application-Specific Optical Sensors And How to Create Them
M.L. Myrick
Presented at Advances in Process Analysis and Control Technologies Conference (APACT04), Bath (UK), April 28, 2004.

Chemical Sensing By Optical Computing: A Practical Tool For Complex Problems
M.L. Myrick
Presented at the 36th Annual Southeastern Regional American Chemical Society Undergraduate Research Conference, Statesboro, GA, April 2, 2004.

Spectroelectrochemical Sensing Using Ultrathin Layer Electrodes Based on Gold Coated Nanoporous Alumina
Maria V. Schiza, Paul Miney and M.L. Myrick
Presented at the Pittsburgh Conference on Analytical Chemistry, Chicago, IL, March 7-12, 2004.

Novel System for Infrared Micro-spectroelectrochemical Measurements
David L. Perkins, Paul G. Miney and M.L. Myrick
Presented at the Pittsburgh Conference on Analytical Chemistry, Chicago, IL, March 7-12, 2004.

Gain Ranging Multivariate Optical Computing: Chemical Imaging of Organophosphates in the Infrared
Ryan J. Priore, M.L. Myrick, M.V. Schiza
Presented at the Pittsburgh Conference on Analytical Chemistry, Chicago, IL, March 7-12, 2004.

Reducing the Search Space to find the "Best" Multivariate Optical Element
F. G. Haibach, M.L. Myrick, D.L. Perkins, R.J. Priore and M.V. Schiza
Presented at the Pittsburgh Conference on Analytical Chemistry, Chicago, IL, March 7-12, 2004.

Organic Nanoparticle Formation for Nanoparticle Beam Deposition Using a Novel Aerosolization Process
A.E. Greer, D.A. Chen, B.R. Genge, K.D. Krantzman and M.L. Myrick
Presented at the Pittsburgh Conference on Analytical Chemistry, Chicago, IL, March 7-12, 2004.

Multivariate Optical Computing: A Tool for Making Simple Sensors
M.L. Myrick
Presented to ACS Process Spectroscopy Topical Group, Wilmington, DE, January 9, 2003

The How-To and Why of Multivariate Optical Computing
M.L. Myrick
Presented at DuPont, Inc., Wilmington, DE, January 9, 2003

Multivariate Optical Computing: A Tool for Making Simple Sensors
M.L. Myrick
Presented at the International Federation of Process Analytical Chemistry, Arlington, VA, January 12-15, 2003.

Multivariate Optical Computing: A Tool for Making Simple Sensors
M.L. Myrick
Presented at Foster-Miller, Inc., Boston, MA, December 15, 2003.

Improved Discrimination of Bacterial Spore Species with FT-IR Spectroscopy by Pretreatment with Autoclaving
D. L. Perkins· C. R. Lovell, B. V. Bronk, P. Setlow, M. L. Myrick
Presented at Joint Service Scientific Conference on Chemical & Biological Defense Research, Towson, MD, November 17-20, 2003.

Determination of Transmission and Reflectance Characteristics of Biological Microorganisms Distributed on Porous Matrices
Maria V. Schiza, M.L. Myrick
Presented at Federation of Analytical Chemistry and Spectroscopy Societies, Ft. Lauderdale, FL October 19-23, 2003.

FT-IR Reflectance Microspectroscopy Study of Bacterial Spores Following the Autoclaving Process
David L. Perkins, M.L. Myrick
Presented at Federation of Analytical Chemistry and Spectroscopy Societies, Ft. Lauderdale, FL October 19-23, 2003.

Nanoparticle Beam Deposition as a Novel Technique for the Formation of Organic Thin Films
Ashley Greer-Reese, M.L. Myrick
Presented at Federation of Analytical Chemistry and Spectroscopy Societies, Ft. Lauderdale, FL October 19-23, 2003.

Novel Imaging Systems: Multivariate Optical Computing from UV to NIR
Ryan Priore, M.L. Myrick
Presented at Federation of Analytical Chemistry and Spectroscopy Societies, Ft. Lauderdale, FL October 19-23, 2003.

Multivariate Optical Computing: A Tool for Making Simple Sensors
M.L. Myrick
Presented at Alliance for Coastal Technology One-Day Meeting, Charleston, SC, October 7, 2003.

Multivariate Optical Computing: A Tool for Making Simple Sensors
M.L. Myrick

Presented at Fall Meeting of the Measurement and Control Engineering Center, Knoxville, TN, October 4, 2003.

Novel Imaging Systems: Multivariate Optical Computing in the UV-Vis

Ryan J. Priore, Ashley E. Greer, Frederick G. Haibach, Maria V. Schiza, David L. Perkins, Michael L. Myrick

Presented at International Conference on Digital Printing Technologies , New Orleans, LA, September 28 - October 3, 2003.

Chemical Sensing by Multivariate Optical Computing

M.L. Myrick

Presented at Chemical Sensors and Interfacial Design Gordon Research Conference, Newport, RI, August 3-8, 2003.

Multivariate Optical Computing: A Tool for Making Simple Sensors

M.L. Myrick

Presented at Advances in Process Analysis and Control Technologies, York (UK), April 30, 2003.

Novel Imaging Systems: Multivariate Optical Computing from UV to NIR

Ryan J. Priore, A.E. Greer, F.G. Haibach, M.V. Schiza, D.L. Perkins and M.L. Myrick

Presented at the Pittsburgh Conference on Analytical Chemistry, Orlando, FL, March 9-14, 2003.

The Design of Multivariate Optical Elements: New Routes to Finding the Best Filter Designs for Chemical Prediction

F.G. Haibach and M.L. Myrick

Presented at the Pittsburgh Conference on Analytical Chemistry, Orlando, FL, March 9-14, 2003.

Diffuse Reflectance Characteristics of Postal Envelopes and Biological Microorganisms as a Potential Basis for their Detection by Multivariate Optical Computing

M.V. Schiza, D.L. Perkins, P. White, A.E. Greer, R.J. Priore, F.G. Haibach and M.L. Myrick

Presented at the Pittsburgh Conference on Analytical Chemistry, Orlando, FL, March 9-14, 2003.

Fourier Transformed Infrared Reflectance Microspectroscopy Study on the Autoclaving Process of Bacterial Spores

D.L. Perkins, M.V. Schiza, R.J. Priore, A.E. Greer, F.G. Haibach, A. Fox, K. Fox and M.L. Myrick

Presented at the Pittsburgh Conference on Analytical Chemistry, Orlando, FL, March 9-14, 2003.

Infrared, Microscopic and Mechanical Characterization of c-BN films Deposited by Reactive Magnetron Sputtering with Ion Bombardment

M.V. Schiza, T.J. Lienert, M.A. Sutton, P. White, A.P. Reynolds and M.L. Myrick
Presented at the Pittsburgh Conference on Analytical Chemistry, Orlando, FL, March 9-14, 2003.

Signal to Noise in the Transmission-Reflection Fliter Multivariate Optical Element
F.G. Haibach, M.V. Schiza, A.E. Greer, R.J. Priore, D.L. Perkins and M.L. Myrick
Presented at the Pittsburgh Conference on Analytical Chemistry, Orlando, FL, March 9-14, 2003.

Temperature Tolerant Multivariate Optical Elements
F.G. Haibach, D.L. Perkins, A.E. Greer, R.J. Priore, M.V. Schiza and M.L. Myrick
Presented at the Pittsburgh Conference on Analytical Chemistry, Orlando, FL, March 9-14, 2003.

Design and Fabrication of Multilayer Films for Multivariate Optical Computing in the Near-Infrared Region
A.E. Greer, R.J. Priore, F.G. Haibach, M.V. Schiza, D.L. Perkins and M.L. Myrick
Presented at the Pittsburgh Conference on Analytical Chemistry, Orlando, FL, March 9-14, 2003.

Nanoparticle Beam Deposition: Generation of Dry Organic Nanoparticle Clusters for Use in a Novel Film Formation Technique
A.E. Greer, B.R. Genge, K.D. Krantzman, D.A. Chen and M.L. Myrick
Presented at the Pittsburgh Conference on Analytical Chemistry, Orlando, FL, March 9-14, 2003.

Speciation of Bacterial Spores by Infrared Microspectroscopy and Concepts for Speciation by Multivariate Optical Computing
David. L. Perkins, M. V. Schiza, R. J. Priore, A. E. Greer, F. G. Haibach, P. Setlow, B. V. Bronk, M. L. Myrick
Presented at Joint Service Scientific Conference on Chemical & Biological Defense Research, Hunt Valley, MD, November 19-21, 2002.

Diffuse Reflectance Characteristics of Papers and Biological Microorganisms as a Potential Basis for Detection by Multivariate Optical Computing
Maria V. Schiza, David L. Perkins, Priscilla White, Ashley E. Greer, Ryan J. Priore, Frederick G. Haibach, M. L. Myrick
Presented at Joint Service Scientific Conference on Chemical & Biological Defense Research, Hunt Valley, MD, November 19-21, 2002.

Diffuse Reflectance Characteristics of Papers and Microorganisms as a potential basis for detection by Multivariate Optical Computing
M.V. Schiza, D.L. Perkins, P.A. White, A.E. Greer, R.J. Priore, F.G. Haibach, P. Setlow, B.V. Bronk and M.L. Myrick
Presented at Southeastern Regional Meeting of the American Chemical Society, Charleston, SC, November 13-16, 2002.

Design and Fabrication of Multilayer Interference Filters for Multivariate Optical Computing
A.E. Greer, R.J. Priore, F.G. Haibach, M.V. Schiza, D.L. Perkins and M.L. Myrick
Presented at Southeastern Regional Meeting of the American Chemical Society, Charleston, SC, November 13-16, 2002.

Multivariate Optical Computing: Factors in the Design of Multivariate Optical Elements
F.G. Haibach, A.E. Greer, M.V. Schiza, R.J. Priore, D.L. Perkins and M.L. Myrick
Presented at Southeastern Regional Meeting of the American Chemical Society, Charleston, SC, November 13-16, 2002.

Novel Imaging Systems: Multivariate Optical Computing from UV to NIR
R.J. Priore, A.E. Greer, M.V. Schiza, F.G. Haibach, D.L. Perkins and M.L. Myrick
Presented at Southeastern Regional Meeting of the American Chemical Society, Charleston, SC, November 13-16, 2002.

Spectral Profiling of Bacterial Spores by Spectral Reflectance and Chemometrics
D.L. Perkins, M.V. Schiza, R.J. Priore, A.E. Greer, F.G. Haibach, P. Setlow, B.V. Bronk and M.L. Myrick
Presented at Southeastern Regional Meeting of the American Chemical Society, Charleston, SC, November 13-16, 2002.

Designing Temperature-Insensitive Multivariate Optical Elements
F.G. Haibach, D.L. Perkins, R.J. Priore, M.V. Schiza, A.E. Greer and M.L. Myrick
Presented at Federation of Analytical Chemistry and Spectroscopy Societies, Providence, RI October 13-18, 2002.

Molecular sensors for the detection and identification of single native DNA nucleotides
P.E. Colavita, A.C. Molliet, M.V. Schiza and M.L. Myrick
Presented at Federation of Analytical Chemistry and Spectroscopy Societies, Providence, RI October 13-18, 2002.

Online Design Reoptimization Algorithm for the Production of Multivariate Optical Elements
A.E. Greer, F.G. Haibach, M.V. Schiza, R.J. Priore, O.O. Soyemi and M.L. Myrick
Presented at Federation of Analytical Chemistry and Spectroscopy Societies, Providence, RI October 13-18, 2002.

Detection of Organophosphorous Compounds in Characteristic Near Infrared Regions by Using Multivariate Optical Elements
M.V. Schiza, A.E. Greer, D.L. Perkins, F.G. Haibach and M.L. Myrick
Presented at Federation of Analytical Chemistry and Spectroscopy Societies, Providence, RI October 13-18, 2002.

Spectral Profiling of Biological Microorganisms by Specular Reflectance and Chemometrics
D.L. Perkins, M.V. Schiza, R.J. Priore, A.E. Greer, F.G. Haibach, P. Setlow, B.V. Bronk, and M.L. Myrick

Presented at Federation of Analytical Chemistry and Spectroscopy Societies, Providence, RI October 13-18, 2002.

Signal to Noise Ratios in Multivariate Optical Computing: A Reprise and Extension to the Transmission-Reflection Filter Spectrometer
F.G. Haibach and M.L. Myrick
Presented at Federation of Analytical Chemistry and Spectroscopy Societies, Providence, RI October 13-18, 2002.

Novel Imaging Systems: Multivariate Optical Computing from UV to NIR
R.J. Priore, A.E. Greer, F.G. Haibach, M.V. Schiza, D.L. Perkins and M.L. Myrick
Presented at Federation of Analytical Chemistry and Spectroscopy Societies, Providence, RI October 13-18, 2002.

Imaging with Multivariate Optical Elements: CCD Imaging of Dye Mixtures in the Visible Region
R. J. Priore, N.E. Schmidt, F.G. Haibach, M.V. Schiza, A.E. Greer and M.L. Myrick
Presented at the Pittsburgh Conference on Analytical Chemistry, New Orleans, LA, March 17-22, 2002.

Middle and Near Infrared Absorption and Raman Characteristics of Organophosphorous Compounds
M. V. Schiza, A.E. Greer, F.G. Haibach, R. Priore, N. J. Farr and M.L. Myrick
Presented at the Pittsburgh Conference on Analytical Chemistry, New Orleans, LA, March 17-22, 2002.

NIR Spectra of Organophosphorus Compounds: Materials and Optical Considerations for Multivariate Optical Detection of OP Compounds on Sand
A.E. Greer, M.V. Schiza, J.R. Farr, F.G. Haibach and M.L. Myrick
Presented at Southeast Association of Analytical Chemistry Conference, Columbia, SC, November 1-3, 2001.

Application of multivariate optical computing to simple near-infrared point measurements, M. L. Myrick, O. O. Soyemi, A. Greer, F. Haibach, H. Li, R. Priore
Presented at SPIE Photonics-Boston Conference, Boston, MA, October 28-November 4, 2001.

Application of multivariate optical computing to near-infrared imaging
M.L. Myrick, O. O. Soyemi, L. Zhang, A. Greer, H. Li
Presented at SPIE Photonics-Boston Conference, Boston, MA, October 28-November 4, 2001.

NIR Spectra of Organophosphorous Compounds: Materials and Optical Considerations for Multivariate Optical Computing of OP Compounds on Sand
A.E. Greer, O.O. Soyemi, N.E. Schmidt, J. Farr, R.J. Priore, U. Evans, F.G. Haibach and M.L. Myrick

Presented at Federation of Analytical Chemistry and Spectroscopy Societies, Detroit, MI October 7-12, 2001.

Chemical Imaging via Multivariate Optical Computing in the Visible Spectral Region
F.G. Haibach, M.L. Myrick, O.O. Soyemi, A.E. Greer and R.J. Priore
Presented at Federation of Analytical Chemistry and Spectroscopy Societies, Detroit, MI October 7-12, 2001.

Molecular Behavior of Organic Polymer in Electroluminescence Devices based on Poly(p-phenyleneethynylene)
H. Li, U. Evans, M. Doescher, A.R. Marshall, U.H.F. Bunz and M.L. Myrick
Presented at Federation of Analytical Chemistry and Spectroscopy Societies, Detroit, MI October 7-12, 2001.

Multivariate Optical Elements for Chemical Measurement
M.L. Myrick, O.O. Soyemi, A.E. Greer, F.G. Haibach
Presented at Federation of Analytical Chemistry and Spectroscopy Societies, Detroit, MI October 7-12, 2001.

Design of Angle-Tolerant Multivariate Optical Elements for Chemical Imaging Applications
O. Soyemi, A. Greer, R. Priore, F. Haibach, N. Schmidt, M. Schiza and M.L. Myrick
Presented at the 5th Joint Conference on Standoff Detection for Chemical and Biological Defense, Williamsburg, VA, September 24-28, 2001.

Chemical Sensing via Multivariate Optical Computing
M.L. Myrick, O. Soyemi, A. Greer
International Symposium On Spectral Sensing Research (ISSSR) 2001, Quebec City, Canada, June 10-15, 2001.

7.0 DISCOVERIES AND INVENTIONS

Novel Filter Design Algorithm for Multivariate Optical Computing
Inventors: M.L. Myrick, O. O. Soyemi, and P.J. Gemperline
Provisional Patent Application Number: 60/235,336.

Optical Computational System
Inventor: M.L. Myrick
U.S. Patent Number 6,529,276 (awarded March 4, 2003)

8.0 OTHER GRANTS RELATED TO F33615-00-2-6059

The most recent grant to support research related to that of F33615-00-2-6059 was grant number DOD-N-000014-97-1-0806, received by the University of South Carolina and in effect from 6/1997-6/2000. The University received a 1-year no-cost extension of this grant from the Office of Naval Research for accounting purposes, although no new work was done that was attributed

to the ONR grant after 6/00. This is the grant that provided support for the acquisition of the visible-light deposition system used during Y1 of the present grant. Publications that were attributed to both DOD-N-000014-97-1-0806 AND F33615-00-2-6059 were:

Spectral Tolerance Determination for Multivariate Optical Element Design
M.L. Myrick, S. Soyemi, H. Li, L. Zhang and D. Eastwood
Fres. J. Anal. Chem. 369(2001), 351.

Interference Filter Refinement for Array-Based Fluorescimetric Sensing
J. Karunamuni, K.E. Stitzer, D. Eastwood, K.J. Albert, D.R. Walt, S.B. Brown and M.L. Myrick
Optical Engineering 40 (2001), 888-95.

Field applications of stand-off sensing using visible/NIR multivariate optical computing
D. Eastwood, O. Soyemi, J. Karunamuni, L. Zhang, H. Li, and M.L. Myrick
SPIE 4199 (2001), 105.

Novel Filter Design Algorithm for Multivariate Optical Computing
O.O. Soyemi, P.J. Gemperline, L. Zhang, D. Eastwood, H. Li, and M.L. Myrick
SPIE 4205 (2001), 288.

For these four publications, acknowledgement of DOD-N-000014-97-1-0806 was for the support of Lixia Zhang and Jeevananda Karunamuni prior to the start of F33615-00-2-6059. All research for these reports (EXCEPT the Optical Engineering report) was conducted in 6/00 and thereafter under the total support of F33615-00-2-6059. Research for the OE report was conducted prior to the beginning of F33615-00-2-6059 with ONR and DARPA support. F33615-00-2-6059 was acknowledged for supporting the salary of D. Eastwood during revision of the manuscript in the summer of 2000.

The ONR grant supported work in molecular computing and fiber-optic technique development, plus optical computing for image and data compression. Other reports totally or partially attributed to DOD-N-000014-97-1-0806, with no attribution to F33615-00-2-6059 are:

The Use of a 2D to 1D Dimension Reduction Fiber-Optic Array for Multi-Wavelength Imaging Sensors
M. V. Schiza, M. P. Nelson, M. L. Myrick, S. M. Angel
Appl. Spectrosc. 55 (2001), 217.

Stripping Voltammetry of Cu Overlayers Deposited on Self-Assembled Monolayers: Field Emission of Electrons Through A Phenylene Ethynylene Oligomer
M.S. Doescher, A. Rawlett, J.M. Tour and M.L. Myrick
J. Phys. Chem. B 105(2001), 105.

Fluorescence Fingerprint of Waters: Excitation-Emission Matrix Spectroscopy as a Tracking Tool
Y. Yan, H. Li and M.L. Myrick

Appl. Spectrosc. 54 (2000), 1539.

Simple Techniques for Chemical Imaging at Many Wavelengths Simultaneously, Using a Novel 2D to 1D Optical Fiber Array
S.M. Angel, M.V. Schiza, M.L. Myrick and M.P. Nelson
SPIE 4074 (2000), 99.

Kinetic and Spectroscopic Profiles of Pyridine Complexes at a Silver Electrode Using Surface-Enhanced Raman Scattering (SERS) and Evolving Factor Analysis
M.A. Nicholson, J.F. Aust, K.S. Booksh, W.C. Bell and M.L. Myrick
Vibrational Spectroscopy 24 (2000), 157.

The Lowest Electronic Excited States of poly(*para*-cyclobutadienylenecyclopentadienyl-cobalt)butadiynylene
B. Craig Harrison, J. Seminario, U. Bunz and M.L. Myrick
J. Phys. Chem. 104 (2000), 5937.

Simultaneous Enantiomeric Determination of Dansyl-D,L-Phenylalanine by Fluorescence Spectroscopy in the Presence of _-Acid Glycoprotein
Yuan Yan and M.L. Myrick
Anal. Chem. 71(1999), 1958.

Time-dependent multivariate single-frame chemical imaging spectroscopy of laser plumes using a dimension reduction fiber optic array"
M. P. Nelson, M. L. Myrick
SPIE 3649(1999), 92-99.

Thermodynamic Characterization of Separation Phenomena at the Silica/Polymer Interface within Glass-Reinforced Composites using Adsorption Chromatography. Part I.
A.R. Muroski, M.P. Nelson and M.L. Myrick
J. Adhesion Sci. Technol. 13(1999), 437.

Fabrication and Evaluation of a Dimension-Reduction Fiber-Optic System for Chemical Imaging Applications
M.P. Nelson and M.L. Myrick
Rev. Sci. Instrum. 70(1999), 2836.

Single-Frame Chemical Imaging: Dimension Reduction Fiber-Optic Array Improvements and Application to Laser-Induced Breakdown Spectroscopy.
M.P. Nelson and M.L. Myrick
Appl. Spectrosc. 53(1999), 751.

New Developments in Two-Dimensional Fluorescence Spectroscopy for Rapid Detection of Organics in Seawater
M.L. Myrick and Y. Yan
SPIE 3854 (1999), 65.

New Approaches to Implementing Predictive Spectroscopy
M.L. Myrick
SPIE 3854 (1999), 98.

Assignment of the Optical Transitions in 1,3-Diethynylcyclobutadiene (cyclopentadienyl)cobalt Oligomers
H. Rengel, M. Altmann, D. Neher, B.C. Harrison, M.L. Myrick and U.H.F. Bunz
J. Phys. Chem. 103(1999),10335.

High-Speed Detection of Explosives.
K.J. Albert, M.L. Myrick, S.B. Brown, F.P. Milanovich and D.R. Walt
SPIE 3710 (1999), 308.

Hyperspectral Imaging Sensors Using a Novel 2D to 1D Fiber Array
M.V. Schiza, M.P. Nelson, M.L. Myrick, and S.M. Angel
SPIE 3860 (1999), 317-325.

Another grant acknowledged jointly with F33615-00-2-6059 is the DARPA grant DAAK-60-97-K-9502. This grant supported the salary of J. Karunamuni for research leading to the report published in Optical Engineering listed above. F33615-00-2-6059 was acknowledged for support of D. Eastwood's salary during the revision of the Optical Engineering manuscript in summer of 2001.

9.0 APPENDIXES

9.1. ORGANOPHOSPHOROUS COMPOUNDS STUDIED AT USC

Compound	MIR	NIR	Raman
Sand/white quartz (NIR)		X	
Methylphosphonic acid (NIR)		X	X
Dimethylmethylphosphonate	X	X	X
Methamidophos	X	X	
Trimethylphosphate	X	X	X
Dichlorvos	X	X	X
Hexamethylphosphoric triamide	X	X	X
Pinacolyl methylphosphonate	X	X	X
Dimethoate (NIR)		X	X
Dylox (NIR)		X	X
Dibrom	X	X	
Phorate	X	X	X
Prophos	X	X	X
Demeton O &S	X	X	
Disulfoton	X	X	X
Dyfonate	X	X	
Monocrotophos	X	X	X
Phosdrin	X	X	X
Dicrotophos	X	X	X
Terbufos	X	X	
Zinophos (NIR)		X	
Fenchlorphos (NIR)		X	X
Methylparathion (NIR)		X	X
Tetraethylpyrophosphate	X	X	
Tetraethyldithiopyrophosphate	X	X	
Tributylphosphorotrithioate	X	X	X
Trichloronate	X	X	
Carbophenothion	X	X	X
Chlorpyrifos (NIR)		X	X
Fensulfothion	X	X	
Parathion	X	X	X
Phosphamidon	X	X	X
Sulprofos (NIR)		X	X
Diazinon	X	X	
Ethion	X	X	X
Famphur (NIR)		X	X
Guthion (NIR)		X	
Imidan (NIR)		X	X
Malathion	X	X	X
Tetrachlorvinphos (NIR)		X	X
Chlorfenvinphos	X	X	
Leptophos (NIR)		X	X
Crotoxyphos	X	X	
EPN (NIR)		X	X
Guthion ethyl (NIR)		X	X
Coumaphos (NIR)		X	X
Dioxathion	X	X	X
Sulfometuron methyl (NIR)		X	X
Fenthion			X

9.2 FIRST PAGES OF ALL PUBLICATIONS

In this section we reproduce the first pages and the abstract from all the open literature publications which were supported by this contract. From these the reader should be able to get an idea of which ones if any he/she would like to obtain for detailed study.

Fresenius J Anal Chem (2001) 369:351–355

SPECIAL ISSUE PAPER

M. L. Myrick · O. Soyemi · H. Li · L. Zhang
D. Eastwood

Spectral tolerance determination for multivariate optical element design

Received: 21 August 2000 / Revised: 30 October 2000 / Accepted: 4 November 2000

Abstract Recent reports from our laboratory have described a method for all-optical multivariate chemometric prediction from optical spectroscopy. The concept behind this optical approach is that a spectral pattern (a regression vector) can be encoded into the spectrum of an optical filter. The key element of these measurement schemes is the multivariate optical element (MOE), a multiwavelength interference-based spectral discriminator that is tied to the regression vector of a particular measurement. The fabrication of these MOEs is a complex operation that requires precise techniques. However, to date, no quantitative means of determining the allowable design/manufacturing errors for MOEs has existed. The purpose of the present report is to show how the spectroscopy of a sample is used to define the accuracy with which MOEs must be designed and manufactured. We conclude this report with a general treatment of spectral tolerance and a worked example. The worked example is based on actual experimental measurements. We show how the spectral bandpass is defined operationally in a real problem, and how the statistics of the theoretical regression vector influence both the bandpass and the minimum tolerances. In the experimental example, we demonstrate that tolerances range continuously between 1 (totally tolerant) to approximately 10^{-3} (0.1% T) in this problem.

Introduction

Multivariate spectroscopy is a powerful tool for analytical determinations of the chemical and physical characteristics of a wide range of sample types via chemometrics. In one common approach for applying multivariate modeling to chemical problems, a spectral pattern that correlates with a dependent variable is found. In subsequent measurements of unknown samples, predictions of the dependent variable are made by computing the magnitude of this spectral pattern in the optical spectrum of the unknown [1].

A recent report from this laboratory [2] describes an all-optical approach to the last step in this procedure, the magnitude calculation given by the scalar product of a regression vector with the spectrum of an unknown sample. The first reports of a fully optical approach to multivariate chemical measurement were those of Bialkowski [3]. The all-optical approach proposed in our laboratory differs from Bialkowski's as it centers around the production of one or more optical interference coatings whose transmission spectra incorporate features of the spectral regression vector. A recently reported permutation on the original concept permits this pattern to be expressed in a single multivariate optical element (MOE) used as a 45-degree beamsplitter in a T-format instrument [4]. This permutation of the MOE based on chemometrics is most similar to a design proposed by Ryabenko and Kasparov [5].

MOEs of the type we have proposed can be designed by commercially-available software packages by assigning the desired spectral transmission profile of the MOE as a target for an iterative solution. However, these programs operate by successive approximations; exact solutions are not, in general, possible. To date, no report has been made of any method for determining the wavelength-dependent limits on spectral errors (i.e., the tolerable spectral variance) that are permissible in the design of MOEs.

The present manuscript describes the development of a general approach to determining the spectral tolerance of MOEs. The approach taken here is to define lower and upper wavelength limits beyond which tolerances are unnecessary, and then to distribute the prediction errors caused by coating misfit even between these limits. Because no *a priori* knowledge of the final iterative solution can be available at the start of the design process, the authors take the conservative approach of assuming that all spectral errors will sum in the result in the worst possible way. All computations are developed for numerical solution in real problems,

M. L. Myrick (✉) · O. Soyemi · H. Li · L. Zhang · D. Eastwood
Department of Chemistry and Biochemistry,
University of South Carolina, Columbia, SC, 29208, USA

THE ANALYST
FULL PAPER
www.rsc.org/analyst

Spectroelectrochemical study of the oxidative doping of polydialkylphenyleneethynylene using iterative target transformation factor analysis

U. Evans, O. Soyemi, M. S. Doescher, U. H. F. Bunz, L. Kloppenburg and M. L. Myrick*

Department of Chemistry and Biochemistry, University of South Carolina, Columbia, SC 29201, USA

Received 6th November 2000, Accepted 10th February 2001
First published as an Advance Article on the web 16th March 2001

Iterative target transformation factor analysis (ITTFA) was used to determine the spectra of the individual species generated during the oxidative p-doping of films of poly(*para*-phenyleneethynylene) (PPE). UV-visible spectra of PPE films on transparent electrodes were obtained *in-situ* during an anodic sweep. ITTFA identified 4 species present during the oxidation, which we assign as neutral polymer, polaron species, bipolaron species, and a species formed by further bipolaron reaction. The region of electrochemical stability for each of these species was identified and their potential-dependent profiles were obtained. This work is the first deconvolution of conjugated polymer spectroelectrochemistry.

Introduction

Electronically conducting polymers with π-conjugated backbones have been actively studied in recent years.[1] The conjugated backbone of these polymers leads to extensive electron delocalization; nevertheless, the quantum-confined nature of the structure leads to large bandgap energies, making the polymers insulators or weak semi-conductors in their neutral (undoped) state.[2] Electrochemical oxidation (p-doping) of conjugated polymers can create mobile charge-carrying defects that result in increased conductivity; these charged sites are balanced by anions that migrate into the polymer. Doping introduces new defect-centered electronic states that exhibit distinctive optical transitions. Undoped polymers exhibit the characteristic $\pi-\pi^*$ transitions of conjugated organic molecules; the new mid-gap states introduced by doping generally result in new red-shifted absorbances. Two major defect types can be formed on oxidation. The first of these are polarons, molecular radical cations, which are formed at low doping levels. Bipolarons, dicationic defects delocalized over a number of repeat units, may be formed at higher doping levels.[3]

In our laboratory, we have recently studied conductivity and charge-carrier mobility in polyphenyleneethynylene-based polymers. Phenylenevinylene and the related phenyleneethynylene polymers constitute an important class of conducting polymers with applications in optoelectronic devices and materials.[4,5]

In this work the spectroelectrochemistry of a novel 2,5-dialkyl(paraphenyleneethynylene) polymer, synthesized by us, has been investigated. This polymer has been shown to emit light blue shifted from poly(*p*-phenylenevinylene), (PPV) and has been investigated as an emitting layer in organic electroluminescent (OEL) devices.[6,7] Efficiency in OEL devices is directly related to the oxidation and reduction potential of the emitting layers.[8,9] Wrighton *et al.*[10] examined the cyclic voltammetry of a dialkoxy-poly(*para*-phenyleneethynylene)-derivative in solution and found that it is irreversibly oxidized at 1.05 V (*vs.* calomel) in liquid SO_2. However, to date the electrochemistry of poly(*para*-phenyleneethynylene)s (PPEs), especially in solid-state films, is largely unexplored.

Spectroelectrochemistry is a powerful technique for the determination of the intermediates in conjugated polymer oxidation.[11] Rapta *et al.* studied the oxidation of polypyrrole by *in-situ* EPR/UV-vis spectroscopy and determined the UV-vis spectra of the neutral, polaronic and bipolaronic states. *In-situ* spectroelectrochemical studies of p-doped PPV have identified the polaronic and bipolaronic states of this polymer.[12,13] Unfortunately, spectroelectrochemistry of conducting polymers is complicated by overlapping spectra for the different charge-carrying defects possible in each material. Factor-analysis-based approaches to interpretation such as iterative target transformation factor analysis (ITTFA) have the power to provide insight into the number of species present, and how their concentrations vary with time and potential. However, to date factor analysis has been used only once to deconvolute spectroelectrochemical data: by Keesey and Ryan who studied the reduction of *E. coli* sulfite reductase hemoprotein and a Mo–Fe–S cluster.[14] In this report, we explore the spectroelectrochemistry of a PPE-based polymer using ITTFA. Using this approach, we obtain the distinct optical spectra of two charged-defect states that we assign as the polaron and bipolaron states on the basis of their potential and doping level dependence.

Experimental

Thin films of **1** and **2** on indium tin oxide (ITO)-coated slides were used for a spectroelectrochemical study.

The polymers **1** and **2** were synthesized according to a literature procedure[15]. Thin films of **1** and **2** were made by spin-coating 150 μl of a 25 mg ml^{-1} chloroform solution of the polymer onto ITO at a speed of 770 rpm for 50 s. In some cases, the film was removed from a portion of the ITO coating with a chloroform-soaked swab prior to making electrical contact with an alligator clip. In other cases, no cleaning protocol was used and a direct connection *via* an alligator clip was made through the film. No difference in the behaviors of these connection types was observed. Film thickness was determined using contact-mode atomic force microscopy by scoring the polymer film with a blade and measuring step heights from the top of the polymer film to the substrate.

The experimental instrumentation for the electrochemical set-up consisted of an EG&G PARC Model 263 potentiostat, connected with a GPIB interface (National Instruments) to a

 DOI: 10.1039/b009038g

Field applications of stand-off sensing using visible/NIR multivariate optical computing

DeLyle Eastwood, Olusola Soyemi, Jeevanandra Karunamuni, Lixia Zhang, Hong Li
Michael Myrick*

Department of Chemistry and Biochemistry,
University of South Carolina
Columbia, SC 29208

ABSTRACT

A novel multivariate visible/NIR optical computing approach applicable to standoff sensing will be demonstrated with porphyrin mixtures as examples. The ultimate goal is to develop environmental or counter-terrorism sensors for chemicals such as organophosphorus (OP) pesticides or chemical warfare simulants in the near infrared spectral region. The mathematical operation that characterizes prediction of properties via regression from optical spectra is a calculation of inner products between the spectrum and the pre-determined regression vector. The result is scaled appropriately and offset to correspond to the basis from which the regression vector is derived. The process involves collecting spectroscopic data and synthesizing a multivariate vector using a pattern recognition method. Then, an interference coating is designed that reproduces the pattern of the multivariate vector in its transmission or reflection spectrum, and appropriate interference filters are fabricated. High and low refractive index materials such as Nb_2O_5 and SiO_2 are excellent choices for the visible and near infrared regions. The proof of concept has now been established for this system in the visible and will later be extended to chemicals such as OP compounds in the near and mid-infrared.

Keywords: Sensors, optical computing, multivariate analysis, visible/NIR, remote sensing, standoff sensing

* - myrick@mail.chem.sc.edu

ound, and Air Pollution Monitoring and Remediation, Tuan Vo-Dinh, Robert L. Spellicy, Editors,
gs of SPIE Vol. 4199 (2001) © 2001 SPIE · 0277-786X/01/$15.00

Anal. Chem. **2001**, *73*, 1069−1079

Accelerated Articles

Design and Testing of a Multivariate Optical Element: The First Demonstration of Multivariate Optical Computing for Predictive Spectroscopy

O. Soyemi,[†] D. Eastwood,[†] L. Zhang,[†] H. Li,[†] J. Karunamuni,[†] P. Gemperline,[‡] R. A. Synowicki,[§] and M. L. Myrick*,[†]

Department of Chemistry and Biochemistry, University of South Carolina, Columbia, South Carolina 29208, Department of Chemistry and Biochemistry, East Carolina University, Greenville, North Carolina 27258, and J. A. Woollam Company Inc., 645 M Street, Suite 102, Lincoln, Nebraska 68508

A demonstration of multivariate optical computing is presented using binary dye mixtures consisting of Bismarck Brown and Crystal Violet. Bismarck Brown was treated as the analyte, while Crystal Violet was treated as a random interfering species. First, a multilayer multivariate optical element (MOE) for the determination of Bismarck Brown was designed using a novel nonlinear optimization algorithm. Next, the MOE was fabricated by depositing alternating layers of two metal oxide films (Nb_2O_5 and SiO_2) on a BK-7 glass substrate via reactive magnetron sputtering. Finally, the MOE was tested on 39 binary dye mixtures using a simple T-format prototype instrument constructed for this purpose. For each sample, measurements of the difference between transmittance through the MOE, and the reflectance from the MOE were made. By setting aside some of the samples for instrument calibration and then using the calibration model to predict the remaining samples, a standard error of prediction of 0.69 μM was obtained for Bismarck Brown using a linear regression model.

Multivariate calibration is an established tool in chemometrics for the correlation of a physical or chemical property of interest to information spanning multiple wavelength channels in optical spectroscopy.[1−3] The conventional application of this tool in chemical analysis entails first the acquisition of optical spectra in the appropriate wavelength region (typically from the ultraviolet to the mid-infrared). Next, chemometric tools are used to extract a spectral pattern (the regression vector) which is correlated to the property of interest but orthogonal to interferences.[4] Prediction of the property in an unknown sample is then carried out by determining the magnitude of the spectral pattern in the optical spectrum of the sample. More specifically, the magnitude is calculated by taking the inner product of the regression vector and the optical spectrum of the unknown sample. A major drawback in the widespread use of multivariate calibration, especially for field applications, is its dependence on expensive and bulky laboratory-type equipment for data acquisition and analysis.

A recent publication from our laboratory[5] addressed from a theoretical standpoint the feasibility of using optical computing in predictive spectroscopy to simplify and harden the apparatus necessary for chemical prediction. The first reports of a related hypothetical optical approach to multivariate chemical measurement were those of Bialkowski.[6] The use of a single multivariate optical element (MOE) in a beam splitter configuration has also

* To whom correspondence should be addressed. Telephone: (803)-777-6018. Fax: (803)-777-9521. E-mail: myrick@psc.sc.edu.

[†] University of South Carolina.

[‡] East Carolina University.

[§] J. A. Woollam Company Inc.

10.1021/ac0012896 CCC: $20.00
Published on Web 02/10/2001

(1) Aust, J. F.; Booksh, K. S.; Myrick, M. L. *Appl. Spectrosc.* **1996**, *50*, 382−387.
(2) Thomas, E. V.; Haaland, D. M. *Anal. Chem.* **1990**, *62*, 1091−1099.
(3) Ruyken, M. M. A.; Visser, J. A.; Smilde, A. K. *Anal. Chem.* **1995**, *67*, 2170−2179.
(4) Martens, H.; Naes, T. *Multivariate Calibration*; John Wiley & Sons: New York, 1989; Chapter 3.
(5) Nelson, M. P.; Aust, J. F.; Dobrowolski, J. A.; Verly, P. G.; Myrick, M. L. *Anal. Chem.* **1998**, *70*, 73−82.
(6) Bialkowski, S. *Anal. Chem.* **1986**, *58*, 2561−2563.

Novel Filter Design Algorithm for Multivariate Optical Computing

Olusola O. Soyemi[a*], Paul J. Gemperline[b], Lixia Zhang[a], DeLyle Eastwood[a], Hong Li[a], Michael L. Myrick[a]

[a]Dept. of Chem. and Biochem., University of South Carolina, Columbia SC 29208

[b]Dept. of Chem. and Biochem., East Carolina University, Greenville, NC 27858

ABSRACT

A new algorithm for the design of optical computing filters for chemical analysis otherwise known as Multivariate Optical Elements (MOEs), is described. The approach is based on the nonlinear correlation of the MOE layer thicknesses to the standard error in sample prediction for the chemical species of interest using a modified version of the Gauss-Newton nonlinear optimization algorithm. The design algorithm can either be initialized by random layer thicknesses or by a pre-existing design. The algorithm has been successfully tested by using it to design a MOE for the determination of copper uroporphyrin in a quaternary mixture of uroporphyrin (freebase), nickel uroporphyrin, copper uroporphyrin, and tin uroporphyrin.

Keywords: optical computing, thin films, chemometrics, spectroscopy, multivariate

1. INTRODUCTION

Multivariate calibration is a well-established tool in chemometrics for the correlation of a physical or chemical property of interest to multiple wavelength channels of optical spectra. (1-3) The conventional application of this tool in chemical analysis entails the acquisition of optical spectra in the appropriate wavelength region (typically from the ultraviolet to the mid-infrared). Next, chemometric tools are used to extract a spectral pattern (or regression vector), which is correlated to the property of interest but orthogonal to interferences (4). Prediction of the property in an unknown sample is carried out by determining the magnitude of the spectral pattern in the optical spectrum of the sample. More specifically, the magnitude is calculated by taking the inner product of the spectral pattern and the optical spectrum of the unknown compound. A major drawback in the widespread use of multivariate calibration, especially for field applications, is its dependence on expensive and bulky laboratory-type equipment for data acquisition and analysis.

In Multivariate Optical Computing (MOC), spectral patterns are encoded into the transmission spectrum of optical interference filters for the purpose of detecting spectral signatures for chemical prediction. Earlier reports by Myrick et al. (5,6), have shown that the prediction step can be optically mimicked by passing light of a fixed bandwidth (which has interacted with the sample either by transmittance through the sample or reflectance from the surface of the sample), through two optical filters whose transmission profiles combine to give a structure that accurately describe the positive and negative portions of the spectral pattern. A more recent study (7) has described a new approach to this method of optical computation, which uses a single filter for prediction.

A typical interference filter (coating) design consists of alternating layers of high- and low-refractive index materials with specified thicknesses. Interference coatings with irregular transmittance profiles are fabrication through the process of reactive magnetron sputtering (8). As was originally envisaged, the

* Correspondence: Email: soyemi@mail.chem.sc.edu; Telephone: 803 777 2652; Fax: 803 777 9521

Advanced Environmental and Chemical Sensing Technology, Tuan Vo-Dinh, Stephanus Buettgenbach, Editors, Proceedings of SPIE Vol. 4205 (2001) © 2001 SPIE. · 0277-786X/00/$15.00

A SIMPLE OPTICAL COMPUTING DEVICE FOR CHEMICAL ANALYSIS

Olusola O. Soyemi[a], Lixia Zhang[a], DeLyle Eastwood[a], Hong Li[a] Paul J. Gemperline[b], Michael L. Myrick[a*]

[a]Dept. of Chem. and Biochem., University of South Carolina, Columbia SC 29208
[b]Dept. of Chemistry, East Carolina University, Greenville, NC 27858

ABSTRACT

Multivariate Optical Computing (MOC) devices have the potential of greatly simplifying as well as reducing the cost of applying the mathematics of multivariate regression to problems of chemical analysis in the real world. These devices utilize special optical interference coatings known as multivariate optical elements (MOEs) that are encoded with pre-determined spectroscopic patterns to selectively quantify a chemical species of interest in the presence of other interfering species. A T-format prototype of the first optical computing device is presented utilizing a multilayer MOE consisting of alternating layers of two metal oxide films (Nb_2O_5 and SiO_2) on a BK-7 glass substrate. The device was tested by using it to quantify copper uroporphyrin in a quaternary mixture consisting of uroporphyrin (freebase), tin uroporphyrin, nickel uroporphyrin, and copper uroporphyrin. A standard error of prediction (SEP) of 0.86μM was obtained for copper uroporphyrin.

Keywords: optical computing, thin films, chemometrics, spectroscopy, interference coatings

1. INTRODUCTION

Multivariate calibration is an established tool in chemometrics for the correlation of a physical or chemical property of interest to information spanning multiple wavelength channels in optical spectroscopy[1-3]. The conventional application of this tool in chemical analysis entails first the acquisition of optical spectra in the appropriate wavelength region (typically from the ultraviolet to the mid-infrared). Next, chemometric tools are used to extract a spectral pattern (the regression vector) which is correlated to the property of interest but orthogonal to interferences[4]. Prediction of the property in an unknown sample is then carried out by determining the magnitude of the spectral pattern in the optical spectrum of the sample. More specifically, the magnitude is calculated by taking the inner product of the regression vector and the optical spectrum of the unknown sample. A major drawback in the widespread use of multivariate calibration, especially for field applications, is its dependence on expensive and bulky laboratory-type equipment for data acquisition and analysis.

A recent publication from our laboratory[5] addressed the feasibility of using optical computing in predictive spectroscopy to simplify and harden the apparatus necessary for chemical prediction from a theoretical standpoint. The first reports of a related hypothetical optical approach to multivariate chemical measurement were those of Bialkowski[6]. The use of a single MOE in a beamsplitter configuration has also been described for the same purpose[7], a permutation most similar to that proposed by Ryabenko and Kasparov[8]. The all-optical approach proposed by our laboratory differs from previous work by centering around the production of one or more optical interference coatings whose transmission spectra incorporate features of a spectral regression vector. Such interference filters based on multivariate spectroscopy will be referred to henceforth as multivariate optical elements (MOEs). MOEs have never been demonstrated as a tool for actual chemical measurement, however.

* Correspondence: Email: myrick@psc.sc.edu; Telephone: 803-777-6018; Fax: 803-777-9521.

...national Integration of Opto-Electro-Mechanical Devices and Systems, Michael R. Descour, ha T. Rantala, Editors, Proceedings of SPIE Vol. 4284 (2001) © 2001 SPIE · 0277-786X/01/$15.00

17

Interference filter refinement for artificial nose fluorescence sensing

Jeevananda Karunamuni, MEMBER SPIE
Katherine E. Stitzer
DeLyle Eastwood, MEMBER SPIE
University of South Carolina
Department of Chemistry
Columbia, South Carolina

Keith J. Albert, MEMBER SPIE
David R. Walt
Tufts University
The Max Tishler Laboratory for Organic Chemistry
Department of Chemistry
Medford, Massachusetts 02155

Steven B. Brown
Lawrence Livermore National Laboratory
P.O. Box 808, L-171
Livermore, California

Michael L. Myrick, MEMBER SPIE
University of South Carolina
Department of Chemistry
Columbia, South Carolina
E-mail: myrick@psc.sc.edu

Abstract. Optical interference coatings are used in filter-based *T*-format fluorimeters to make beamsplitters, bandpasses, and bandblocking filters that separate excitation and emission signals. Commercially available filters usually perform well in these applications, but better performance may be possible if the system of optical filters is tailored to the specific analysis. We provide a general method for designing optical filters for the optical train of a specific fluorescence sensor system simultaneously using two light-emitting diode (LED) excitation sources (blue and green) and two different fluorescent indicators. We approach the problem of designing the optics of the system by first constructing a hypothetical target spectrum for each filter using the optical spectrum of the excitation source, and the excitation and emission spectra of the fluorescence sensors. Structural designs for Nb_2O_5/SiO_2 multilayer interference filters are then synthesized. An iterative evaluation procedure is then used to improve the performance of the system for minimal leakage of the excitation sources onto our detector array. We also provide experimental results for the construction of these filters using reactive magnetron sputtering. [DOI: 10.1117/1.1367255]

Subject terms: fluorescence; interference filter; artificial nose; filter synthesis.

Paper 200269 received July 5, 2000; revised manuscript received Jan. 23, 2001; accepted for publication Jan. 29, 2001.

1 Introduction

One common type of optical instrument is the filter-based T-format (an epi-illumination geometry) fluorimeter. The purpose of such an instrument is to either directly measure an analyte's fluorescence intensity, or to interrogate a fluorescence transducer that is sensitive to an analyte concentration or an environmental condition, e.g., temperature. A basic T-format instrument has three arms: the excitation, detection, and sensor arms. It normally uses a beamsplitter of some type to separate the beam paths of the excitation and detection arms of the instrument, while combining them into a single optical train on the sensor arm. Optical filters are incorporated into these instruments because they reduce costs, have higher throughput efficiencies, and are smaller and thus more portable than other wavelength selection devices. Commercially available optical filters make the job of constructing a basic *T*-format system simple: once the excitation and emission wavelengths are defined for the sensor arm, and the excitation source and detector are selected, adequate filters for the application are often available from various companies that manufacture multilayer interference filters. A number of companies produce optical filters specifically for *T*-format instruments, among which are Omega Optical, Inc., Chroma, Inc., and Corion, Inc.

The recent introduction of fiber optic-based sensors for the measurement of various analytes using arrays of different fluorescence transducers[1–11] has complicated the design of these systems. For example, recent work by Walt et al.[6–11] focuses on previously developed "artificial nose" technology to detect low-level nitroaromatic vapors that may be present on the soil surface above buried land mines. This work employs an array of multiple transducer types for vapor detection by computational analysis.[6–11] Many of the available fluorescence-based transducers have different optimal excitation and emission wavelengths. One possible approach to instrument design for these array-based sensors is, in effect, to design a separate *T*-format system for each transducer. The basic concepts governing the design of such instruments is well known.[12,13] Another approach is to design more complex optics that permit a single instrument to excite and detect fluorescence of multiple transducers and/or analytes.

The complex combinations of excitation and emission spectra possible for these arrays has prompted us to investigate systematic means for filter selection or synthesis in systems combining fluorescence sensors with very different spectroscopies. It is often possible to retain the simple layout of a filter-based *T*-format instrument even when multiple excitation and emission bandpasses are needed. The purpose of the present report is to illustrate an integrated method for designing a complete system of optics for a sensor array, considering the details of light sources and the spectroscopies of more than one transducer type. In the following discussion, we consider a recent sensor package for 2,4,6-trinitrotoluene (TNT) vapor detection that resulted

 0091-3286/2001/$15.00

ELSEVIER

Vibrational Spectroscopy 28 (2002) 73–81

VIBRATIONAL SPECTROSCOPY

www.elsevier.com/locate/vibspec

A single-element all-optical approach to chemometric prediction

M.L. Myrick[a,*], O. Soyemi[a], J. Karunamuni[a], D. Eastwood[a], H. Li[a], L. Zhang[a], A.E. Greer[a], P. Gemperline[b,1]

[a]*Department of Chemistry and Biochemistry, University of South Carolina, Columbia, SC 29208, USA*
[b]*Department of Chemistry and Biochemistry, East Carolina University, Greenville, NC 27858, USA*

Received 1 August 2000; received in revised form 14 September 2001; accepted 17 September 2001

Abstract

A single-element approach to multivariate optical computing is described. Data for mixtures of Crystal Violet and Bismarck Brown dyes are analyzed as an example application. Radiometric information is combined with transmission spectra of the samples to obtain representative system responses for the samples. Direct synthesis of a multivariate optical element (MOE) is compared to a novel new approach for synthesizing simpler MOEs. The results show that less complex spectral vectors can be designed that perform adequately in this example. Experimental results for fabrication of an MOE are shown.

Keywords: Multivariate; Chemometrics; Optical computing; Thin films; Spectroscopy

1. Introduction

Multivariate spectroscopy is a powerful tool for analytical determinations of the chemical and physical characteristics of a wide range of sample types. In one common approach for applying multivariate modeling to chemical problems, a spectral pattern that correlates with a dependent variable is found. In subsequent measurements of unknown samples, predictions of the dependent variable are made by computing the magnitude of this spectral pattern in the optical spectrum of the unknown.

After collecting spectra of solutions containing various amounts of the component of interest and interferent(s), principal component analysis (PCA) is used to decompose this set of independent variables into a set of principal components (PCs). These PCs are linear combinations of the original variables and can be thought of as a new set of orthogonal axes in the space defined by the original spectra and their detector channels. The primary axis, PC1, is the vector which describes the greatest variability in the data, while each successive PC describes smaller variability. Principal component regression (PCR) is then used to relate the dependent variable (concentration of a component of interest) to the independent variables (the coordinates of each spectrum on the PCs). A regression vector is determined in this way which correlates with the dependent variable. A calibration curve can then be created by taking the direct product of each spectrum and the regression vector.

A recent report from this laboratory [1,2] describes an all-optical interference-filter-based approach to the last step in this procedure, the magnitude calculation

* Corresponding author. Tel: +1-803-777-9521; fax: +1-803-777-9521.
E-mail addresses: myrick@mail.chem.sc.edu (M.L. Myrick), gemperlinep@mail.ecu.edu (P. Gemperline).
[1] Fax: +1-252-328-6767.

0924-2031/02/$ – see front matter
PII: S0924-2031(01)00160-6

Multivariate optical elements simplify spectroscopy

BY MICHAEL MYRICK

Interference filters with carefully designed spectral properties perform optical computations for spectroscopic analysis that replace complex mathematical computations.

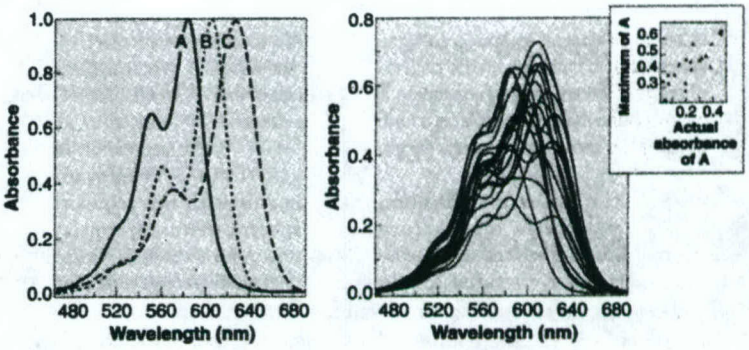

FIGURE 1. While the visible absorption spectra of three dyes are distinct from one another, they have a great deal of spectral overlap (left). For 21 mixtures of the three dyes (spectra at right), the absorbance of the mixtures at the maximum absorption wavelength of dye A as a function of the actual absorbance can be plotted (right, inset). This method of estimation can give poor results.

Pattern-recognition techniques can be applied to optical spectra of complex mixtures (gasoline, blood, environmental samples, and so on) for the purpose of detecting the presence of specific compounds, measuring their concentrations, or estimating properties that depend on sample chemistry. Based on multivariate (multiwavelength) calibration, this approach to chemical measurement is powerful, but is used infrequently because of the expense and complexity of the spectroscopic tools required. In contrast, instruments can be made with the mathematics of pattern recognition designed directly into optical interference filters. These filters extract information from light without recording a spectrum. This approach points to a revolution in low-cost, rugged, high-quality instruments.

The problem of interferents

Optical spectroscopy is an effective tool for "fingerprinting" the composition of matter. Identification of sample chemistry, however, requires that enough of the spectroscopic fingerprint be observed to be useful, which can require measurement at many different optical wavelengths. Sensible use of multiwavelength optical spectroscopy of complex samples requires techniques of simple multivariate pattern recognition and calibration.

Multivariate calibration is the process by which multivariate data are analyzed to reveal patterns specific to a chemical measurement. For example, when three different dyes whose optical absorption spectra overlap are mixed randomly to make solutions, estimating the concentration of one of the dyes (the analyte) from the spectra alone in the presence of the others becomes a complex process. The difficulty arises because the other dyes serve as "interferents"—that is, chemical species whose spectra are convoluted with that of the species we hoped to measure.

The simplest way to estimate the amount of one of the dyes in a three-dye mixture is to measure the absorbance of the mixtures at the wavelength of maximum absorbance of the analyte dye. A comparison of this estimation against the actual absorbance of the analyte in the mixtures usually shows poor results (see Fig. 1).

PCR: a mathematical approach

A better approach makes use of pattern recognition. Using a technique known as principal components regression (PCR), a pattern in the spectra of the mixtures can be identified that gives good prediction of the analyte (see Fig. 2).[1] A simple form of pattern recognition, PCR dramatically improves the estimation of analytes in the mixtures.

MICHAEL MYRICK is an associate professor in the Department of Chemistry and Biochemistry at the University of South Carolina, 631 Sumter Street, Columbia, SC 29208; email: myrick@mail.chem.sc.edu.

Application of multivariate optical computing to simple near-infrared point measurements

M. L. Myrick, O. O. Soyemi, M. V. Schiza, J. R. Farr, F. G. Haibach, A. E. Greer, H. Li, R. J. Priore

Department of Chemistry and Biochemistry
University of South Carolina
Columbia, SC 29208

ABSTRACT

Quantitative multivariate spectroscopic methods seek spectral patterns that correspond to analyte concentrations even in the presence of interferents. By embedding a spectral pattern that corresponds to a target analyte in an interference filter in a beamsplitter arrangement; bulky and complex instrumentation can be eliminated with the goal of producing a field-portable instrument. A candidate filter design for an organic analyte, of military interest, and an interferent is evaluated.

1. INTRODUCTION

Multivariate spectroscopy is a powerful tool for analytical determinations of the chemical and physical characteristics of a wide range of sample types. In one common approach for applying multivariate modeling to chemical problems, a spectral pattern that correlates with a dependent variable is found. In subsequent measurements of unknown samples, predictions of the dependent variable are made by computing the magnitude of this spectral pattern in the optical spectrum of the unknown. In this paper we were using transmission spectra of two organic compounds, one as analyte and one as interferent as proof of concept for chemicals of interest to the military in the near and mid infrared spectral region

A recent report from this laboratory [1,2] describes an all-optical interference-filter-based approach to the last step in this procedure, the magnitude calculation given by the scalar product of a regression vector with the spectrum of an unknown sample. The idea of using incoherent linear optical signal processing for computation of an analytical parameter in a sample mixture was described as early as 1986 by Bialkowski [3]. The all-optical approach taken by this laboratory centers on the production of one or more optical interference coatings whose transmission spectra incorporate features of the spectral regression vector. The concept behind this approach is shown schematically in Figure 1. An identified spectral property is transferred to a spectral target spectrum for an optical filter. This target is used to synthesize an optical coating design through an iterative procedure, and then the design is used to guide the fabrication of a device.

The present work describes background work toward the application of this general method in the near-infrared spectral region.

Instrumentation for Air Pollution and Global Atmospheric Monitoring, James O. Jensen, Robert L. Spellicy, Editors, Proceedings of SPIE Vol. 4574 (2002) © 2002 SPIE · 0277-786X/02/$15.00

Application of multivariate optical computing to near-infrared imaging

M. L. Myrick, O. O. Soyemi, F. G. Haibach, L. Zhang, A. E. Greer, H. Li, R. J. Priore, M. V. Schiza, J. R. Farr

Department of Chemistry and Biochemistry
University of South Carolina
Columbia, SC 29208

ABSTRACT

Rapid quantitative imaging of chemical species is an important tool for investigating heterogenous mixtures, such as laminated plastics, biological samples and vapor plumes. Using traditional spectroscopic methods requires difficult computations on very large data sets. By embedding a spectral pattern that corresponds to a target analyte in an interference filter in a beamsplitter arrangement; the chemical information in an image can be obtained rapidly and with a minimal amount of computation. A candidate filter design that is tolerant to the angles present in an imaging arrangement is evaluated in near-infrared spectral region for an organic analyte and an interferent.

1. INTRODUCTION

Optical spectroscopy coupled with multivariate mathematics is routinely used in analytical chemistry for species quantification and chemical/biomedical imaging. However, the widespread application of this type of analytical spectroscopy has been limited by heavy reliance on bulky and expensive multichannel instruments, as well as the need for fast computing technology to process the vast amounts of multivariate data that are generated. [1]. In 1986, Bialkowski proposed that optical filters could be designed to aid in this process [2], an idea refined by Ryabenko in 1991 [3] and our laboratory in 1998 [4]. In each of these studies, the use of an optical interference filter to project a spectral pattern out from collimated multiwavelength light was proposed, a simple form of optical computing. Recent reports of optical regression studies using conventional acousto-optical tunable spectrometer systems show the potential for such multivariate optical computing methods as supplements to, or replacements for, conventional spectrometer systems [5].

Our laboratory recently demonstrated this promise by designing, fabricating and characterizing the performance of an optical interference filter for a chemical measurement [6]. These interference filters, which we refer to as multivariate optical elements or MOEs, permit the estimation of chemical properties based on the measurement of a spectral pattern. While conventional spectroscopy is still needed to characterize samples so that a suitable spectral pattern on which to base an analytical measurement can be found, MOEs permit the magnitude of these spectral patterns to be measured without the necessity of recording spectra for unknown samples.

Vibrational Spectroscopy-based Sensor Systems, Steven D. Christesen, Arthur J. Sedlacek III, Editors,
Proceedings of SPIE Vol. 4577 (2002) © 2002 SPIE · 0277-786X/02/$15.00

Nonlinear Optimization Algorithm for Multivariate Optical Element Design

OLUSOLA O. SOYEMI, FREDERICK G. HAIBACH, PAUL J. GEMPERLINE, and MICHAEL L. MYRICK*

LifeScan Inc., 100 Gibraltar Dr., Milpitas, California 95035 (O.O.S.); Dept. of Chemistry and Biochemistry, University of South Carolina, Columbia, South Carolina 29208 (F.G.H., M.L.M.); and Dept. of Chemistry, East Carolina University, Greenville, North Carolina 27858 (P.J.G.)

A new algorithm for the design of optical computing filters for chemical analysis, otherwise known as multivariate optical elements (MOEs), is described. The approach is based on the nonlinear optimization of the MOE layer thicknesses to minimize the standard error in sample prediction for the chemical species of interest using a modified version of the Gauss–Newton nonlinear optimization algorithm. The design algorithm can either be initialized with random layer thicknesses or with layer thicknesses derived from spectral matching of a multivariate principal component regression (PCR) vector for the constituent of interest. The algorithm has been successfully tested by using it to design various MOEs for the determination of Bismarck Brown dye in a binary mixture of Crystal Violet and Bismarck Brown.

Index Headings: **Optical computation; Chemometrics; Principal component regression; PCR; Nonlinear optimization.**

INTRODUCTION

Multivariate calibration is a well-established tool in chemometrics for the correlation of a physical or chemical property of interest to multiple wavelength channels of optical spectra.[1-3] The conventional application of this tool in chemical analysis entails the acquisition of optical spectra in the appropriate wavelength region (typically from the ultraviolet to the mid-infrared). Next, chemometric tools such as principal component regression (PCR) and partial least-squares (PLS) are used to estimate multivariate regression vectors correlated to the property of interest but orthogonal to interferences.[4] Prediction of the property in an unknown sample is carried out by taking the inner product of the spectral pattern in the regression vector with the optical spectrum of the unknown compound. A major drawback in the widespread use of multivariate calibration, especially for field applications, is its dependence on expensive and bulky laboratory-type equipment for data acquisition and analysis.

In multivariate optical computing (MOC), spectral patterns are encoded into the transmission spectrum of optical interference filters for the purpose of chemical prediction. Earlier reports by Myrick et al. have shown that the prediction step in multivariate calibration can be optically mimicked by passing light of a fixed bandwidth that has interacted with the sample through two optical filters whose combined transmission profiles accurately describe the positive and negative portions of the spectral patterns in a multivariate regression vector.[5,6] A more recent study has described a new approach to this method of optical computation that uses a single filter for prediction.[7]

A typical interference filter consists of alternating layers of high- and low-refractive index materials with specified thicknesses. Interference coatings with irregular transmittance profiles are fabricated through the process of reactive magnetron sputtering (RMS).[8] An initial approach to filter design entailed the transfer of a predetermined spectral pattern to the optical coating by a process of iterative synthesis.[9] This filter design technique synthesizes a multilayer coating by minimizing a merit function (F) that describes the sum of squared differences between the desired spectral pattern (e.g., a multivariate regression vector) and the filter's computed spectral pattern. A generic form of the merit function is shown in Eq. 1, where Z_j^D is the calculated response (e.g., filter transmittance) at wavelength j, Z_j is the target value, Tol_j is the design tolerance, m is the number of discretely sampled wavelengths, and k is a gain factor used to change the relative importance of the mismatched regions (with integer values of 1, 2, 4, or 16).

$$F = \left(\frac{1}{m} \sum_{j=1}^{m} \frac{|Z_j^D - Z_j|^k}{Tol_j} \right)^{1/k} \quad (1)$$

A variant of this approach has been used by Heavens and Liddell[10] to create a filter design algorithm that minimizes the following function:

$$F(x) = \sum_{k=1}^{m} [R_0(\lambda_k) - R(x, \lambda_k)]^2 \quad (2)$$

where x is the vector of design variables (optical coating layers), R_0 is the specified reflectance at wavelength λ_k, and R is the computed value of reflectance at λ_k for particular values of x. For multivariate calibration problems, however, the complex spectral patterns encoded in regression vectors result in filter designs with a large number of layers when using this approach. Multilayer filters having an excessive thickness tend to have rough surfaces that scatter incident radiation, absorb significant amounts of incident light, and break easily due to increased internal stress.

As a way of overcoming this limitation in filter design, we present the description of two alternative design algorithms that can result in designs having substantially fewer layers. Both methods employ a nonlinear least-squares optimization technique to design an optical coating that minimizes the sample prediction error for the chemical species of interest. In other words, instead of

Received 9 June 2001; accepted 13 November 2001.

* Author to whom correspondence should be sent.

0003-7028/02/5604-0477$2.00/0

Design of angle-tolerant multivariate optical elements for chemical imaging

Olusola O. Soyemi, Frederick G. Haibach, Paul J. Gemperline, and Michael L. Myrick

Multivariate optical elements (MOEs) are multilayer optical interference coatings with arbitrary spectral profiles that are used in multivariate pattern recognition to perform the task of projecting magnitudes of special basis functions (regression vectors) out of optical spectra. Because MOEs depend on optical interference effects, their performance is sensitive to the angle of incidence of incident light. This angle dependence complicates their use in imaging applications. We report a method for the design of angle-insensitive MOEs based on modification of a previously described nonlinear optimization algorithm. This algorithm operates when the effects of deviant angles of incidence are simulated prior to optimization, which treats the angular deviation as an interferent in the measurement. To demonstrate the algorithm, a 13-layer imaging MOE (IMOE, with alternating layers of high-index Nb_2O_5 and low-index SiO_2) for the determination of Bismarck Brown dye in mixtures of Bismarck Brown and Crystal Violet, was designed and its performance simulated. For angles of incidence that range from 42° to 48°, the IMOE has an average standard error of prediction (SEP) of 0.55 μM for Bismarck Brown. This compares with a SEP of 2.8 μM for a MOE designed by a fixed-angle algorithm.

OCIS codes: 110.2960, 110.2970, 120.4610, 070.5010, 070.4790.

1. Introduction

Optical spectroscopy coupled with multivariate mathematics is routinely used in analytical chemistry for species quantification and chemical and biomedical imaging. However, the widespread application of this type of analytical spectroscopy has been limited by heavy reliance on bulky and expensive multichannel instruments, as well as the need for fast computing technology to process the vast amounts of multivariate data that are generated.[1] In 1986, Bialkowski proposed that optical filters could be designed to aid in this process,[2] an idea refined by Kasparov and Ryabenko in 1991[3] and by our laboratory in 1998.[4] In each of these studies, use of an optical interference filter to project a spectral pattern out from collimated multiwavelength light was proposed, a simple form of optical computing. Recent reports of optical regression studies that use conventional acousto-optical tunable spectrometer systems show the potential for such multivariate optical computing methods as supplements to, or replacements for, conventional spectrometer systems.[5]

Our laboratory recently demonstrated this promise by designing, fabricating, and characterizing the performance of an optical interference filter for a chemical measurement.[6] These interference filters, which we refer to as multivariate optical elements or MOEs, permit the estimation of chemical properties based on the measurement of a spectral pattern. Although conventional spectroscopy is still needed to characterize samples so that a suitable spectral pattern on which to base an analytical measurement can be found, MOEs permit the magnitude of these spectral patterns to be measured without having to record spectra for unknown samples.

A further application for MOEs is as color-separation-type elements in imaging systems. Hypothetically, a MOE can be designed to provide immediate imaging of chemical distributions. For example, if light from a scene (the source scene) transmitted through a MOE were imaged and mapped to the red channel of a red-green-blue display, while the reflectances were imaged and mapped to the green and blue channels of the same display, the resulting image should contain an implicit color coding of the MOE projection of the light source. However, this relatively simple concept is compli-

O. O. Soyemi is with LifeScan, Incorporated, Milpitas, California 95035. F. G. Haibach and M. L. Myrick (myrick@mail.chem.sc.edu) are with the Department of Chemistry and Biochemistry, University of South Carolina, Columbia, South Carolina 29208. P. J. Gemperline is with the Department of Chemistry, East Carolina University, Greenville, North Carolina 27858.

Received 10 July 2001; revised manuscript received 27 November 2001.

On-line reoptimization of filter designs for multivariate optical elements

Frederick G. Haibach, Ashley E. Greer, Maria V. Schiza, Ryan J. Priore, Olusola O. Soyemi, and Michael L. Myrick

An automated method for producing multivariate optical element (MOE) interference filters that are robust to errors in the reactive magnetron sputtering process is described. Reactive magnetron sputtering produces films of excellent thickness and uniformity. However, small changes in the thickness of individual layers can have severe adverse effects on the predictive ability of the MOE. Adaptive reoptimization of the filter design during the deposition process can maintain the predictive ability of the final filter by changing the thickness of the undeposited layers to compensate for the errors in deposition. The merit function used, the standard error of calibration, is fundamentally different from the standard spectrum matching. This new merit function allows large changes in the transmission spectrum of the filter to maintain performance. © 2003 Optical Society of America

OCIS codes: 000.1570, 200.4560, 120.4570, 120.4610, 120.6200, 310.0310.

1. Introduction

In chemical systems, one is often interested in the concentration of a single component, the analyte, in the presence of other chemical compounds. In remote sensing applications, or when rapid analysis is needed, spectroscopy is often the method of choice. However, it can be difficult to find regions in the spectrum where only the analyte absorbs. In particularly difficult situations, the other compounds may absorb at all wavelengths that the analyte does. These other compounds are known as spectroscopic interferents.

Multivariate calibration provides quantitative results from these types of system. Typically the analyte concentration in solution is the variable of interest. The analyte concentration is predicted when the optical spectrum is projected onto a set of orthogonal loading vectors.[1,2] Each loading vector L accounts for a linear change in the predicted variable. If there are multiple effects, such as optical absorption by interferents, or if the effect is nonlinear, then many loading vectors may be needed to predict the variable. Typically, we restrict ourselves to cases in which only one loading vector is needed to predict a given property. The process of building a calibration model and prediction is typically carried out with a digital computer, a spectrometer, and an experienced analyst. The substitution of the computer and the spectrometer with a simple filter instrument offers the potential of increased reliability and lower cost.

Multivariate optical computing is a technique that utilizes optical interference effects to perform the fundamental mathematical operations required for the chemometric prediction of component species from their optical spectra.[3–15] A multivariate optical element (MOE) constructed as an interference filter can represent only one loading vector.

To have predictive accuracy, the single loading vector must be chosen so that it is orthogonal to the spectral patterns of the interferents and have a spectral component parallel to the analyte.

We chose to encode the loading vector into a filter using both the reflection and the transmission characteristics of an interference filter.[7,10,14] To accomplish this, we use a loading vector that is a function of the difference of the transmittance $\mathbf{T}$ and reflectance $\mathbf{R}$ of a multilayer interference filter held at 45° to predict the concentration of the sample $\hat{y}$ from the light transmitted through the sample $\mathbf{x}$.

$$\hat{y} = G(\mathbf{T} - \mathbf{R}) \cdot \mathbf{x} + \text{offset}. \quad (1)$$

F. G. Haibach, A. E. Greer, M. V. Schiza, R. J. Priore, and M. L. Myrick (myrick@mail.chem.sc.edu) are with the Department of Chemistry and Biochemistry, University of South Carolina, 631 Sumter Street, Columbia, South Carolina 29208. O. O. Soyemi is with LifeScan, Incorporated, 100 Gibraltar Drive, Milpitas, California 95035.

Received 17 May 2002; revised manuscript received 13 November 2002.

0003-6935/03/101833-06$15.00/0

Electrochemical and Solid-State Letters, **6** (10) B42-B45 (2003)
0013-4651/2003/6(10)/B42/4/$7.00 © The Electrochemical Society, Inc.

Growth and Characterization of a Porous Aluminum Oxide Film Formed on an Electrically Insulating Support

Paul G. Miney, Paula E. Colavita, Maria V. Schiza, Ryan J. Priore, Frederick G. Haibach, and Michael L. Myrick[z]

Department of Chemistry and Biochemistry, University of South Carolina, Columbia, South Carolina 29208, USA

Thin films of porous anodic aluminum oxide have been prepared on an electrically insulating support by the anodization of aluminum films sputtered onto glass slides. The resulting transparent aluminum oxide films were characterized by scanning electron microscopy and variable angle ellipsometry. Subsequently, the film was modeled from the ellipsometric data taken. An underlying conductive medium is not necessarily needed to bring about nearly complete anodization of the aluminum layer.

Manuscript submitted February 10, 2003; revised manuscript received May 26, 2003. Available electronically July 29, 2003.

The anodization (anodic oxidation) of aluminum metal in certain strong acid electrolytes leads to the formation of an anodic oxide film on its surface. This film is comprised of a relatively thick porous outer layer with regularly spaced pores extending from the outer surface toward the metal substrate, and a relatively thin nonporous barrier layer adjacent to the metal/oxide interface. With increasing anodization time, the metal is converted to oxide at the metal/oxide interface, and the pores extend further into the film.[1,2] This porous oxide typically exhibits a uniform array of hexagonal cells, each cell containing a cylindrical pore.[3] Many variations of the anodizing process have been used, typically employing sulfuric,[4-6] oxalic,[7,8] and phosphoric acid[9,10] electrolytes. In recent years, various research teams have formed porous anodic aluminum oxide from aluminum layers sputter-deposited onto tantalum,[11,12] titanium,[13] and silicon substrates.[14,15] Very recently, Chu *et al.*[16] have described the formation of porous aluminum oxide on glass substrates coated with tin-doped indium oxide (ITO) and silicon dioxide (SiO_2) films. The ITO film was used as a conductive medium to bring about complete anodization of the aluminum metal, as most investigators assume an underlying conductor is a requirement for complete conversion. However, Das and McGinnis[15] have claimed that they have formed porous anodic aluminum oxide from aluminum evaporated onto both silicon and glass, although they report only one study where p-doped silicon was used as a substrate.

Here, we present a study of the anodization of aluminum films sputter-deposited onto an electrically insulating support (a plain float glass microscope slide) with no additional electrode materials than the aluminum film itself. Aluminum is among the most optically dense metals, so that incomplete conversion to the oxide should be sensitively detected by optical methods. The model obtained from ellipsometry data suggests that the aluminum is almost completely anodized, leaving only a 1.2 nm average thickness of metallic aluminum behind. Because of the important role that alumina plays as a substrate for catalysis, it is hoped that this result will lead to further developments where other, more common insulating materials (such as cloth or paint) can be used as substrates for aluminum oxide formation.

Experimental

Plain, precleaned microscope slides (25 × 75 × 1.2 mm), commercially available from Fisher Scientific, were used as supports. Prior to aluminum deposition, these slides were further cleaned by a piranha etch which consisted of a 3:1 solution of sulfuric acid (Fisher Scientific) and 30% hydrogen peroxide (Mallinckrodt).[a] Following this, they were rinsed with copious amounts of deionized water. All aqueous solutions were prepared with deionized water.

An aluminum layer with an approximate thickness of 500 nm was produced by magnetron sputtering in a vacuum chamber (CVC). The layer was produced in nine cycles (approx. 57.3 nm per cycle). The aluminum target (Pure Tech) had a purity of 99.99%. The base chamber pressure was 5×10^{-6} Torr or lower. The chamber was pumped down using a helium cryopump (Cryo-Torr, Helix Technology Corporation) and was backed up by a mechanical pump (Varian DS 402). The argon (99.9999%, Matheson Tri-Gas) flow rate was 16 cm^3 min^{-1} and the sputtering power was 2.0 kW. After the sputtering process, the back side of the slide was scribed with a diamond pen and was cut into three 25 × 25 mm pieces (each of which was used as a sample). Prior to anodization, the samples were degreased in acetone. The anodization of aluminum was carried out using a regulated dc power supply (EC-420) in a 10% phosphoric acid solution (Fisher Scientific). The samples were anodized at 80 ± 2 V at 298 K while the electrolyte was mechanically stirred. A platinum gauze was used as a counter electrode. Electroplating tape (3M) was placed across the width of the aluminum coated side of the sample where it crossed the solution/air interface when the sample was placed in solution. This was done because we had previously observed this region to be very active in anodization, causing a thin section of aluminum at this interface to erode across the entire width of the sample, breaking the electrical contact to the rest of the film. Covering this interface area eliminated the problem. Electroplating tape was also placed on the back side of the sample to provide a visual background for the anodization process (as described below). The change in current throughout the anodization process was monitored by a multimeter. The anodization process was also monitored photographically.

The morphology and microstructure of the anodized samples were characterized using a scanning electron microscope (SEM, Hitachi S-2500) with the samples sputtered with a thin film of gold to avoid the effect of charging. Side views of the films were made by scribing the reverse side of the glass slide and breaking the sample to reveal a cross section before metallizing for SEM.

Ex situ spectroscopic ellipsometry was also used to characterize the porous alumina layer. The spectroscopic polarization data were acquired at 60, 65, 70, and 75° incident angles and over a spectral range of 300-800 nm using a J.A. Woollam Co. V-VASE ellipsometer. This particular instrument employs a retarder to permit measurement of depolarization and anisotropy. The range of angles was chosen to maximize the variation in the acquired Δ and Ψ data for aluminum.

Ellipsometric models were developed for each material. The glass layer model was built from ellipsometric measurements of a clean microscope slide, identical to the one on which the aluminum film was deposited, using the Sellmeier formula and a Tauc-Lorentz absorption in the UV range. The aluminum layer was described using the Sellmeier formula[17] and Tauc-Lorentz absorption.[18] The effects of surface roughness and a native oxide layer were removed by including these layers in the model of the aluminum ellipsometric

[a] N.B. Extreme caution should be exercised when handling this solution.

[z] E-mail: myrick@mail.chem.sc.edu

Full Paper

A New Optically Reflective Thin Layer Electrode (ORTLE) Window: Gold on a Thin Porous Alumina Film Used to Observe the Onset of Water Reduction

*Paul G. Miney, Maria V. Schiza, Michael L. Myrick**

Department of Chemistry and Biochemistry University of South Carolina, Columbia, SC 29208;
*e-mail myrick@mail.chem.sc.edu

Received: July 1, 2003
Final version: September 8, 2003

Abstract
The fabrication and unique characteristics of a new type of thin layer electrode, an optically reflective thin layer electrode (ORTLE), are described. The electrode was fabricated by the anodization of a thin layer of aluminum sputtered onto a plain glass microscope slide to create a 750 nm-thick porous alumina film. A thin film of gold was then sputtered atop the porous and transparent alumina film. The gold layer remained porous to allow solution into the pores but was optically thick and reflective. Reflectance measurements made through the microscope slide did not interrogate the bulk solution, but show spectral features that shift with the optical properties of the material filling the pores of the alumina film. A simple series of experiments, in which the potential of the ORTLE was stepped negatively to various values in an aqueous sodium sulfate solution, shows that interference fringes shift measurably in the ORTLE spectrum at potentials several hundred millivolts positive of the potential at which gas evolution was visible to the naked eye.

Keywords: OTTLE, Porous alumina, Spectroelectrochemistry, Specular reflectance spectroscopy

1. Introduction

Spectroelectrochemistry is a combination of electrochemical and spectroscopic techniques in which optical measurements are referred to the potential of a working electrode. Thin-layer spectroelectrochemistry is possibly the simplest type of spectroelectrochemistry and has advantages such as rapid and exhaustive electrolysis and small volume features [1]. Since the first report in 1967 [2], optically transparent thin layer electrodes (OTTLEs) have been used for such thin layer studies [3–5]. A typical application of an OTTLE is the spectroscopic study of redox processes [6–8]. Various spectroscopic techniques such as luminescence spectroscopy [6], FTIR difference spectroscopy [9] and UV/vis/NIR [10–12] have been coupled with electrochemical techniques via OTTLEs, and a variety of OTTLE designs for many purposes have been developed [13–15].

As a consequence of our work with nanoelectrode arrays [16, 17] we have carried out studies into the anodization of aluminum thin films on various substrates. We recently reported a study of the anodization of aluminum thin films sputtered onto an electrically insulating substrate – a plain float glass microscope slide [18]. The resulting porous aluminum oxide (alumina) films are transparent and contain pores varying from approximately 80 to 100 nm in diameter. In this article, we describe the design and characterization of a new type of thin layer electrode which is a variation on the concept of an OTTLE. The essential difference between an OTTLE and our new electrode is that reflectance is collected instead of transmittance. For this reason, the electrode is called an optically reflective thin layer electrode (ORTLE) in the following discussion. This new electrode is based on the porous alumina thin films in [18]. In the case of the ORTLE, spectroscopy interrogates a solution phase within the pores of the alumina film between the electrode face and a window behind it. The electrode is created by thin-film deposition of gold onto the exposed face of the porous alumina, creating a gold electrode filled with holes having a diameter much less than the wavelength of visible light. The thickness of the alumina film – and thus the depth of the pores – can be altered by controlling the thickness of the original aluminum film. Through the use of a combination of specular reflectance spectroscopy and chronoamperometry, we can confine our spectroelectrochemical study to that solution contained within the pores. The ORTLE described here interrogates the thinnest sample of which the authors are aware and is the first based on porous alumina. In this report, we describe the preparation of the ORTLE in detail, plus how the ORTLE is incorporated into spectroscopic measurements. We also characterize the stability of the ORTLE spectrum and its origin, and show how an applied potential affects the observed spectrum in a simple solution.

  DOI: 10.1002/elan.200302926

Miniature Stereo Spectral Imaging System for Multivariate Optical Computing

RYAN J. PRIORE, FREDERICK G. HAIBACH, MARIA V. SCHIZA, ASHLEY E. GREER, DAVID L. PERKINS, and M. L. MYRICK*

Dept. of Chemistry and Biochemistry, University of South Carolina, Columbia, South Carolina 29208 (R.J.P., M.V.S., A.E.G., D.L.P., M.L.M.); and Detect-X, Inc., 2150 Northwest Parkway, Marietta, Georgia 30067 (F.G.H.)

Index Headings: **Optical computation; Optical fabrication; Stereoimaging; Thin films.**

INTRODUCTION

Chemical or hyperspectral imaging is a rapidly developing field that has applications ranging from materials characterization to remote environmental sensing.[1] Thanks to developments in processing and instrumentation over the past two decades,[2–4] it is now possible to use hyperspectral imaging routinely in the laboratory.[5–9] However, the technique still suffers from long data collection times and the need for post-collection computer processing.[10] Other than satellite remote earth sensing, uses of hyperspectral imaging outside the laboratory have been limited because of the restricted portability of most instruments. Speed, size, maintenance, sensitivity, complexity, and cost remain significant challenges to widespread adoption of hyperspectral measurement platforms outside a laboratory or satellite setting.

Interference filter based multivariate optical computing (MOC) attempts to combine the data collection and processing steps of a traditional multivariate chemical analysis in a single step, offering an all-optical computing technology with no moving parts.[11] MOC instruments have characteristics that lend themselves well to compact, portable, rapid, and sensitive imaging of multivariate information content in optical spectra. In filter-based MOC, a specialized interference filter called a multivariate optical element (MOE) is used as an optical beamsplitter. The intensity difference between the light rays that are transmitted and reflected by the MOE is designed to equate to the magnitude of a specific multivariate pattern in the light spectrum. Details of the theory and design of these MOEs have been previously reported.[12–14] Traditional MOEs are designed to perform with collimated light for point detection measurements, and they require two separate point detectors. MOEs can also be designed for chemical imaging applications by a modified design process.[15]

In this report, we present a catadioptric optical system designed for MOE stereo imaging applications. Catadioptric systems incorporate both reflective and refractive components into the optical system and have been explored by several researchers.[16] The system reported is based on a rectified catadioptric imager that allows both the transmitted- and reflected-light MOE images to be collected simultaneously by a single ¼-inch miniature charge-coupled device (CCD) detector. To demonstrate this miniature stereoimaging prototype, *Bacillus globigii* spore solutions were deposited on a paper background to serve as targets for a simple MOE-type imaging system. We report sample, light source and detector response spectra, instrumental prototype design and fabrication results, and example data.

EXPERIMENTAL

The diffuse reflectance imaging instrument was fabricated in house. Four ¼-inch right angle prisms (Edmund Industrial Optics, Barrington) and an aluminum coated glass slide (Fisher Scientific, Pittsburgh, PA) were used to form the stereo imaging block, enabling a single camera to collect both transmittance and reflectance images simultaneously. This is shown in Fig. 1.

A monochrome CCD camera (model WAT-660A, Watec America Corp., Las Vegas, NV) was radiometrically calibrated as the detector using an OL Series 750D grating double-monochromator (Optronic Laboratories, Inc., Orlando, FL). Battery-powered light emitting diodes (LEDs) (5 blue, model E198, λ_{max} = 430 nm and 2 yellow, model E472, λ_{max} = 595 nm, Gilway, Woburn) were calibrated as the source package against an OL Series 455 integrating sphere calibration standard lamp (Optronic Laboratories, Inc.) using the same system used to calibrate the camera. The CCD camera spectral sensitivity and LED spectral intensity are shown in Fig. 2.

A 23-layer bandpass filter was developed using a library design and fabricated using power and time estimates by reactive magnetron sputtering (RMS) onto the hypotenuse of a single prism. The block was masked, sand blasted, and coated with graphite adhesive (Electron Microscopy Sciences, Fort Washington, PA) to reduce stray light and cemented together with lens bond (type DB–99, Summers Optical, Fort Washington, PA). A drop of *Bacillus globigii* suspension (concentration = 26.09 × 10^7 spores/mL) was placed on a paper envelope and imaged with the miniature prototype controlled by a Hewlett Packard IPAQ (model 3870, Palo Alto, CA) equipped with a LifeView, Inc. FlyJacket (Fremont, CA).

Received 10 September 2003; accepted 22 March 2004.
* Author to whom correspondence should be sent.

CONCLUSION

The results presented in this work demonstrate the usefulness of 2D Raman correlation spectroscopy in determining the glycosidic linkages in amylose and amylopectin, which are not readily obtainable from conventional one-dimensional spectra.

The intensity of the 954 cm^{-1} band exhibits an increase with the amylose amount, while the 938 and 850 cm^{-1} bands decrease. The asynchronous spectrum indicates that the spectral intensity reduction of the 938 and 850 cm^{-1} bands happens before the intensity increase of the 954 cm^{-1} band. All of the observations suggest that that the 954 and 938 cm^{-1} bands be assigned to symmetric C–O–C stretching modes involving the α-D-(1→4) linkages and the α-D-(1→6) linkages in amylose and amylopectin, respectively, while the 850 cm^{-1} band should be assigned to symmetric C–O–C vibrations (ring breathing) in the glucose unit.

In addition, the appearance of several additional bands around 954, 938, and 850 cm^{-1} represents the effects of various conformational structures of the glucose unit and the interactions through hydrogen bonding on the vibrational environments of the C–O–C fractions.

ACKNOWLEDGMENTS

The authors wish to express their sincere thanks to Prof. James de Haseth of University of Georgia, Georgia, for the discussion of band assignments and Ms. Jennifer Herringa of ARS/USDA, Georgia, for recording the Raman spectra.

1. D. A. Rees, *Polysaccharide Shapes* (John Wiley and Sons, New York, 1977).
2. Y. Pomeranz, Ed., *Wheat: Chemistry and Technology* (American Association of Cereal Chemists, Inc., St. Paul, MN, 1988), vol. 1, 3rd ed., pp. 277–296.
3. J. J. Cael, J. L. Koenig, and J. Blackwell, Carbohydr. Res. **29,** 123 (1973).
4. J. L. Koenig, J. Polym. Sci., Part D **6,** 59 (1972).
5. F. S. Parker, *Applications of Infrared, Raman, and Resonance Raman Spectroscopy in Biochemistry* (Plenum Press, New York, 1983), pp. 315–347.
6. D. Phillips, J. Xing, H. Liu, D.-H. Pan, and H. Corke, Cereal Chem. **76,** 821 (1999).
7. D. S. Himmelsbach, F. E. Barton, A. M. McClung, and E. T. Champagne, Cereal Chem. **78,** 488 (2001).
8. J. R. Ferraro and K. Nakamoto, *Introductory Raman Spectroscopy* (Academic Press, San Diego, CA, 1994).
9. P. R. Carey, *Biochemical Applications of Raman and Resonance Raman Spectroscopies* (Academic Press, New York, 1982).
10. Y. Ozaki, "Raman Spectroscopy", in *Spectral Methods in Food Analysis,* M. M. Mossoba, Ed. (Marcel Dekker, New York, 1999), pp. 427–462.
11. I. Noda, "Progress in 2D Correlation Spectroscopy", in *Two-Dimensional Correlation Spectroscopy,* Y. Ozaki and I. Noda, Eds. (American Institute of Physics, AIP conference proceedings 503, Melville, New York, 2000), pp. 3–17.
12. I. Noda, Y. Liu, and Y. Ozaki, J. Phys. Chem. **100,** 8674 (1996).
13. K. Ebihara, H. Takahashi, and I. Noda, Appl. Spectrosc. **47,** 1343 (1993).
14. A. T. Tu, J. Lee, and Y. C. Lee, Carbohydr. Res. **67,** 295 (1978).
15. A. T. Tu, J. Lee, and F. P. Milanovich, Carbohydr. Res. **76,** 239 (1979).
16. D. L. Vien, N. B. Colthup, W. G. Fateley, and J. G. Grasselli, *The Handbook of Infrared and Raman Characteristic Frequencies of Organic Molecules* (Academic Press, New York, 1991), p. 68.

Effects of Autoclaving on Bacterial Endospores Studied by Fourier Transform Infrared Microspectroscopy

D. L. PERKINS, C. R. LOVELL, B. V. BRONK, B. SETLOW, P. SETLOW, and M. L. MYRICK*

Department of Chemistry and Biochemistry, University of South Carolina, 631 Sumter St., Columbia, South Carolina 29208 (D.L.P., M.L.M.); Department of Biological Sciences, University of South Carolina, Columbia, South Carolina 29208 (C.R.L.); Air Force Research Laboratory at U.S. Army Edgewood Chemical Biological Center, Aberdeen Proving Ground, Maryland 21010-5424 (B.V.B.); and Department of Molecular, Microbial and Structural Biology, University of Connecticut Health Center, Farmington, Connecticut 06030 (B.S., P.S.)

Index Headings: **Bacteria; Bacillus; Clostridium; Endospores; Fourier transform infrared spectroscopy; Microspectroscopy; Autoclaving.**

INTRODUCTION

Classifying, discriminating, and identifying endospores of bacteria are extremely important due to the pathogenic properties possessed by some of these microorganisms. Although many biochemical techniques exist and are well established, there exists a need for rapid, complementary techniques to screen for bacteria that present a public health problem. Although not directly used as a screening tool, a common technique used by health care institutions and other organizations in the study of microorganisms is the autoclaving process. For example, it is used routinely to sterilize materials and instruments in medical and research applications. Autoclaving provides sterilization by employing pressurized steam (15 psi) to obtain a saturation temperature of 121 °C. The intense heat and pressure of autoclaving denatures and damages macromolecules and subcellular structures including proteins, cytoplasmic membranes, and nucleic acids, and if done correctly, autoclaving is a very dependable method for sterilization.

Fourier transform infrared (FT-IR) spectroscopy has been utilized in the past by others to classify, discriminate, and identify species of bacteria.[1–5] This work has shown that the mid-infrared spectral absorptions of whole vegetative bacterial cells are highly specific fingerprints, and it is possible to differentiate bacteria down to the subspecies level utilizing multivariate analysis. Furthermore, FT-IR has also been used to identify cellular components, or bio-markers, of both bacteria and bacterial endospores.[6–9]

The aim of this study is to evaluate the effect of the autoclaving process on bacterial endospores of *Bacillus*

Received 22 September 2003; accepted 28 January 2004.

* Author to whom correspondence should be sent.

Precision in multivariate optical computing

Frederick G. Haibach and Michael L. Myrick

Multivariate optical computing (MOC) is an instrumentation design concept for optically demultiplexing the spectroscopic signals in radiometric measurements. The advantages of optically demultiplexing are improved precision, optical throughput, improved reliability, and reduced cost of instrumentation. Conceptually, the instrument implements a multivariate regression vector whose dot product with the spectrum yields a single value related to a spectroscopically active physical property of interest. Instrumentation designs for implementing MOC are diverse, and there has been no systematic comparison of the performance of these designs. This report develops a general expression for comparing the precision of the different instrumentation designs of MOC. Additionally, an expression is given for the transition from low- to high-signal-limited performance of MOC instrumentation. These two general expressions are applied to the traditional multivariate analysis and five examples of MOC.

OCIS codes: 000.1570. 120.4570, 120.4610. 120.5630. 120.6200. 200.4560. 200.4860.

1. Introduction

The goal of multivariate optical computing (MOC) is the construction of spectroscopic instrumentation that is simple and rugged enough to place in the hands of a nonexpert and that yet captures the advantages of classic multivariate calibration methods. Several related approaches to MOC have now been developed to achieve this goal. Some methods are based on optical interference filters known as multivariate optical elements (MOEs).[1] Others rely on acousto-optical tunable filters or other tunable wavelength selectors.[2–4] Still others might rely on spectrometers employing digital mirror array technology[5–7] or holographic gratings. Each of these approaches has advantages and disadvantages.

A key factor differentiating MOC approaches is their relative level of measurement precision. In their report on MOC,[1] Nelson *et al.* made estimates of noise in MOC compared with traditional spectroscopy. Prakash *et al.* later evaluated signal-to-noise ratios for an acousto-optical tunable filter MOC instrument.[2] However, no systematic comparisons of precision in the variants of interference-filter-based MOC instrumentation[1,8–10] have yet been made. Understanding how the shape and amplitude of the transmission function of a given interference filter affect precision is also important for comparing MOE filter designs, yet few analytical expressions exist to permit this comparison.[11] The lack of general expressions for measurement precision in MOC is the motivating factor for this paper.

In this paper, measurement-precision expressions are developed from a generalized approach. We have followed, to the extent possible, the approach taken by Prakash *et al.*[2] but with a more explicit treatment of signal intensities and measurement time. Signal intensities are divided into channels to reflect the fact that most measurements are recorded either wavelength by wavelength or as a series of simultaneous detector samples (i.e., a diode array). This nomenclature is retained in the discussion of MOC measurements for ease of comparison, even though many of these measurements are not so divided. Total experiment time is used as a parameter in the general discussion to permit comparison of measurements that more efficiently sample light, for example, by recording all wavelengths simultaneously, with those that sample inefficiently (e.g., one wavelength at a time).

The approach we take in Section 2 is to first obtain a set of simple equations describing measurement variance in general terms. Next, we show how these simple equations can be applied to real measurements by a series of instrument types. We have necessarily made some approximations. For exam-

F. G. Haibach is with Detect-X, Incorporated, 2150 Northwest Parkway, Marietta, Georgia 30067. M. L. Myrick (myrick@mail.chem.sc.edu) is with the Department of Chemistry and Biochemistry, University of South Carolina, Columbia, South Carolina 29208.

Received 18 June 2003; revised manuscript received 1 December 2003; accepted 14 January 2004.

0003-6935/04/102130-11$15.00/0